[UCI]I804:24011-200000263542

February, 2013

Ph.D. Thesis

Isolation and Characterization of New Sirtuin1 (SIRT1) Activators from Medicinal Plants

Chosun University Graduate School

College of Pharmacy

Dao Trong Tuan

Isolation and Characterization of New Sirtuin1 (SIRT1) Activators from Medicinal Plants

약용 식물자원으로부터 새로운 서투인 단백질 활성화 물질의 분리 및 특징 규명

February 25th, 2013

Chosun University Graduate School

College of Pharmacy

Dao Trong Tuan

Isolation and Characterization of New Sirtuin1 (SIRT1) Activators from Medicinal Plants

지도교수 오원근

이 논문을 약학 박사학위신청 논문으로 제출함

2012년 10월

조선대학교 대학원

약학과

다오트롱투완

This thesis is examined and approved for

Dao Trong Tuan's Ph.D. degree

Chairman	Seoul National Univ.	Dr. Kang Keon Wook
Member	Chosun Univ.	Dr. Woo Eun Rhan
Member	KRIBB	Dr. Lee Chul Ho
Member	Chosun Univ.	Dr. Oh Won Keun
Member	Chosun Univ.	Dr. Cho Tae Oh

December 2012

Chosun University Graduate School

Contents

List of Shemes

List of Tables

List of Figures

List of Abbreviations

ADP: adenosine diphosphate
$[\alpha]^{T}_{D}$: specific rotation
CD: circular dichroism
COSY: H–H correlation spectroscopy
CR: calorie restriction
DMSO: dimethyl sulfoxide
FOXO: forkhead box class O
HEK: human embryonic kidney
HFD: high fat diet
HMBC: heteronuclear multiple bond correlation
HMQC: heteronuclear multiple quantum coherence
HPLC: high performance liquid chromatography
HR-EI-MS: high resolution electro impact mass spectroscopy
IR: infrared absorption
MAR: mating-type regulator
MyoD: myogenic differentiation antigen
m/z: mass to charge ratio
NAD^{+}: the oxidized form of nicotinamide adenine
NMR: nuclear magnetic resonance
NOESY: nuclear overhauser effect spectroscopy
PGC: proliferator activated receptor gamma coactivator
PPAR: peroxisome proliferator activated receptor
ppm: parts per million
RANTES: regulated on activation normal T cell expressed and secreted
RP: reverse phase
SIRT1: silent information regulator two ortholog 1
Tat: trans activator of transcription
TGF: transforming growth factor
UV: ultraviolet absorption

(국문 초록)

약용 식물자원으로부터 새로운 서투인 단백질 활성화 물질의 분리 및 특징 규명

다오 트롱 투완
조선대학교 대학원
약학과
지도교수: 오원근

Silent information regulator two ortholog 1 (SIRT1)는 처음으로 발견된 포유류의 sirtuin이고 일곱개의 알려진 SIRTs (SIRTs 1-7) 가운데 가장 많이 연구된 단백질이다. SIRT1을 활성화 시키는 문질은 노화 관련 질환의 치료에 도움이 될 수 있다는 거으로 알려지고 있다. 그러나, 비록 지금까지 많은 저분자 SIRT1 활성화물질이 보고되었다 할 지라도 새로운 물질의 개발은 SIRT1 생물학적 기능에 대한 이해를 향상시키기 치료학적인 적용을 위하여 계속 요구되고 있디. SIRT1의 효능을 증가시키는 새로운 골격의 화합물을 화합물을 얻기위하여, 우리는 전통 약용 식물자원으로부터 선택적이며 높은 활성을 갖는 화합물에 대한 검색을 실시하였다. In vitroSIRT1 분석법을 사용하여 약용식물자원을 탐색한 후 두가지 식물자원인 *Ailanthus altissima*와 *Curcuma longa* 가 연구를 위한 식물 대상으로 선택되었다.

활성 추적 검색법을 사용하여 12개의 새로운 화합물을 포함한 활성 화합물의 분리하는 성과를 얻었다. 신규 화합물의 목록은 다음과 같다: (2′*R*,3′*R*)-7-(2′,3′-dihydroxy-3′,7′-dimethylocta-6′-enyloxy)-6,8-dimethoxycoumarin, 6,8-dimethoxy-7-(3′,7′-dimethylocta-2′,6′-

dienyloxy)coumarin, (2′*R*,3′*R*,6′*R*)-7-(2′,3′-dihydroxy-6′,7′-epoxy-3′,7′-dimethyloctaoxy)-6,8-dimethoxycoumarin, (2′*R*,3′*R*,4′*S*,5′*S*)-6,8-dimethoxy-7-(3′,7′-dimethyl-4′,5′-epoxy-2′-hydroxyocta-6′-enyloxy)coumarin, (3′*R*,4′*S*)-6,8-dimethoxy-7-(3′,7′-dimethylocta-3′,4′-epoxy-6′-enyloxy)coumarin, (2′*R*,3′*R*,6′*R*)-7-(6′,7′-dihydroxy-2′,3′-epoxy-3′,7′-dimethyloctaoxy)-6,8-dimethoxycoumarin, (3′*R*,4′*S*)-7-(2′,3′:6′,7′-diepoxy-6′-hydroxy-3′,7′-dimethyloctaoxy)-6,8-dimethoxycoumarin, (2′*R*,3′*R*,6′*S*)-6,8-dimethoxy-7-(6′-hydroxy-2′,3′-epoxy-3′,7′-dimethylocta-7′-enyloxy)coumarin, (2′*R*,3′*R*,6′*S*)-6,8-dimethoxy-7-(2′,3′6′-trihydroxy-3′,7′-dimethylocta-7′-enyloxy)coumarin (altissimacoumarins C-K), 2-(4,5-dihydroxy-3-methoxyphenyl)methenyl-5-(4-hydroxyphenyl)ethenyl-3(2*H*)-furanone, 2-(4,5-dihydroxy-3-methoxyphenyl)methenyl-5-(4-hydroxy-3-methoxyphenyl)ethenyl-3(2*H*)-furanone 과 (1*R*,3*R*,5*S*)-trihydroxy-1-(4,5-dihydroxy-3-methoxyphenyl)-7-(4-hydroxy-3-methoxyphenyl)heptane (curcuminlongins A-B 와 D).

분리된 신규화합물의 구조분석을 위하여, 1D, 2D-NMR, UV, IR, 및 MS등의 분광학적인 방법과 물리화학적인 기술들이 사용되었다. 본 학위 논문에서, 모든 신규 화합물의 분리 및 구조 해석등이 시도 되었다. 또한, 화합물의 SIRT1에 대한 작용 및 그들의 구조 - 활성 관계에 대한 연구가 시도되었다. 이러한 결과는 *A. altissima*와 *C. longa*로부터 분리된 화합물은 새로운 SIRT1 활성화물질로 가능성을 갖고있어 보다 후속적인 연구가 필요한 것으로 사료된다.

ABSTRACT

Isolation and Characterization of New Sirtuin1 (SIRT1) Activators from Medicinal Plants

Dao Trong Tuan

Advisor: Prof. Oh Won-Keun Ph.D.

College of Pharmacy,

Graduate School of Chosun University

Silent information regulator two ortholog 1 (SIRT1) was discovered as the first mammalian sirtuin discovered and is the most studied of the seven human sirtuin family members. It has been postulated that activators of SIRT1 might be beneficial in the treatment of aging-associated diseases. However, although some small molecular activators of SIRT1 have been identified recently, new activators are still needed to improve the understanding of SIRT1 biological functions and to discover its possible therapeutic indication. With the hope of gaining promising substances served as lead compounds for stimulating SIRT1 activity, we have focused our efforts on search for highly active compounds isolated from traditional medicinal plants source. After screening thousands of plants by using an in vitro SIRT1 assay, two candidates have been selected for further studies, including *Ailanthus altissima* and *Curcuma longa*.

Bioactivity guided fractionation of these candidates has resulted in the isolation of a series of substances as active principles, including twelve new compounds:

(2′*R*,3′*R*)-7-(2′,3′-dihydroxy-3′,7′-dimethylocta-6′-enyloxy)-6,8-dimethoxycoumarin, 6,8-dimethoxy-7-(3′,7′-dimethylocta-2′,6′-dienyloxy)coumarin, (2′*R*,3′*R*,6′*R*)-7-(2′,3′-dihydroxy-6′,7′-epoxy-3′,7′-dimethyloctaoxy)-6,8-dimethoxycoumarin, (2′*R*,3′*R*,4′*S*,5′*S*)-6,8-dimethoxy-7-(3′,7′-dimethyl-4′,5′-epoxy-2′-hydroxyocta-6′-enyloxy)coumarin, (3′*R*,4′*S*)-6,8-dimethoxy-7-(3′,7′-dimethylocta-3′,4′-epoxy-6′-enyloxy)coumarin, (2′*R*,3′*R*,6′*R*)-7-(6′,7′-dihydroxy-2′,3′-epoxy-3′,7′-dimethyloctaoxy)-6,8-dimethoxycoumarin, (3′*R*,4′*S*)-7-(2′,3′:6′,7′-diepoxy-6′-hydroxy-3′,7′-dimethyloctaoxy)-6,8-dimethoxycoumarin, (2′*R*,3′*R*,6′*S*)-6,8-dimethoxy-7-(6′-hydroxy-2′,3′-epoxy-3′,7′-dimethylocta-7′-enyloxy)coumarin, (2′*R*,3′*R*,6′*S*)-6,8-dimethoxy-7-(2′,3′6′-trihydroxy-3′,7′-dimethylocta-7′-enyloxy)coumarin (altissimacoumarins C-K), 2-(4,5-dihydroxy-3-methoxyphenyl)methenyl-5-(4-hydroxyphenyl)ethenyl-3(2*H*)-furanone, 2-(4,5-dihydroxy-3-methoxyphenyl)methenyl-5-(4-hydroxy-3-methoxyphenyl)ethenyl-3(2*H*)-furanone and (1*R*,3*R*,5*S*)-trihydroxy-1-(4,5-dihydroxy-3-methoxyphenyl)-7-(4-hydroxy-3-methoxyphenyl)heptane (curcuminlongins A-B and D).

Their structures were elucidated on the basic of spectral (including 1D, 2D-NMR, UV, IR, and MS) and physicochemical analyses. Herein, my thesis deals with the isolation, structural elucidation of these compounds. Furthermore, the preliminarily studies on evaluation of stimulating SIRT1 activity of the compounds and their structure-activity relationship are described and discussed. These data suggest that terpenylated coumarins from *A. altissima*, and curcuminoids from *C. longa* can be considered as promising classes of SIRT1 activators.

I. INTRODUCTION

Sirtuin 1 (SIRT1) is a member out of seven evolutionarily conserved sirtuin enzymes (SIRT1 to SIRT7) in human that require the co-factor nicotinamide adenine dinucleotide (NAD^+) and primarily catalyze the deacetylation of ε-acetyl-Lys residues in protein substrates. SIRT1, of particular interest, has been implicated in a number of age-related diseases and biological functions involving cell survival, apoptosis, stress resistance, fat storage, insulin production, and glucose and lipid homeostasis.

1. The discovery of sirtuins

About 10 years ago, the longevity effect of calorie restriction (CR) was first hypothesized to be mediated by a family of ancient enzymes, found throughout all species, known as "sirtuin" proteins (Guarente, 2005; Guarente & Picard, 2005; Sinclair, 2005). The founding member of this family, the SIR2 gene from the yeast *S. cerevisiae*, was originally called MAR1 (mating-type regulator 1) (Klar *et al*., 1979). Following this initial work, other mutations that led to sterility were also isolated in this gene and in 3 others, so this set of four genes was collectively renamed in the literature as SIR 1-4 (for "silent information regulator") (Rine & Herskowitz, 1987; Ivy *et al*., 1985; Shore *et al*., 1984). Subsequent work further elucidated that over expression of SIR2 led to notably higher deacetylation of histone proteins at the mating-type loci, a unique feature of SIR2 that is not shared by the other SIR proteins (Braunstein *et al*., 1993). A few years later, four more yeast genes were discovered with homology to SIR2 and these genes were named as HST (or "homologues of SIR2") 1-4 (Derbyshire *et al*., 1996; Brachmann *et al*., 1995). Thus,

there are a total of five sirtuin genes in *S. cerevisiae*: SIR2, the founding member of the family, and the four homologues, HST1-HST4. Although it was shown that none of the four HST genes were essential for survival, they do participate in silencing at telomeres and at the mating-type loci, in addition to maintaining integrity of the genome and progression through the cell cycle. SIR2 was then subsequently discovered across diverse species ranging from bacteria to plant and human. There have been seven sirtuins characterized in human:

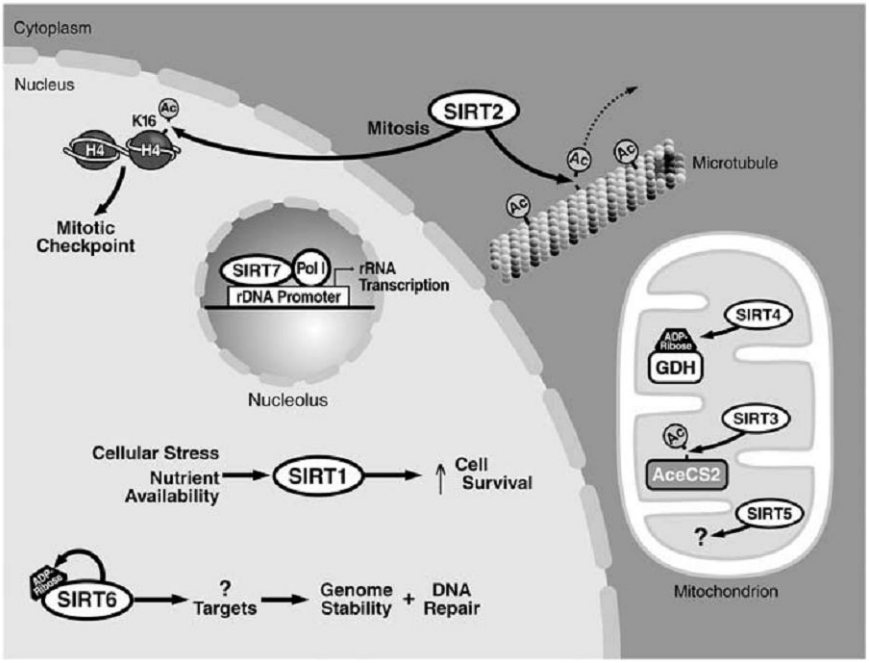

Fig. 1. Cellular localization, enzymatic activities and targets of the mammalian sirtuins (Saunders & Verdin, 2007)

Sirtuins link with CR that was first made in *S. cerevisiae*. Increased dosage of the SIR2 gene was shown to suppress the formation of extra chromosomal rDNA circles (ERCs) and thereby extend yeast lifespan by 30% (Kaeberlein *et al.*, 1999). Later, it was

observed that the replicative lifespan of cells was extended by about 30% using media with 0.5% glucose (weight/volume), when compared to cells grown on the standard recipe of 2% glucose, and this CR-induced longevity effect was shown to be dependent on the SIR2 gene (Anderson *et al*., 2003; Lin *et al*., 2000). Although controversy exists, the life-extending function of SIR2 was conserved across other organisms: increasing the level (or activity) of the Sir2 enzyme extends the lifespan of models like *C.elegans* and *Drosophila* (Rogina and Helfand, 2004; Tissenbaum and Guarente, 2001). Indeed, even the protozoan para site, *Leishmania*, encodes a Sir2 enzyme to promote its survival (Vergnes *et al*., 2002). Importantly, recent studies in mice have shown that SIRT1 knockout animals (SIRT1 is the mammalian orthologue of Sir2) fail to exhibit increased physical activity characteristic of CR (Chen *et al*., 2005) and CR also fails to extend lifespan (Boily *et al*., 2009), yet these changes may be attributed to a systemic decrease in overall fitness, as the animals may have other unknown defects/phenotypes. Conversely, transgenic mice over-expressing SIRT1 exhibit phenotypes that mimic the CR state, including increased metabolism, leaner body composition, lowered blood cholesterol and adipokines, and increased performance upon rotarod challenge (Bordone *et al*., 2007). Today, the mammalian SIRT1 have emerging roles in a variety of fundamental age-associated processes including cancer, diabetes, obesity, inflammation, muscle differentiation, heart failure, and neurodegeneration, thereby attracting wide interest for promising therapeutic intervention (Gan & Mucke, 2008; Porcu & Chiarugi, 2005).

2. Role of SIRT1 in metabolic regulation

SIRT1 regulates a variety of cellular processes like energy metabolism, cell-

cycle progression, muscle differentiation, fat mobilization, and aging, through the deacetylation of its substrates, including histones H1, H3, and H4, p53, p300, FOXOs 1, 3a, and 4, p65, HIVTat, PGC-1*α*, PCAF, MyoD, peroxisome proliferation-activated receptor γ, Ku70, and others (Sauve *et al.*, 2006; Vaziri *et al.*, 2001; Yeung *et al.*, 2004). Most striking is SIRT1's ability to coordinate metabolic pathways in different tissues, facilitating appropriate physiological responses to changes in cellular energy levels and strongly supporting a key role of sirtuins as metabolic sensor (**Fig. 2**). Human SIRT1 is expressed in all organs with strong expression in the major metabolic tissues liver, skeletal muscle, adipose tissue, pancreatic *β*-cells and brain (Michishita *et al.*, 2005). In the liver SIRT1 regulates cholesterol flux. During fasting deacetylation of PGC1-α by SIRT1 activates transcription programs promoting fatty acid oxidation and glucose production by enhancing gluconeogenesis and repressing glycolysis in the liver. Mitochondrial fatty acid oxidation is also induced by SIRT1 in skeletal muscle upon fasting. In white adipose tissue, on the other hand, SIRT1 promotes lipolysis and fatty-acid mobilization by binding and repressing the nuclear receptor PPAR-γ. SIRT1 also modulates the production and secretion of adiponectin, which improves insulin sensitivity. In pancreatic *β*-cells SIRT1 positively regulates insulin secretion. There is increasing evidence that SIRT1 might have a protective function against type-2 diabetes, as mice overexpressing SIRT1 specifically in the pancreatic *β*-cells (BESTO) exhibit increased glucose-stimulated insulin secretion and improved glucose tolerance (Ramsey *et al.*, 2008). Interestingly, several SIRT1 activating compounds (including resveratrol and other non-polyphenolic substances) were shown to improve glucose homeostasis and insulin sensitivity in diet-induced and genetic type-2 diabetes animal models (Baur *et al.*, 2006; Feige *et al.*, 2008; Lagouge *et al.*, 2006; Milne

et al., 2007; Yamazaki *et al.*, 2009). Thus, SIRT1 seems to be a key energy sensor linking NAD^+-dependent protein deacetylation to energy metabolism and physiological responses during nutrient deprivation.

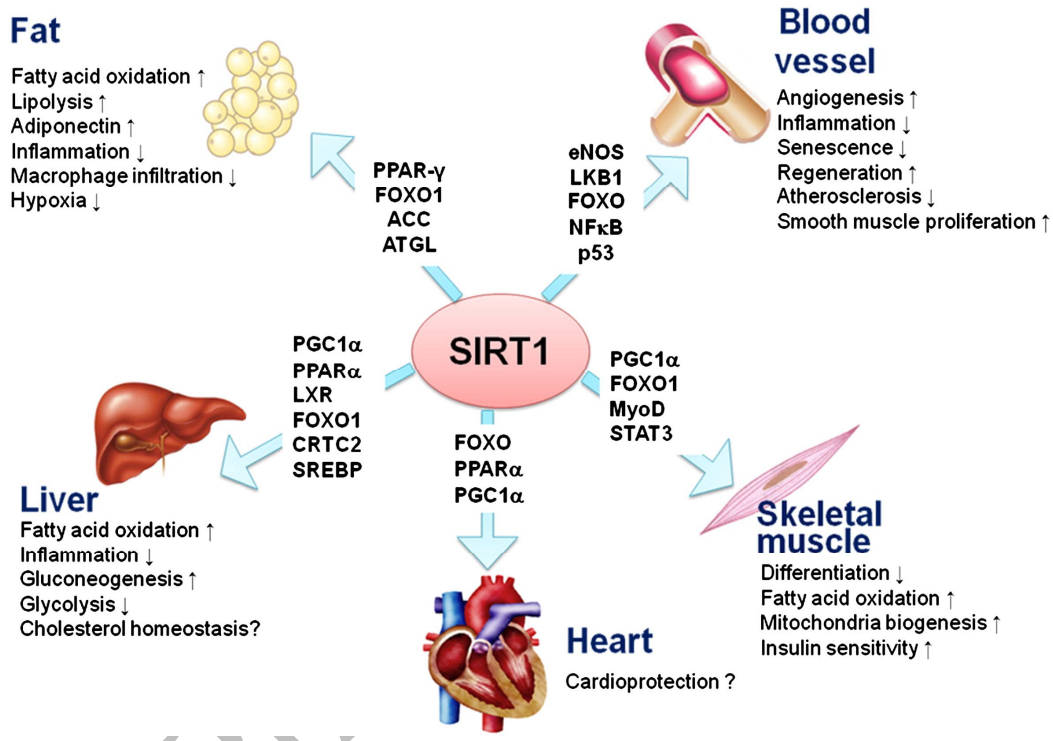

Fig. 2. SIRT1 is a metabolic master switch that modulates lifespan

3. SIRT1 as promising therapeutic targets to treat age-associated diseases

3.1. Cardiovascular disease

SIRT1 activation can improve cardiac function through effects on multiple pathways including improved vaso-relaxation (possibly through K-channel inhibition), anti-inflammatory activity on macrophages and foam cell formation. This is in addition to increased scavenging of reactive oxygen species, increased nitric oxide synthase activity,

reduced platelet aggregation, angiogenesis activity and anti-apoptosis activity (Delmas *et al.*, 2005; Das *et al.*, 2006; Labinskyy *et al.*, 2006; Mattagajasingh *et al.*, 2007; Stef *et al.*, 2006; Zbikowska *et al.*, 1999; Zhang *et al.*, 2006; Teisseyre & Michalak 2006). As an example, SIRT1 regulates the activity of PGC1α, a central factor in controlling energy state and contractile function in cardiac muscle (Arany *et al.*, 2005). Furthermore, activity of the histone variant H2A.Z, which is upregulated during cardiac hypertrophy (Chen *et al.*, 2006), is regulated by SIRT1 resulting in its ubiquitin-mediated degradation and a consequential moderation of cell growth and apoptosis.

3.2. Neurodegenerative diseases

Both SIRT1 activators and overexpression of SIRT1 have been shown to slow in vitro cell death as well as in vivo neurodegeneration (Pallas *et al.*, 2008). Further evidence to support a role of SIRT1 in neuroprotection comes from the literature on the beneficial health effects of calorie restriction. Recent epidemiological evidence suggests that humans who maintain a low calorie diet have a reduced risk of developing Alzheimer's disease (Hendrie *et al.*, 2001; Luchsinger *et al.*, 2002; Mattson, 2003). Axonal degeneration is a major component of neuropathies and therefore compounds that lead to axonal protection represent useful therapeutic agents. Interestingly, studies in rodents have established that degeneration of distal neurons occurs within 24–48 hours after axotomy (Coleman *et al.*, 2002). Cellular NAD levels decline after axotomy and prevention of this by overexpression of the NAD-synthesizing enzyme NMNAT or exogenous NAD treatment can protect neurons from degeneration (Wang *et al.*, 2005; Araki *et al.*, 2004).

3.3. Inflammatory diseases

SIRT1 activation may lead to anti-inflammatory activity through attenuation of NF-κB activity, the master regulator of innate immune responses (Yeung *et al.*, 2004). A comprehensive review of SIRT1 regulation of NF-κB, via RelA/p65 subunit deacetylation, has recently been published (Salminen *et al.*, 2008). The interaction between SIRT1 and NF-κB may also involve other factors including transducin-like enhancer of split 1 (TLE1) (Ghosh *et al.*, 2007), with both SIRT1 and TLE1 being required to suppress NF-κB activity indicating a further level of complexity. Moreover, expression of multiple pro-inflammatory mediators such as intracellular adhesion molecule 1 (ICAM1), MCP1, RANTES (or CCL5), macrophage colony stimulating factor (MCSF), granulocyte macrophage CSF (GMCSF), GCSF, transforming growth factor-β (TGF-β) are all reduced by SIRT1 activator (Leiro *et al.*, 2005). This suggests that SIRT1 activation has profound effects on inflammation through multiple downstream pathways. In addition, SIRT1 activators can inhibit TNF-α following a challenge with lipopolysaccharide (Nayagam *et al.*, 2006). SIRT1 activity is also decreased in the lungs of patients with chronic obstructive pulmonary disease, and its activity is reduced when human macrophages are exposed to cigarette smoke (Rajendrasozhan *et al.*, 2008).

3.4. Cancer

There have been conflicting data reported in the literature that support both activation and inhibition of SIRT1 as a strategy for cancer therapy. At the level of gene suppression, there is evidence of involvement of SIRT1 in epigenetic silencing of tumour suppressor genes such as SFRP1, CDH1 and GATA5 promoters. Inhibition and

knockdown of SIRT1 led to re-expression of these silenced genes with potential implications for tumour growth (Pruitt *et al.*, 2006). Specifically, silencing of the SFRP1 and SFRP2 genes is important for aberrant activation of the Wnt pathway in colon cancer. Re-expression of these genes by nicotinamide and splitomycin, both weak/nonspecific SIRT1 inhibitors, or by knockdown of SIRT1 causes downregulation of Wnt pathway function leading to apoptosis. However, recent evidence indicates that SIRT1 can directly inhibit β-catenin, another member of the Wnt signalling pathway. Ectopic expression of wild-type SIRT1, but not a catalytic deficient mutant, reduces proliferation in colon cancer cell lines (Firestein *et al.*, 2008). An increase in SIRT1 can result in deacetylation of multiple proteins including the tumour suppressors, p53, p73 and Ku70, which hypothetically may lead to increased tumorigenesis (Luo *et al.*, 2001; Cohen *et al.*, 2004; Dai *et al.*, 2007).

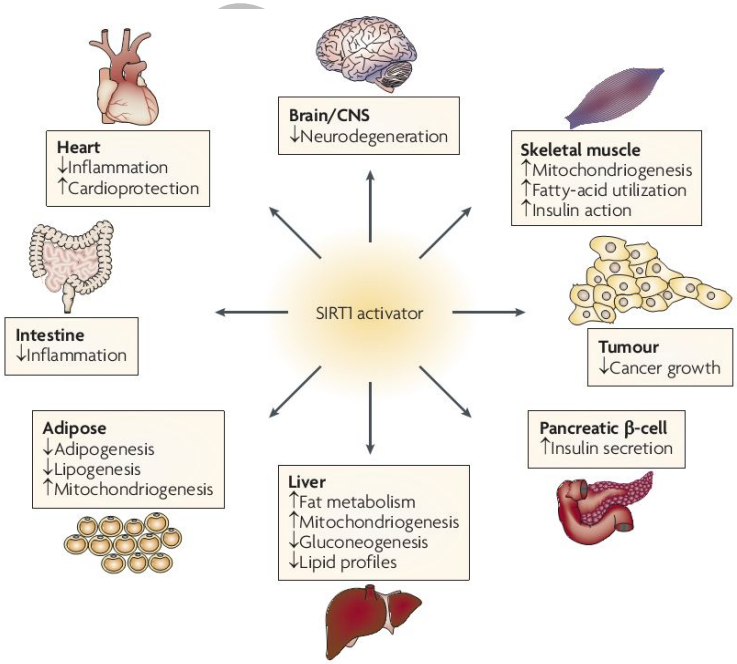

Fig. 3. Multiple target organs of SIRT1 activators in the treatment of ageing diseases

4. Molecular mechanisms of SIRT1

SIRT1 utilizes a unique two-step biochemical process to catalyze their deacetylase reaction (Sauve & Schramm, 2003). During catalysis, one NAD^+ molecule and one acetyl-lysine (histone or non-histone protein) substrate are utilized, and progress by a base-exchange step coupled to the deacetylation step (**Fig. 4**). Importantly, the major by product of this reaction, nicotinamide, must be cleared as it accumulates, for it can bind to a regulatory C-pocket in the sirtuin (discovered by structural studies) and greatly inhibit the enzymatic function (Zhao *et al*., 2004; Bitterman *et al*., 2002).

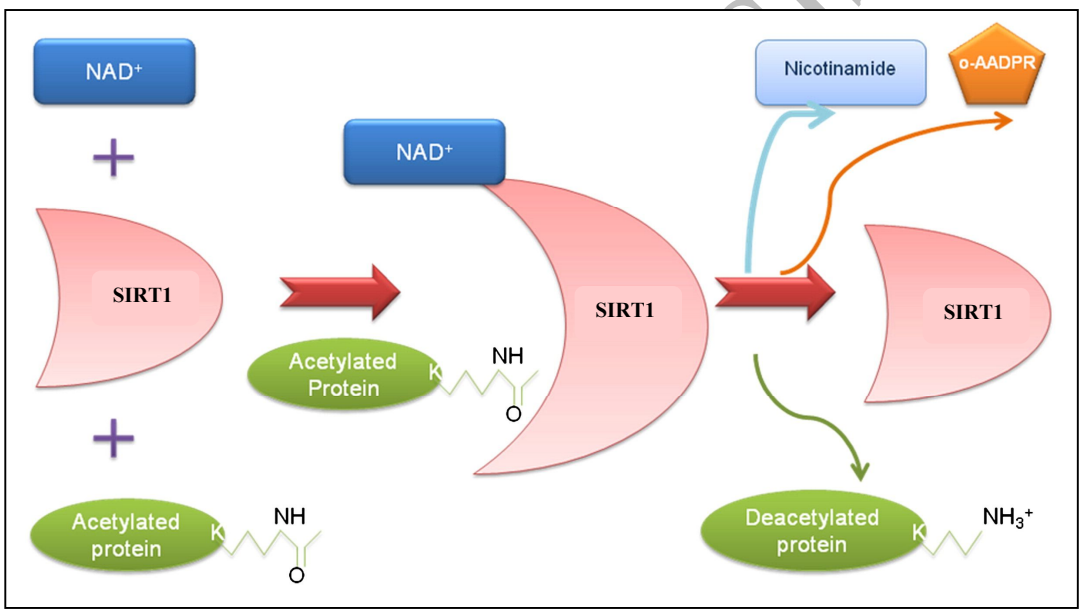

Fig. 4. NAD^+-dependent protein deacetylation reaction catalyzed by SIRT1

5. General characterization of SIRT1 enzyme activation

Recently, several assays to measure the enzymatic activity of SIRT1 have been described. These assays are including radioactive methods with ^{14}C-NAD^+, ^{14}C-acetylated p53 or ^{3}H-acetylated histone groups as radioactive substrate (Bedalov *et al*.,

2001; Borra *et al*., 2005; Luo *et al*., 2001), and HPLC methods to analyze substrate conversion/product formation (Jackson & Denu, 2002). These methods pose drawbacks for large-scale screening and management of hazardous wastes. In 2003, Howitz *et al*., reported the first screen for SIRT1 activators using the Fluor de Lys assay (Enzo Life Sciences, Formingdale, NY). Steady state kinetic characterization revealed that resveratrol activates by lowering the Km for the peptide substrate (Howitz *et al*., 2003). Investigations of the molecular detail of SIRT1 activation have emphasized the dependence on substrate structural features, that was highlighted by two reports in 2005 Borra *et al.* and Kaeberlein *et al*., demonstrating that resveratrol enhances the SIRT1 catalyzed deacetylation of Ac-Arg-His-Lys(Ac)-AMC but not the corresponding peptide lacking the AMC group, Ac-Arg-His-Lys-Lys(Ac)-NH_2. The observation that activation requires a fluorophore covalently attached to the peptide substrate was later confirmed by Beher *et al*. (2009) and extended by Pacholec *et al*. (2010) with using the TAMRA-labeled peptide, Ac-Glu-Glu-Lys-Gly-Gln-Ser-Thr-Ser-Ser-His-Ser-Lys(Ac)-Nle-Ser-Thr-Glu-Gly-Lys(TAMRA)-Glu-Glu-NH_2 (Milne *et al*., 2007). Pacholec *et al*. (2010) further reported that the previous SIRT1 activators do not activate full-length protein substrate. These results raised concerns that activation of SIRT1 was only relevant to fluorescently labeled substrates although a specific mechanism for how the compound binding to the fluorophore could result in activation of SIRT1 was not proposed.

6. SIRT1 activators

Some small-molecule activators of SIRT1 have been identified by utilizing a commercially available deacetylase activity assay, almost all of them are synthetic

compounds (Vu *et al*., 2009; Bernis *et al*., 2009; Smith *et al*., 2009; Yamazaki *et al*., 2009; Mai *et al*., 2009). Howitz and colleagues have identified some compounds of natural origin, such as resveratrol, fisetin and butein, but these compounds have a low bioavailability (Howitz *et al*., 2003). Moreover, this particular method for the determination of SIRT1 activity is controversial due to its dependence on the use of a specific fluorophore substrate (Borra *et al*., 2005; Pacholec *et al*., 2010). Other previous researchers have reported synthesized compounds with SIRT1 stimulatory activity, including quinoxalines, SRT derivatives, oxazolo-[4,5-*b*]pyridines, dihydropyridines and imidazol-[1,2-*b*]thiazoles (Vu *et al*., 2009; Bernis *et al*., 2009; Smith *et al*., 2009; Yamazaki *et al*., 2009; Mai *et al*., 2009). There has been little clinical data available for the selective SIRT1 activators, among which, SRT1720 has been the most extensively tested compound with data in several disease models, including models of diabetes (Milne *et al*., 2007; Feige *et al*., 2008; Yoshizaki *et al*., 2010), inflammation (Lappas *et al*., 2007) and fatty liver disease (Walker *et al*., 2010). Minor *et al*. (2011) after SRT1720 in food was administered at doses of 30 and 100 mg/kg in 1-year-old mice fed a HFD for the remainder of their lifespan. SRT1720 strongly increased the mean and maximum lifespan of the mice while conferring significant health benefits including reduced liver steatosis, increased insulin sensitivity, and a reduction in inflammation and apoptotic markers. Moreover, the altered gene expression profile of the HFD diet fed mice was normalized to that of normal chow mice in the HFD animals receiving SRT1720 (Minor *et al*., 2011).

Anyway to date, only a few activators of SIRT1 have been reported, and almost all of them are synthetically derived compounds or identified from library screening studies.

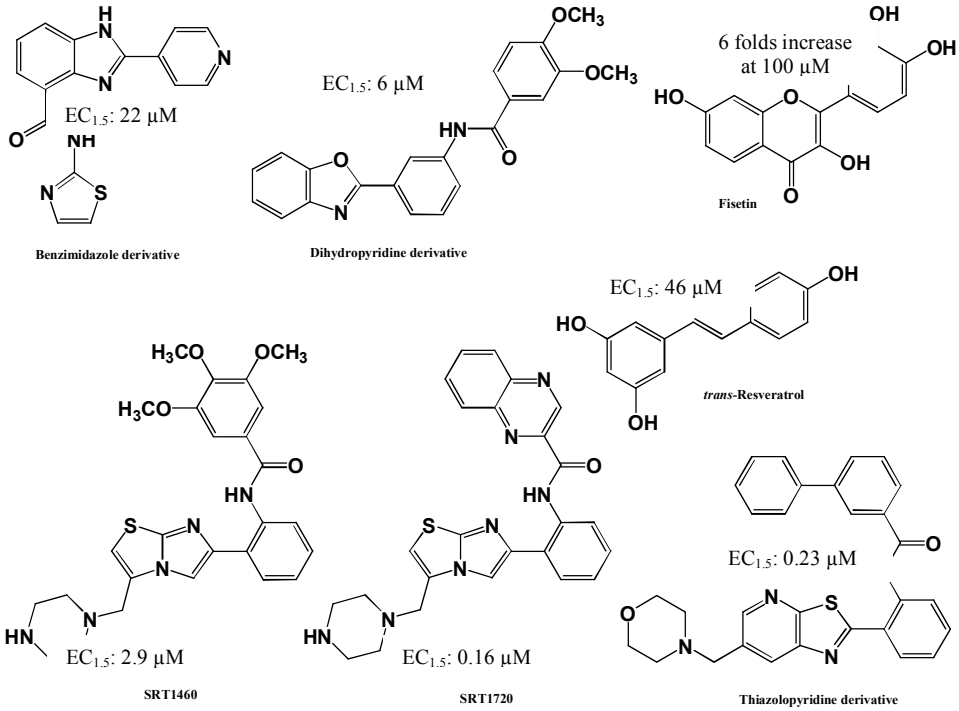

Fig. 5. SIRT1 activators derived from natural resources or synthesis

7. Research objectives and content

With the hope of gaining promising substances served as lead compounds for stimulating SIRT1 activity, we have focused on screening thousands of plants by using an in vitro SIRT1 assay, and two candidates have been finally selected for further studies, including *Ailanthus altissima* and *Curcuma longa*. Bioactivity guided fractionation of these candidates has resulted in the isolation of a series of substances as active principles, including twelve new compounds. Herein, my thesis deals with the isolation, structural elucidation of these compounds. Additionally, the preliminarily studies on evaluation of stimulating SIRT1 activity of the compounds and their structure-activity relationship are described and discussed.

II. MATERIALS AND METHODS

1. Chemicals, reagents and chromatography

Column chromatography was conducted on silica gel (Merck, 63–200 μm particle size) and C-18 silica gel (Merck, 40–63 μm particle size) from Merck. HPLC was carried out using a Gilson System with UV detector and an ODS-H80 column (20 × 150 mm, 4 μm particle size, YMC Co., Ltd., Japan). Baker analyzed HPLC solvents MeOH and MeCN were purchased from Mallinckrodt Baker, Inc. USA. Deuterated solvent for NMR analysis $CDCl_3$ was purchased from CIL (Cambridge Isotope Lab., USA).

Nicotinamide and resveratrol were purchased from Sigma Chemical Company (St Louis, MO, USA), Dulbecco's modified Eagle's medium (DMEM), fetal bovine serum (FBS), and trypsin were purchased from GIBCO-BRL (Grand Island, NY, USA). Human recombiniant SIRT1, NAD^+ and the buffer used for assays were purchased from Biomol (Plymouth Meeting, PA)

2. General experimental procedures

Optical rotations were determined on a Rudolph Autopol IV polarimeter using a 100 mm glass microcell. UV spectra were recorded in MeOH on a JASCO V-550 UV/Vis spectrometer with a 0.5 nm resolution, and IR spectra (KBr) were obtained using a Nicolet 6700 FT-IR (Thermo Electron Corp.). CD spectra were measured on a JASCO J-715 spectropolarimeter (Japan spectroscopic Ltd., Japan). NMR spectra were recorded on a Varian Unity Inova 500 MHz spectrometer with TMS as the internal standard at the Korea Basic Science Institute (KBSI, Gwangju Center, Korea). EIMS and HREIMS data were

recorded on a Micromass QTOF2 (Micromass, Wythenshawe, UK) mass spectrometer. HPLC was carried out using a Gilson system with a UV detector and Optima Pak C_{18} column (10 × 250 mm, 10 µm particle size, RS Tech, Korea). All solvents used for extraction and isolation were of analytical grade.

3. Cell culture and transfection

HEK293 cells were maintained in Dulbecco's Modified Eagle's Medium (DMEM) (Welgene) supplemented with 10% fetal bovine serum and 1% antibiotic/antimycotic at 37 ^{o}C and 5% CO2. The cells were counted and plated in 24-well plates at a density of 10^5 cells/well in 1 mL of medium. After 24 h, the plasmid DNA was introduced into each well by using PEI transfection reagent (Polyscience, Inc.), according to the manufacturer's instructions. Briefly, the cells were incubated with 0.6 µg of DNA and 3 µg PEI reagent for 12 h at 37 ^{o}C. After transfection, the cultures were maintained in 10% FBS-DMEM medium. At 24 h post-transfection, the cells were treated with the test compounds or the positive control.

4. In vitro SIRT1 deacetylation in a bioluminescence assay

The SIRT1 enzyme assay was performed as previously reported (Liu *et al.*, 2008). Briefly, this was performed using acetylated p53 (Ac-p53) [HLKSKKGQSTSRHKK(Ac)LMFK] peptide, NAD^+ and SIRT1 in the absence or presence of the compound in the SIRT1 reaction buffer (100 mM Tris/Cl pH 8.0, 20 mM NaCl, 4 mM DTT, 100 µg/mL BSA). The enzyme reaction was initiated by the addition of the Ac-p53 peptide and NAD^+, and incubated for 2 h. The reaction was quenched by the

addition of 10 μL of LDH reagent (5 mM nicotinamide, 10 mM lactic acid, 62.5 U/mL LDH, 600 μM glycine, 500 μM hydrazine). After 1 h of incubation, 4 μL of the SIRT1/LDH mixture were added to 50 μL of a luminescence reaction mixture [50 mM Hepes, pH 7.5, 1 mM DTT, 1.5 mM EDTA, 100 μg/mL BSA, 10 μg/mL luciferase, 0.05 U/mL NAD(P)H:FMN-oxidoreductase, 500 μM decanal, 5 μM FMN]. Finally, luminescence in the reaction was measured within 15 min using a SpectraMax Luminescence System (Molecular Devices, Inc.). The positive control for each plate was a SIRT1 reaction in the presence of DMSO, and the negative control was a reaction mixture without enzyme.

5. In vitro SIRT1 deacetylation in a NAD/NADH assay

The SIRT1 enzyme reaction was performed in a final volume of 25 μL per well in a 384-well microplate. A standard SIRT1 reaction solution contained 0.1 U/mL enzyme, 10 μM NAD^+, and 20 μM Ac-p53 peptide in the absence or presence of the compound in the SIRT1 assay buffer (25 mM Tris/Cl pH 8.0, 137 mM NaCl, 2.7 mM KCl, 1mM $MgCl_2$, 1mg/mL BSA). The assay buffer and the enzyme/compound mixture (10 μL) were incubated for 10 min at room temperature. The reaction was then initiated by the addition of 15 μL of a solution containing Ac-p53 peptide and NAD^+. After incubation for 6 h at ambient temperature, the reaction was quenched by the addition of 25 μL of a NAD/NADH recycling enzyme mixture containing 1 mM nicotinamide. After 2 h of incubation, the absorbance increase in the reaction was measured using VersaMax Absorbance Microplate Reader (Molecular Devices, Inc.). The positive control for each plate was a SIRT1 reaction in the presence of DMSO, and the negative control was a

reaction mixture without enzyme.

6. In vivo SIRT1 deacetylation in a luciferase reporter assay

Cells were transiently transfected with the reporter plasmid, PG13-luc (wt p53 binding sites), in combination with the plasmid encoding myc tagged p53 (myc-p53), and the plasmid encoding flag tagged SIRT1 (flag SIRT1) with RSV-*β*-gal plasmid as an internal control. The total amount of transfected DNA was the same in each well. The luciferase activity was measured by adding 40 µL of luciferin into 60 µL of lysate using an analytical luminescence luminometer. Promoter activity was measured using a Dual Luciferase Assay Kit (Promega, Madison, WI), measuring both luciferase and renilla luciferase with a luminometer (Promega). Cells were lysed and assayed for p53, myc-p53 and flag SIRT1 reporter activities, which were corrected for constitutive *β*-galactosidase luciferase expression. Normalized values were calculated by dividing the luciferase activity by the renila luciferase activity.

7. NAD^+-to-NADH ratio assay

The NAD+-to-NADH ratio was measured from whole cell extracts of HEK293 cells using the Biovision NAD/NADH Quantitation kit, performed according to the manufacturer's instructions.

8. Statistical analysis

A statistical calculation was carried out using Microsoft Excel 2003. The results are expressed as the means ± SD of three to five independent experiments.

III. RESULTS

1. Isolation of SIRT1 activators from *Ailanthus altissima*

1.1. Introduction

Ailanthus altissima (Mill.) Swingle (Simaroubaceae), commonly known as the "tree of heaven", is a deciduous tree (6–20 m in height). It is native to mainland China and is now naturalized in many temperate regions of the world (Kowarik *et al*., 1995). Its leaves have been used in traditional medicine to treat gastric ailments, while the root bark and stem bark have been used as folk remedies for colds, fever, and tumors of the breast in the Peoples Republic of China and Korea (Feo *et al*., 2003; Jin *et al*., 2006). Previous phytochemical studies have led to the characterization of quassinoids, alkaloids, lipids, coumarins, and other phenolic derivatives, of which quassinoids are the major components with antitumor, antimalarial, antifeedant, anti-inflammatory, and other activities (Okano *et al*., 1990; Hwang *et al*., 2005). However, there have been no studies on the effects of *A. altissima* on SIRT1 activity.

1.2. Plant material

The stem barks of *A. altissima* were purchased from Kangwon Herbal Medicine Company (Kangwon-do, Republic of Korea), in November 2009 and botanically identified by Prof. Y. H. Moon. A voucher specimen (CU2009–18) has been deposited at the Herbarium of Chosun University, Gwangju, Republic of Korea.

1.3. Extraction and isolation

The dried stem barks of *A. altissima* (4.0 kg) were extracted with MeOH (10.0 L × 2 times) at room temperature for one week. The combined MeOH extracts were concentrated to yield a dry residue (210.0 g). This crude extract was then suspended in H_2O (2.0 L) and partitioned successively with *n*-hexane (3 × 1.5 L), EtOAc (3 × 1.5 L), and *n*-BuOH (3 × 1.5 L). The EtOAc fraction (95.0 g), which exhibited strong SIRT1

activity, was chromatographed over a silica gel column (10 × 30 cm; 63–200 μm particle size) and eluted with gradient mixtures of *n*-hexane/acetone (9:1, 8:2…1: 9, each 2.5 L) to yield seven pooled fractions (F1: 10.8 g; F2: 6.5 g; F3: 7.5 g; F4: 5.3 g; F5: 5.8 g; F6: 6.2 g; F7: 11.5 g; F8: 17.0 g). Fraction F4 was applied to an RP-18 column (7 × 30 cm; 40–63 μm particle size) and eluted with a stepwise gradient of MeOH-H_2O (2:1 to 10:1) to afford five subfractions (F4.1–F4.5). F4.4 (550.0 mg) was purified by HPLC [Optima Pak C_{18} column (10 × 250 mm, 10 μm particle size, RS Tech, Korea); mobile phase MeOH in H_2O containing 0.1% HCO_2H (0–70 min: 74% MeOH, 70–75 min: 74–100% MeOH, 75–85 min: 100% MeOH); flow rate 2 mL/min; UV detection at 205 and 254 nm] to yield compound **1** (t_R = 55 min, 22.0 mg) and compound **10** (t_R = 63 min, 85.0 mg). Fraction F5 was chromatographed over a Sephadex LH-20 column (7 × 30 cm) using MeOH as the eluting solvent to give three subfractions (F5.1–F5.3). F5.2 (4.2 g) was then fractionated into five subfractions (F5.2.1–F5.2.5), using an RP-18 column (5 × 30 cm; 40–63 μm particle size), with a stepwise gradient of MeOH-H_2O (1:1 to 10:1). Subfraction F5.2.1 (150.0 mg) was further purified by HPLC (0–45 min: 52% MeOH, 45–50 min: 52–100% MeOH, 50–60 min: 100% MeOH) to yield compound **11** (t_R = 40 min, 7.5 mg) and compound **2** (t_R = 43 min, 6.5 mg). Compounds **3** (t_R = 54 min, 6.5 mg) and **4** (t_R = 60 min, 8.0 mg) were isolated by HPLC (0–65 min: 58% MeOH, 65–70 min: 58–100% MeOH, 70–80 min: 100% MeOH) from subfraction F5.2.3 (140.0 mg). Fraction F5.2.4 (220.0 mg) was continuously purified by HPLC (0–60 min: 62% MeOH, 60–70 min: 62–100% MeOH, 70–80 min: 100% MeOH) to yield compound **5** (t_R = 47 min, 17.5 mg), compound **6** (t_R = 50 min, 2.5 mg) and compound **7** (t_R = 58 min, 9.0 mg). Next, fraction F6 was chromatographed over a Sephadex LH-20 column (7 × 30 cm) using MeOH as the eluting

solvent to give four subfractions (F6.1–F6.4). F6.3 (2.8 g) was futher fractionated into seven subfractions (F6.3.1–F6.3.7), using an RP-18 column (5 × 30 cm; 40–63 µm particle size), with a stepwise gradient of MeOH-H_2O (1:1 to 10:1). Subfraction F6.3.3 (120.0 mg) was then purified by HPLC (0–45 min: 55% MeOH, 45–50 min: 55–100% MeOH, 50–60 min: 100% MeOH) to yield compound **8** (t_R = 35 min, 14.5 mg) and compound **9** (t_R = 39 min, 3.5 mg).

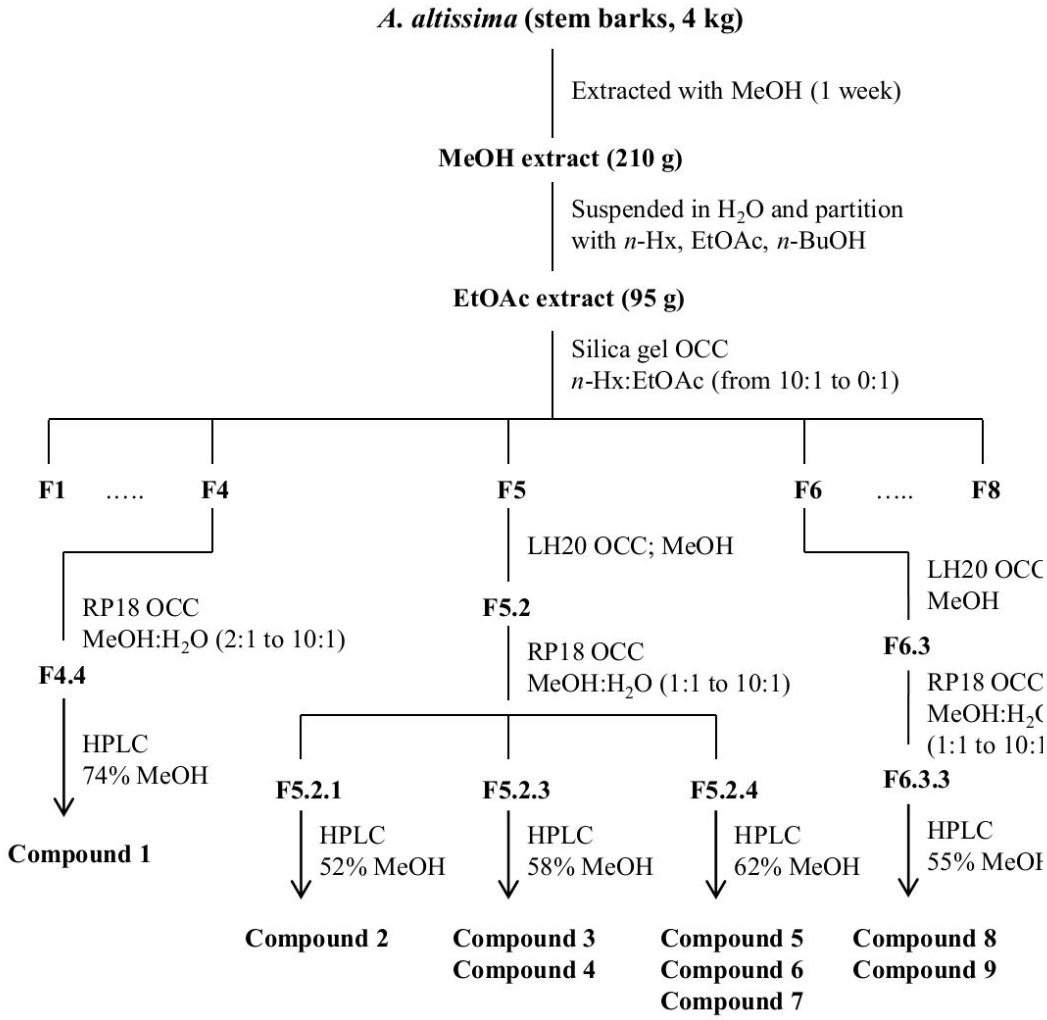

Scheme 1. Isolation of new compounds (**1**–**9**) from *A. altissima*

*Altissimacoumarin C (**1**):* colorless oil; $[\alpha]_D^{25}$ +17 (*c* 0.1, MeOH); UV (MeOH) λ_{max} (log ε) 208 (4.32), 225 (4.13), 293 (3.59), 335 (3.18) nm; IR (KBr) ν_{max} 3430 (OH), 2928, 1727 (C=O), 1564, 1460, 1269, 1086 cm^{-1}; CD (MeOH, Δε) λ_{max} 325 (-4.14), 300 (+3.37); ^1H (500 MHz) and ^{13}C (125 MHz) NMR data, see **Table 1**; EIMS *m/z* 392 ($[M]^+$, 9), 374 (7), 265 (71), 222 (100), 207 (69), 176 (38), 109 (50); HREIMS *m/z* 392.1837 $[M]^+$ (calcd for $C_{21}H_{28}O_7$, 392.1835).

*Altissimacoumarin D (**2**):* colorless oil; $[\alpha]_D^{25}$ 0.0 (*c* 0.1, MeOH); UV (MeOH) λ_{max} (log ε) 210 (4.27), 230 (3.74), 295 (3.09), 340 (3.14) nm; IR (KBr) ν_{max} 1716 (C=O), 1563, 1456, 1290, 1122 cm^{-1}; ^1H (500 MHz) and ^{13}C (125 MHz) NMR data, see **Table 2**; EIMS *m/z* 358 ($[M]^+$, 1), 222 (100), 207 (20), 179 (16), 123 (15); HRFABMS *m/z* 359.1848 $[M+H]^+$ (calcd for $C_{21}H_{27}O_5$, 359.1858).

*Altissimacoumarin E (**3**):* colorless oil; $[\alpha]_D^{25}$ +13 (*c* 0.1, MeOH); UV (MeOH) λ_{max} (log ε) 208 (4.42), 225 (4.16), 295 (3.23), 335 (3.05) nm; IR (KBr) ν_{max} 3490 (OH), 2937, 1715 (C=O), 1564, 1488, 1291, 1044 cm^{-1}; CD (MeOH, Δε) λ_{max} 317 (-7.42), 251 (+2.28); ^1H (500 MHz) and ^{13}C (125 MHz) NMR data, see **Table 3**; EIMS *m/z* 408 ($[M]^+$, 4), 350 (4), 307 (9), 267 (3), 222 (100), 169 (17), 143 (92), 125 (32), 107 (23); HREIMS *m/z* 408.1786 $[M]^+$ (calcd for $C_{21}H_{28}O_8$, 408.1784).

*Altissimacoumarin F (**4**):* colorless oil; $[\alpha]_D^{25}$ +12 (*c* 0.1, MeOH); UV (MeOH) λ_{max} (log ε) 208 (4.26), 225 (4.19), 291 (3.62), 335 (3.38) nm; IR (KBr) ν_{max} 3490 (OH), 2938, 1715 (C=O), 1563, 1457, 1291, 1042 cm^{-1}; ^1H (500 MHz) and ^{13}C (125 MHz) NMR data, see **Table 4**; EIMS *m/z* 390 ($[M]^+$, 47), 375 (26), 309 (19), 265 (32), 222 (100), 207 (29), 194 (21), 151 (52); HREIMS *m/z* 390.1679 $[M]^+$ (calcd for $C_{21}H_{26}O_7$, 390.1679).

*Altissimacoumarin G (**5**):* colorless oil; $[\alpha]_D^{25}$ +11 (*c* 0.1, MeOH); UV (MeOH) λ_{max} (log ε) 208 (4.30), 225 (4.03), 295 (3.19), 340 (3.11) nm; IR (KBr) ν_{max} 2920, 1718 (C=O), 1568, 1455, 1227, 1089 cm^{-1}; CD (MeOH, Δε) λ_{max} 325 (-3.88), 281 (+2.65); ^1H (500 MHz) and ^{13}C (125 MHz) NMR data, see **Table 5**; EIMS *m/z* 374 ($[M]^+$, 4), 284 (7), 265 (19), 222 (100), 207 (9), 191 (33), 141 (55); HREIMS *m/z* 374.1732 $[M]^+$ (calcd for $C_{21}H_{26}O_6$, 374.1729).

*Altissimacoumarin H (**6**):* colorless oil; $[\alpha]_D^{25}$ +19 (*c* 0.1, MeOH); UV (MeOH) λ_{max} (log ε) 210 (4.45), 230 (3.72), 295 (3.17), 340 (3.01) nm; IR (KBr) ν_{max} 3500 (OH), 2972, 1715 (C=O), 1564, 1488, 1291, 1039 cm^{-1}; CD (MeOH, Δε) λ_{max} 317 (-5.08), 280 (+2.35); ^1H (500 MHz) and ^{13}C (125 MHz) NMR data, see **Table 6**; EIMS *m/z* 408 ($[M]^+$, 6), 350 (3), 307 (6), 267 (6), 222 (95), 169 (19), 143 (100), 125 (50), 107 (10); HREIMS *m/z* 408.1784 $[M]^+$ (calcd for $C_{21}H_{28}O_8$, 408.1784).

Altissimacoumarin I (7): colorless oil; $[\alpha]_D^{25}$ +10 (*c* 0.1, MeOH); UV (MeOH) λ_{max} (log ε) 208 (4.35), 230 (4.02), 295 (3.05), 345 (3.44) nm; IR (KBr) ν_{max} 3445 (OH), 2940, 1732 (C=O), 1566, 1456, 1292, 1153 cm^{-1}; CD (MeOH, Δε) λ_{max} 325 (-7.77), 271 (+1.75); ^1H (500 MHz) and ^{13}C (125 MHz) NMR data, see **Table 7**; EIMS *m/z* 406 ($[M]^+$, 4), 327 (3), 267 (12), 222 (85), 207 (12), 194 (6), 113 (100); HREIMS *m/z* 406.1631 $[M]^+$ (calcd for $C_{21}H_{26}O_8$, 406.1628).

*Altissimacoumarin J (**8**):* colorless oil; $[\alpha]_D^{25}$ +10 (*c* 0.1, MeOH); UV (MeOH) λ_{max} (log ε) 208 (4.25), 230 (3.95), 295 (3.32), 340 (3.01) nm; IR (KBr) ν_{max} 3448 (OH), 2942, 1728 (C=O), 1560, 1415, 1389, 1039 cm^{-1}; CD (MeOH, Δε) λ_{max} 311 (-5.42), 267 (+1.71); ^1H (500 MHz) and ^{13}C (125 MHz) NMR data, see **Table 8**; EIMS *m/z* 390 ($[M]^+$,

6), 290 (2), 265 (2), 222 (65), 207 (10), 176 (5), 125 (100); HREIMS *m/z* 390.1679 $[M]^+$ (calcd for $C_{21}H_{26}O_7$, 390.1679).

*Altissimacoumarin K (**9**):* colorless oil; $[\alpha]_D^{25}$ +14 (*c* 0.1, MeOH); UV (MeOH) λ_{max} (log ε) 210 (4.55), 230 (4.17), 290 (3.65), 340 (3.34) nm; IR (KBr) ν_{max} 3451 (OH), 2922, 1715 (C=O), 1593, 1470, 1265, 1173 cm^{-1}; CD (MeOH, Δε) λ_{max} 325 (-3.86), 270 (+2.38); ^1H (500 MHz) and ^{13}C (125 MHz) NMR data, see **Table 9**; EIMS *m/z* 390 ($[M-H_2O]^+$, 5), 327 (2), 267 (8), 222 (80), 207 (16), 153 (51), 125 (100); HREIMS *m/z* 390.1677 $[M-H_2O]^+$ (calcd for $C_{21}H_{26}O_7$, 390.1679).

Preparation of (*S*) and (*R*)-MTPA ester derivatives of 1, 3, 4, 6 and 8: Compound **1** (1.0 mg) was dissolved in 100 µL of pyridine and stirred at room temperature (rt). For the preparation of the (*S*)-MTPA ester (**1a**) of **1**, 10 µL of (*R*)-MTPA-Cl were added to the reaction vial. After being stirred at rt for 3 h, the mixture was evaporated to dryness and purified by RP-HPLC with 87% MeOH to give **1a** (0.8 mg). Treatment of **1** (1.0 mg) with (*S*)-MTPA-Cl afforded a (*R*)-MTPA ester (**1b**) (1.0 mg). Using a similar procedure, the (*S*)-MTPA esters **3a** (0.6 mg), **4a** (0.6 mg), **6a** (1.0 mg), **8a** (0.9 mg), and (*R*)-MTPA esters **3b** (0.7 mg), **4b** (0.9 mg), **6b** (1.2 mg), **8b** (0.9 mg) were obtained from **3** (each 0.9 mg), **4** (each 1.0 mg), **6** (each 1.1 mg), and **8** (each 1.0 mg), respectively.

*Compound **1a**:* colorless oil; ^1H NMR data ($CDCl_3$, 500 MHz) δ_H 6.36 (1H, d, *J* = 9.5 Hz, H-3), 7.59 (1H, d, *J* = 9.5 Hz, H-4), 6.63 (1H, s, H-5), 3.81 (3H, s, OCH_3-6), 3.92 (3H, s, OCH_3-8), 5.04 (1H, dd, *J* = 10.5, 2.0 Hz, H-1′a), 4.40 (1H, dd, *J* = 10.5, 8.0 Hz, H-1′b), 4.32 (1H, dd, *J* = 8.0, 2.0 Hz, H-2′), 1.27 (1H, m, H-4′a), 1.25 (1H, m, H-4′b), 2.17

(1H, m, H-5′a), 1.68 (1H, m, H-5′b), 5.36 (1H, t, J = 7.0 Hz, H-6′), 1.61 (3H, s, H-8′), 1.25 (3H, s, H-9′), 1.58 (3H, s, H-10′), 3.56 (3H, s, OCH_3), 7.58 (2H, m, aromatic H), 7.37 (3H, m, aromatic H).

*Compound **1b**:* colorless oil; ^{1}H NMR data ($CDCl_3$, 500 MHz) δ_H 6.34 (1H, d, J = 9.5 Hz, H-3), 7.58 (1H, d, J = 9.5 Hz, H-4), 6.61 (1H, s, H-5), 3.74 (3H, s, OCH_3-6), 3.90 (3H, s, OCH_3-8), 4.48 (1H, dd, J = 10.5, 2.0 Hz, H-1′a), 3.94 (1H, dd, J = 10.5, 8.0 Hz, H-1′b), 4.32 (1H, dd, J = 8.0, 2.0 Hz, H-2′), 1.60 (1H, m, H-4′a), 1.47 (1H, m, H-4′b), 2.18 (1H, m, H-5′a), 1.73 (1H, m, H-5′b), 5.62 (1H, t, J = 7.0 Hz, H-6′), 1.71 (3H, s, H-8′), 1.26 (3H, s, H-9′), 1.69 (3H, s, H-10′), 3.56 (3H, s, OCH_3), 7.58 (2H, m, aromatic H), 7.37 (3H, m, aromatic H).

*Compound **3a**:* colorless oil; ^{1}H NMR data ($CDCl_3$, 500 MHz) δ_H 6.37 (1H, d, J = 9.5 Hz, H-3), 7.61 (1H, d, J = 9.5 Hz, H-4), 6.66 (1H, s, H-5), 3.82 (3H, s, OCH_3-6), 3.96 (3H, s, OCH_3-8), 4.54 (1H, dd, J = 10.5, 2.0 Hz, H-1′a), 4.35 (1H, dd, J = 10.5, 8.0 Hz, H-1′b), 5.55 (1H, dd, J = 8.0, 2.0 Hz, H-2′), 2.06 (1H, m, H-4′a), 1.60 (1H, m, H-4′b), 1.99 (1H, m, H-5′a), 1.97 (1H, m, H-5′b), 3.82 (1H, m, H-6′), 1.19 (3H, s, H-8′), 1.14 (3H, s, H-9′), 1.10 (3H, s, H-10′), 3.64 (3H, s, OCH_3), 7.67 (2H, m, aromatic H), 7.37 (3H, m, aromatic H).

*Compound **3b**:* colorless oil; ^{1}H NMR data ($CDCl_3$, 500 MHz) δ_H 6.35 (1H, d, J = 9.5 Hz, H-3), 7.60 (1H, d, J = 9.5 Hz, H-4), 6.64 (1H, s, H-5), 3.77 (3H, s, OCH_3-6), 3.88 (3H, s, OCH_3-8), 4.44 (1H, dd, J = 10.5, 2.0 Hz, H-1′a), 4.26 (1H, dd, J = 10.5, 8.0 Hz, H-1′b), 5.56 (1H, dd, J = 8.0, 2.0 Hz, H-2′), 2.17 (1H, m, H-4′a), 1.88 (1H, m, H-4′b), 2.07 (1H, m, H-5′a), 2.04 (1H, m, H-5′b), 3.85 (1H, m, H-6′), 1.25 (3H, s, H-8′), 1.24 (3H, s, H-

9′), 1.13 (3H, s, H-10′), 3.55 (3H, s, OCH_3), 7.64 (2H, m, aromatic H), 7.37 (3H, m, aromatic H).

*Compound **4a**:* colorless oil; ^{1}H NMR data ($CDCl_3$, 500 MHz) δ_H 6.35 (1H, d, *J* = 9.5 Hz, H-3), 7.59 (1H, d, *J* = 9.5 Hz, H-4), 6.65 (1H, s, H-5), 3.85 (3H, s, OCH_3-6), 4.00 (3H, s, OCH_3-8), 4.28 (1H, dd, *J* = 10.5, 3.0 Hz, H-1′a), 4.26 (1H, dd, *J* = 10.5, 8.0 Hz, H-1′b), 5.23 (1H, dd, *J* = 8.0, 3.0 Hz, H-2′), 2.48 (1H, m, H-3′), 4.54 (1H, m, H-4′), 4.70 (1H, dd, *J* = 15.0, 8.0 Hz, H-5′), 5.26 (1H, d, *J* = 8.0, H-6′), 1.87 (3H, s, H-8′), 1.64 (3H, s, H-9′), 1.72 (3H, s, H-10′), 3.57 (3H, s, OCH_3), 7.55 (2H, m, aromatic H), 7.43 (3H, m, aromatic H).

*Compound **4b**:* colorless oil; ^{1}H NMR data ($CDCl_3$, 500 MHz) δ_H 6.35 (1H, d, *J* = 9.5 Hz, H-3), 7.60 (1H, d, *J* = 9.5 Hz, H-4), 6.66 (1H, s, H-5), 3.85 (3H, s, OCH_3-6), 4.00 (3H, s, OCH_3-8), 4.30 (1H, dd, *J* = 10.5, 3.0 Hz, H-1′a), 4.28 (1H, dd, *J* = 10.5, 8.0 Hz, H-1′b), 5.23 (1H, dd, *J* = 8.0, 3.0 Hz, H-2′), 2.46 (1H, m, H-3′), 4.50 (1H, m, H-4′), 4.62 (1H, dd, *J* = 15.0, 8.0 Hz, H-5′), 5.21 (1H, d, *J* = 8.0, H-6′), 1.86 (3H, s, H-8′), 1.61 (3H, s, H-9′), 1.70 (3H, s, H-10′), 3.57 (3H, s, OCH_3), 7.55 (2H, m, aromatic H), 7.43 (3H, m, aromatic H).

*Compound **6a**:* colorless oil; ^{1}H NMR data ($CDCl_3$, 500 MHz) δ_H 6.37 (1H, d, *J* = 9.5 Hz, H-3), 7.63 (1H, d, *J* = 9.5 Hz, H-4), 6.70 (1H, s, H-5), 3.85 (3H, s, OCH_3-6), 4.00 (3H, s, OCH_3-8), 4.52 (1H, dd, *J* = 10.5, 2.0 Hz, H-1′a), 3.91 (1H, dd, *J* = 10.5, 8.0 Hz, H-1′b), 3.88 (1H, dd, *J* = 8.0, 2.0 Hz, H-2′), 1.85 (1H, m, H-4′a), 1.69 (1H, m, H-4′b), 2.22 (1H, m, H-5′a), 1.92 (1H, m, H-5′b), 4.03 (1H, m, H-6′), 1.23 (3H, s, H-8′), 1.22 (3H, s, H-9′), 1.11 (3H, s, H-10′), 3.60 (3H, s, OCH_3), 7.66 (2H, m, aromatic H), 7.34 (3H, m,

aromatic H).

*Compound **6b**:* colorless oil; ^{1}H NMR data ($CDCl_3$, 500 MHz) δ_H 6.37 (1H, d, J = 9.5 Hz, H-3), 7.62 (1H, d, J = 9.5 Hz, H-4), 6.69 (1H, s, H-5), 3.82 (3H, s, OCH_3-6), 4.00 (3H, s, OCH_3-8), 4.49 (1H, dd, J = 10.5, 2.0 Hz, H-1′a), 3.87 (1H, dd, J = 10.5, 8.0 Hz, H-1′b), 3.85 (1H, dd, J = 8.0, 2.0 Hz, H-2′), 1.76 (1H, m, H-4′a), 1.65 (1H, m, H-4′b), 2.16 (1H, m, H-5′a), 1.89 (1H, m, H-5′b), 4.03 (1H, m, H-6′), 1.26 (3H, s, H-8′), 1.20 (3H, s, H-9′), 1.18 (3H, s, H-10′), 3.54 (3H, s, OCH_3), 7.63 (2H, m, aromatic H), 7.33 (3H, m, aromatic H).

*Compound **8a**:* colorless oil; ^{1}H NMR data ($CDCl_3$, 500 MHz) δ_H 6.37 (1H, d, J = 9.5 Hz, H-3), 7.62 (1H, d, J = 9.5 Hz, H-4), 6.69 (1H, s, H-5), 3.88 (3H, s, OCH_3-6), 4.03 (3H, s, OCH_3-8), 4.80 (1H, dd, J = 10.5, 2.0 Hz, H-1′a), 3.98 (1H, dd, J = 10.5, 9.0 Hz, H-1′b), 3.86 (1H, dd, J = 9.0, 2.0 Hz, H-2′), 2.33 (1H, m, H-4′a), 1.86 (1H, m, H-4′b), 2.22 (1H, m, H-5′a), 1.70 (1H, m, H-5′b), 4.54 (1H, m, H-6′), 5.02 (1H, s, H-8′a), 4.82 (1H, s, H-8′b), 1.25 (3H, s, H-9′), 1.60 (3H, s, H-10′), 3.64 (3H, s, OCH_3), 7.68 (2H, m, aromatic H), 7.33 (3H, m, aromatic H).

*Compound **8b**:* colorless oil; ^{1}H NMR data ($CDCl_3$, 500 MHz) δ_H 6.36 (1H, d, J = 9.5 Hz, H-3), 7.62 (1H, d, J = 9.5 Hz, H-4), 6.66 (1H, s, H-5), 3.85 (3H, s, OCH_3-6), 4.02 (3H, s, OCH_3-8), 4.68 (1H, dd, J = 10.5, 2.0 Hz, H-1′a), 3.90 (1H, dd, J = 10.5, 9.0 Hz, H-1′b), 3.82 (1H, dd, J = 8.0, 2.0 Hz, H-2′), 2.29 (1H, m, H-4′a), 1.74 (1H, m, H-4′b), 2.15 (1H, m, H-5′a), 1.66 (1H, m, H-5′b), 4.53 (1H, m, H-6′), 5.08 (1H, s, H-8′a), 4.89 (1H, s, H-8′b), 1.24 (3H, s, H-9′), 1.69 (3H, s, H-10′), 3.59 (3H, s, OCH_3), 7.66 (2H, m, aromatic H), 7.35 (3H, m, aromatic H).

Fig. 6. $\Delta\delta_{SR}$ values (in ppm) for the MTPA esters of **1**, **3**, **4**, **6** and **8**

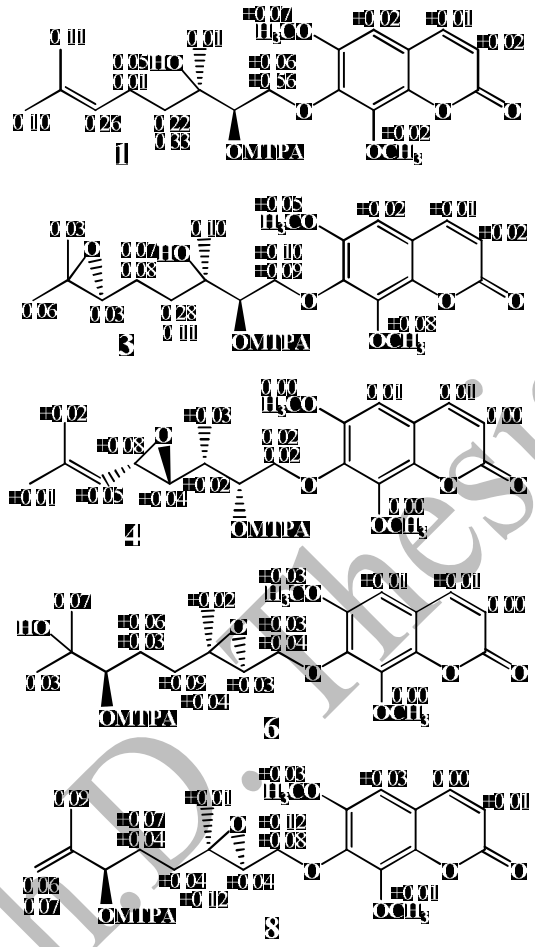

Fig. 7. Chemical structures of known compounds isolated from *A. altissima*

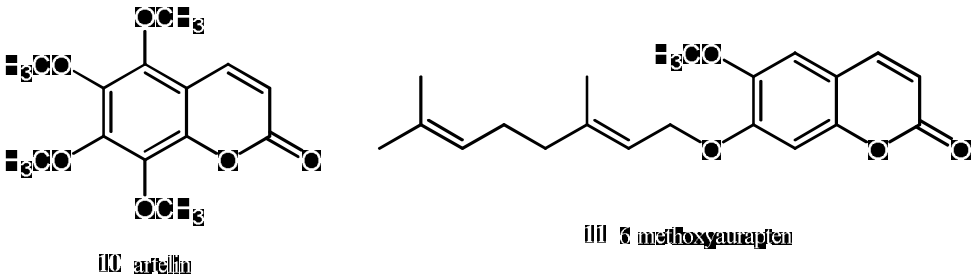

1.4. Structural determination of new compounds isolated from *A. altissima*

In order to isolate the compounds with stimulating SIRT1 activity, the methanol extract of *A. altissima* was subjected to a succession of chromatographic procedures including silica gel chromatography, Shephadex LH-20, RP-C18, and HPLC to afford eleven compounds, including 9 new (**1–9**) and 2 known (**10–11**) coumarin derivatives (Hwang *et al*., 2005; Ito *et al*., 1990) (**Fig. 7**).

1.4.1. Structural determination of compound 1

Compound **1** was obtained as a colorless oil. Its molecular formula of $C_{21}H_{28}O_7$ was established by HREIMS, *m/z* 392.1837 $[M]^+$ (calcd for $C_{21}H_{28}O_7$, 392.1835). Strong UV peaks at λ_{max} 225, 293, and 335 nm, and an IR band at ν_{max} 1727 cm^{-1} suggested a 7-oxygenated coumarin skeleton (Hwang *et al*., 2005). In the ^1H NMR spectrum (**Table 1**), the apparent characteristic signals of a 6,7,8-trisubstituted coumarin, with doublets at δ_H 7.62 (1H, d, J = 9.5 Hz, H-4) and 6.36 (1H, d, J = 9.5 Hz, H-3), a singlet at δ_H 6.69 (1H, s, H-5), and two methoxy signals at δ_H 4.06 (3H, s, OCH_3-8) and 3.90 (3H, s, OCH_3-6) were observed. The positions of the methoxy groups were inferred as C-6 and C-8 by the HMBC correlations from the methoxy protons to C-6 (δ_C 149.7) and C-8 (δ_C 141.0), respectively (**Fig. 8**), and a diagnostic fragment peak at *m/z* 222 ($[M–170]^+$) in the EIMS (Hwang *et al*., 2005; Banthorpe & Brown, 1989). In addition, its ^1H NMR spectrum showed eight other signals due to three methyls [δ_H 1.67 (3H, s, H-8′), 1.61 (3H, s, H-10′) and 1.22 (3H, s, H-9′)], two methylenes [δ_H 2.13 (1H, m, H-5′a), 2.05 (1H, m, H-5′b), and 1.62 (1H, m, H-4′a), 1.40 (1H, m, H-4′b)], an oxymethine [δ_H 3.70 (1H, dd, J = 8.0, 2.0 Hz, H-2′)], an oxymethylene [δ_H 4.55 (1H, dd, J = 10.5, 2.0 Hz, H-1′a), 4.02 (1H, dd, J = 10.5, 8.0 Hz, H-1′b)], and an olefinic proton [δ_H 5.11 (1H, t, J = 7.0 Hz, H-6′)]. On the basis of

the observed HMQC correlations, these signals correspond to the ^{13}C NMR signals for an oxygenated C_{10} terpenyl side-chain [$-OCH_2CHOHC(CH_3)OHCH_2CH_2CH=C(CH_3)_2$] (Hwang *et al*., 2005; Ito *et al*., 2005). This terpenyl group was attached to the C-7 position because the H-1′ proton at δ_H 4.02 displayed HMBC connectivity with C-7 (δ_C 144.6). Furthermore, the HMBC correlations between oxymethylene at H-1′/C-2′, C-3′, and between H-9′/C-2′, C-3′, and C-4′ indicated that two hydroxy groups are attached at C-2′ and C-3′, respectively. The planar structure of **1** was confirmed by additional HMBC correlations of H-4′/C-2′, C-3′, C-5′, C-6′ and C-9′; H-5′/C-3′, C-4′, C-6′ and C-7′; H-6′/C-4′, C-7′, C-8′ and C-10′; and H-8′/C-6′, C-7′ and C-10′. The *syn* relative configuration of the 2′,3′-diol of compound **1** was determined by 2D-NOESY experiments, which showed a strong NOE cross peak between H-2′ and H-9′ (**Fig. 8**) (Hwang *et al*., 2005; Xin *et al*., 2008). Assignment of the absolute configuration of the 2′,3′-diol of **1** was also confirmed by the Mosher ester method (Phoopichayanun *et al*., 2008; Seco *et al*., 2004). Compound **1** was treated individually with (*R*)- and (*S*)-*α*-methoxy-*α*-(trifluoromethyl)phenylacetyl chloride (MTPA-Cl) in dry pyridine to yield the (*S*)- or (*R*)- MTPA ester derivatives **1a** and **1b**, respectively. Analysis of the ^1H NMR chemical shift differences ($\Delta\delta_{S-R}$) (**Fig. 6**) of these derivatives allowed the assignment of the absolute configuration of C-2′ of **1** as *R*. The absolute configuration of C-3′ was thus assigned as *R*. Therefore, compound **1**, named altissimacoumarin C, was assigned as (2′*R*,3′*R*)-7-(2′,3′-dihydroxy-3′,7′-dimethylocta-6′-enyloxy)-6,8-dimethoxycoumarin.

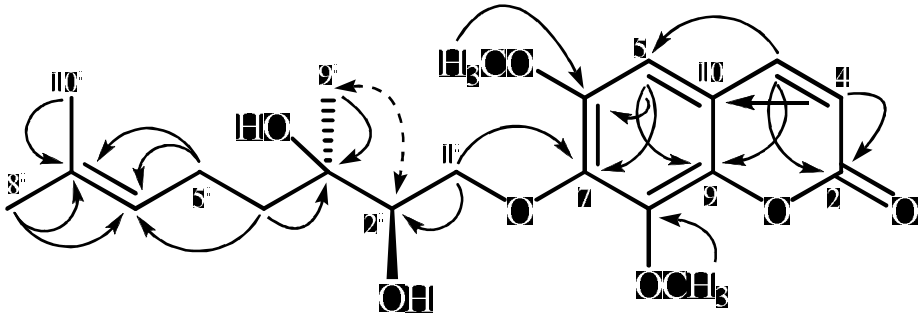

Fig. 8. Key HMBC (H→C) and NOSEY (**↔**) correlations of altissimacoumarin C (**1**)

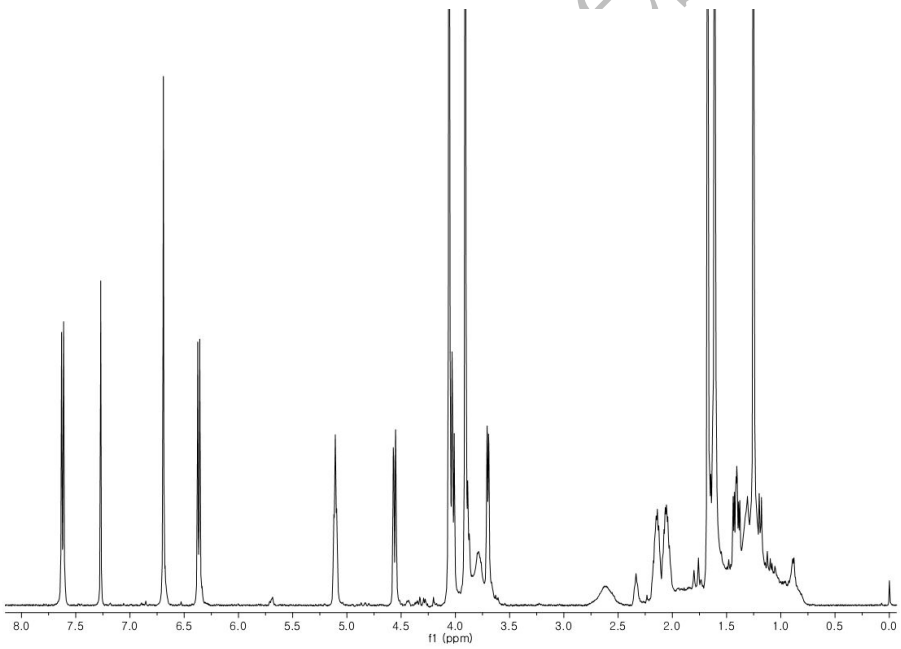

Fig. 9. ^{1}H-NMR spectrum of altissimacoumarin C (**1**)

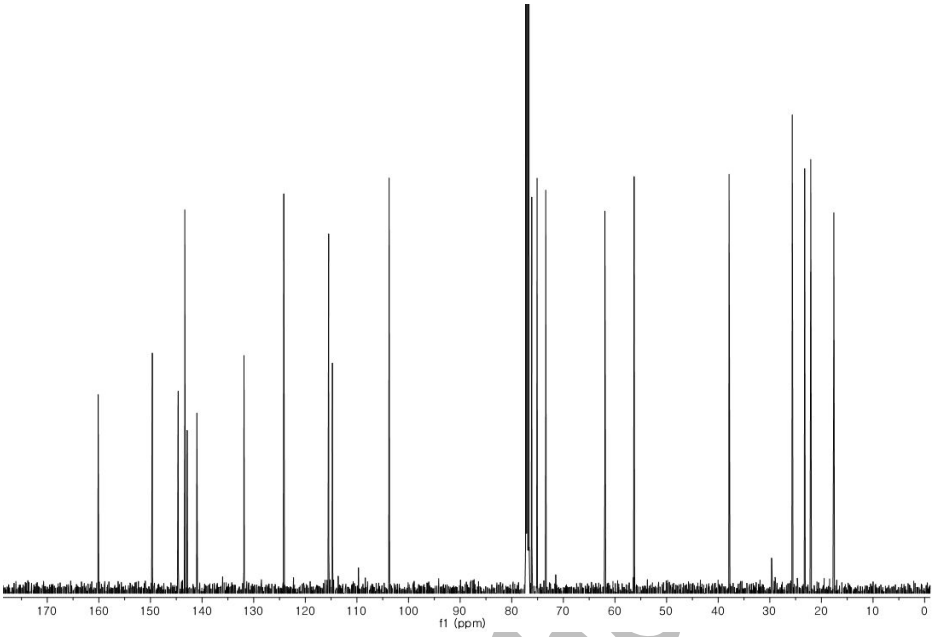

Fig. 10. ^{13}C-NMR spectrum of altissimacoumarin C (**1**)

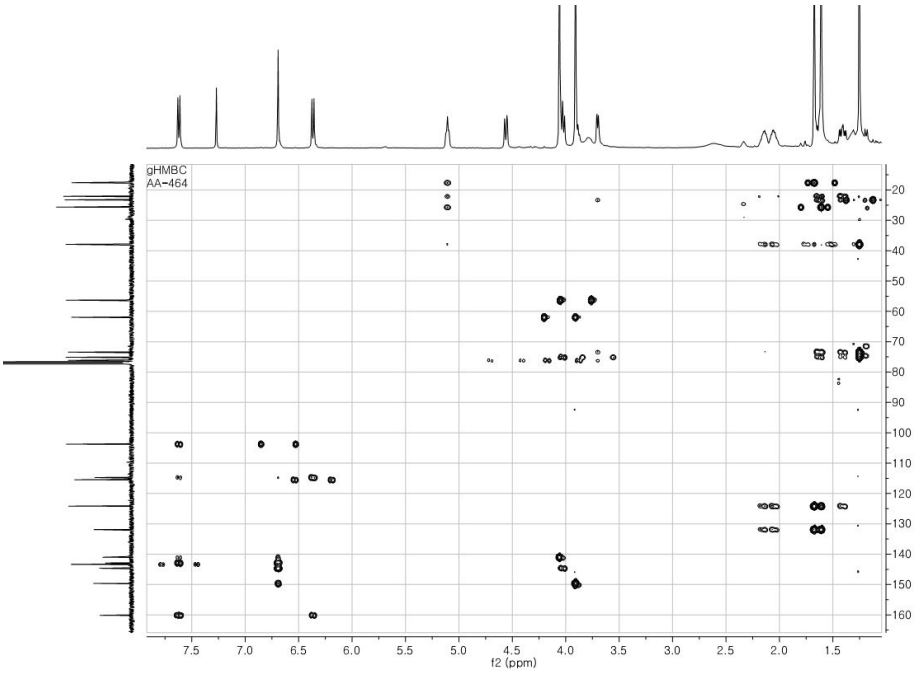

Fig. 11. HMBC spectrum of altissimacoumarin C (**1**)

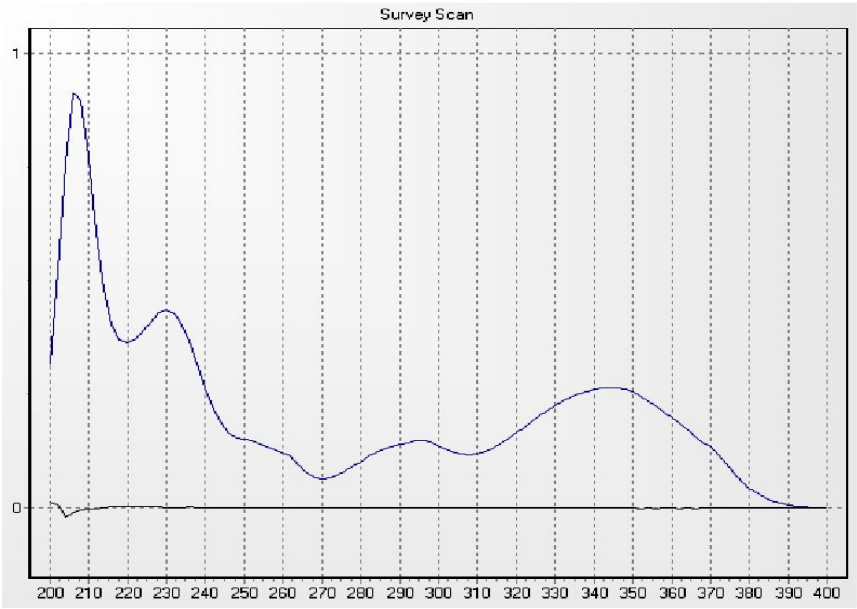

Fig. 12. UV spectrum of altissimacoumarin C (**1**)

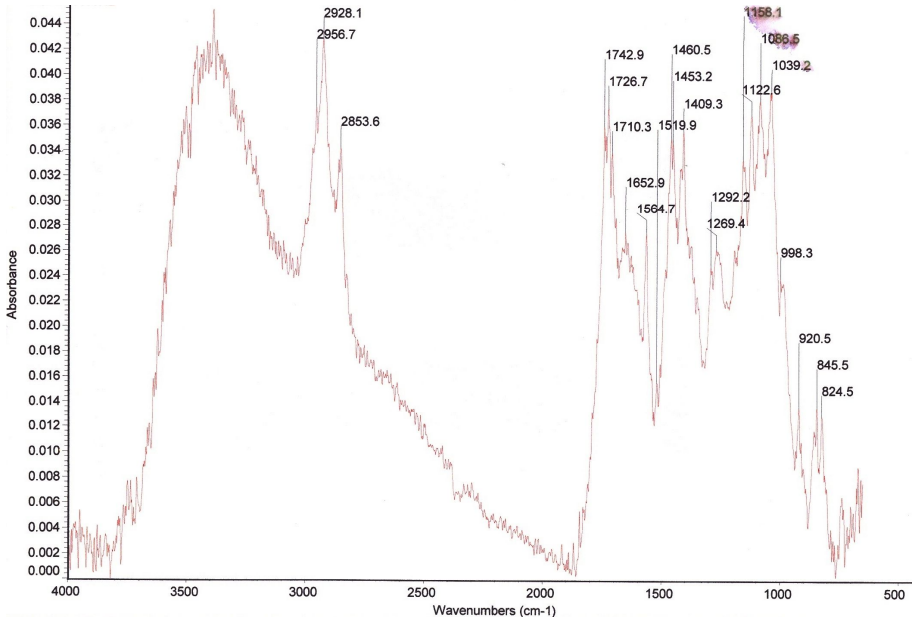

Fig. 13. IR spectrum of altissimacoumarin C (**1**)

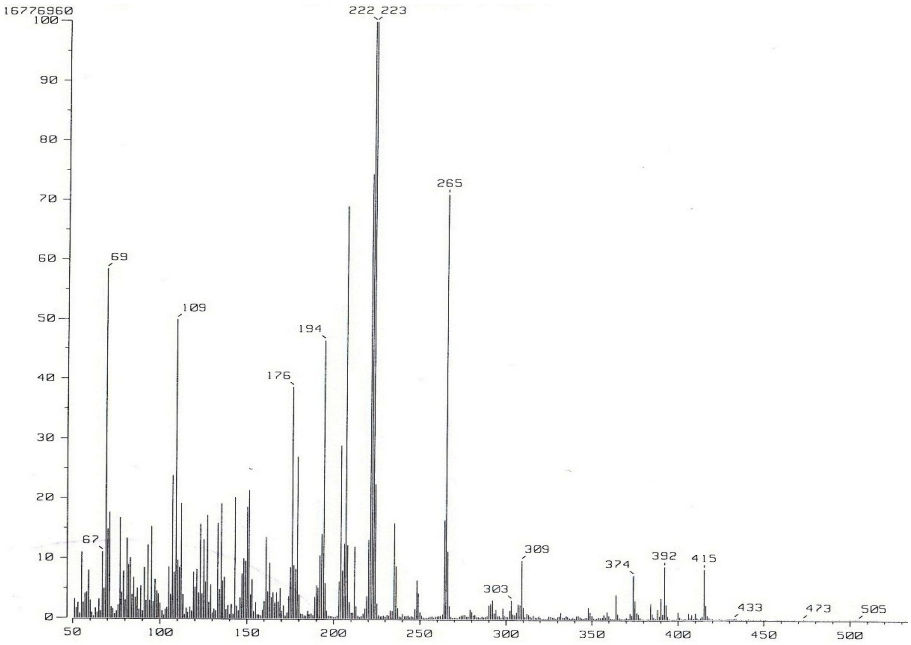

Fig. 14. EIMS spectrum of altissimacoumarin C (**1**)

Table 1. ^{1}H and ^{13}C-NMR data of altissimacoumarin C (**1**)[a] (in $CDCl_3$)

Position	δ_H mult. (*J* in Hz)	δ_C	HMBC (H→C)
2		160.2	
3	6.36 d (9.5)	115.5	C-2, C-4, C-10
4	7.62 d (9.5)	143.4	C-2, C-3, C-5, C-9, C-10
5	6.69 s	103.8	C-4, C-6, C-7, C-9, C-10
6		149.7	
7		144.6	
8		141.0	
9		142.9	
10		114.8	
1′	4.55 dd (10.5, 2.0)	76.1	C-7, C-2′, C-3′
	4.02 dd (10.5, 8.0)		C-7, C-2′, C-3′
2′	3.70 dd (8.0, 2.0)	75.1	C-1′, C-3′, C-4′, C-9′
3′		73.4	
4′	1.62 m	37.9	C-2′, C-3′, C-5′, C-6′, C-9′
	1.40 m		C-3′, C-5′, C-6′, C-9′
5′	2.13 m	22.1	C-3′, C-4′, C-7′
	2.05 m		C-3′, C-4′, C-6′, C-7′
6′	5.11 t (7.0)	124.2	C-4′, C-7′, C-8′, C-10′
7′		131.9	
8′	1.67 s	25.6	C-6′, C-7′, C-10′
9′	1.22 s	23.2	C-2′, C-3′, C-4′
10′	1.61 s	17.6	C-6′, C-7′, C-8′
OCH_3-6	3.90 s	56.3	C-6
OCH_3-8	4.06 s	61.9	C-8

[a] Assignments were based on HSQC, HMBC experiments.

1.4.2. Structural determination of compound 2

Compound **2** was obtained as a colorless oil. The presence of 6,8-dimethoxy-7-substituted coumarin was indicated from the UV absorptions at λ_{max} 230, 295 and 340 nm, an IR band at ν_{max} 1716 cm^{-1}, the typical AB-type signals at δ_H 7.61 (1H, d, J = 10.0 Hz, H-4), 6.34 (1H, d, J = 10.0 Hz, H-3), a singlet at δ_H 6.66 (1H, s, H-5), and two methoxy signals at δ_H 4.03 (3H, s, OCH_3-8) and 3.89 (3H, s, OCH_3-6) in the ^1H NMR spectrum (Hwang *et al.*, 2005). In addition, the ^1H and ^{13}C NMR spectra (**Table 2**) revealed signals for a geranyl group [δ_H 4.68 (2H, d, J = 7.0 Hz, H-1′), 5.56 (1H, t, J = 7.0 Hz, H-2′), 2.05 (2H, m, H-4′), 2.08 (2H, m, H-5′), 5.06 (1H, t, J = 6.5 Hz, H-6′), 1.67 (3H, s, H-8′), 1.69 (3H, s, H-9′), 1.59 (3H, s, H-10′); δ_C 70.3, 119.6, 142.5, 39.6, 26.3, 123.8, 131.7, 25.6, 16.4 and 17.6, respectively]. This geranyl group was placed at the C-7 position because the H-1′ proton displayed a HMBC connectivity with C-7 (δ_C 144.9). These NMR data were similar to those of 6-methoxyaurapten, except for an additional methoxy group at C-8 (Talapatra *et al.*, 1973). This was supported further by the molecular ion peak at *m/z* 359.1848 $[M+H]^+$ in the HRFABMS, which indicated a molecular formula of $C_{21}H_{26}O_5$ (calcd for $C_{21}H_{27}O_5$, 359.1858). The location of this methoxy group was established through a HMBC correlation from the methoxy protons to C-8 (δ_C 141.8) (**Fig. 15**). From the above data, the structure of **2**, named altissimacoumarin D, was proposed as 6,8-dimethoxy-7-(3′,7′-dimethylocta-2′,6′-dienyloxy)coumarin.

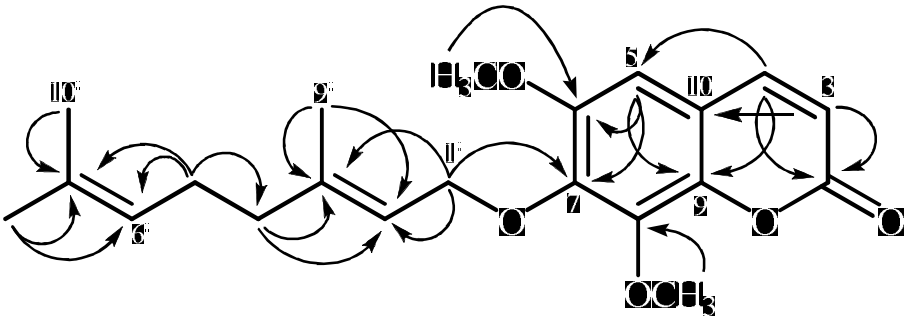

Fig. 15. Key HMBC (H→C) correlation of altissimacoumarin D (**2**)

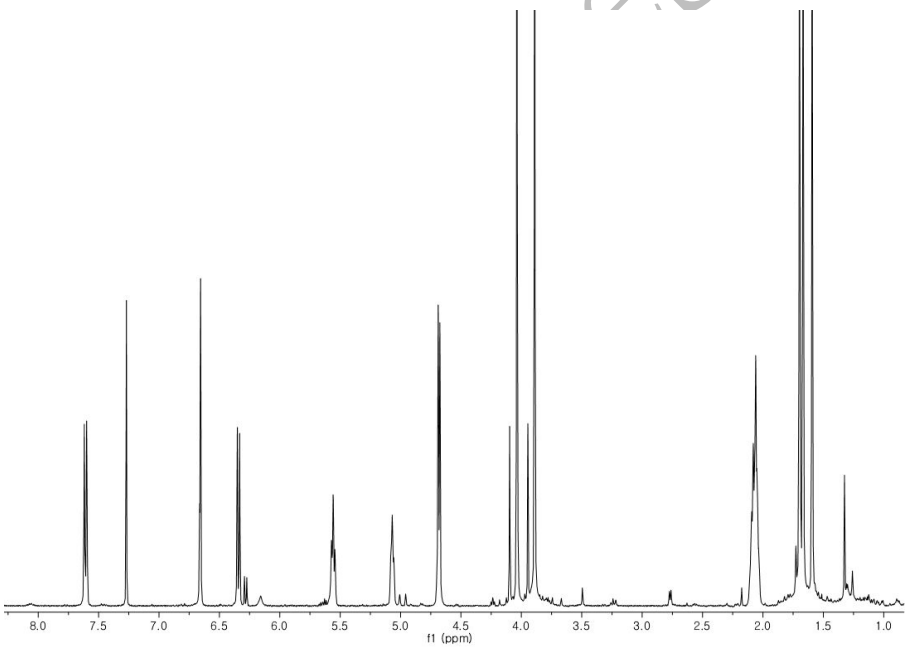

Fig. 16. ^{1}H-NMR spectrum of altissimacoumarin D (**2**)

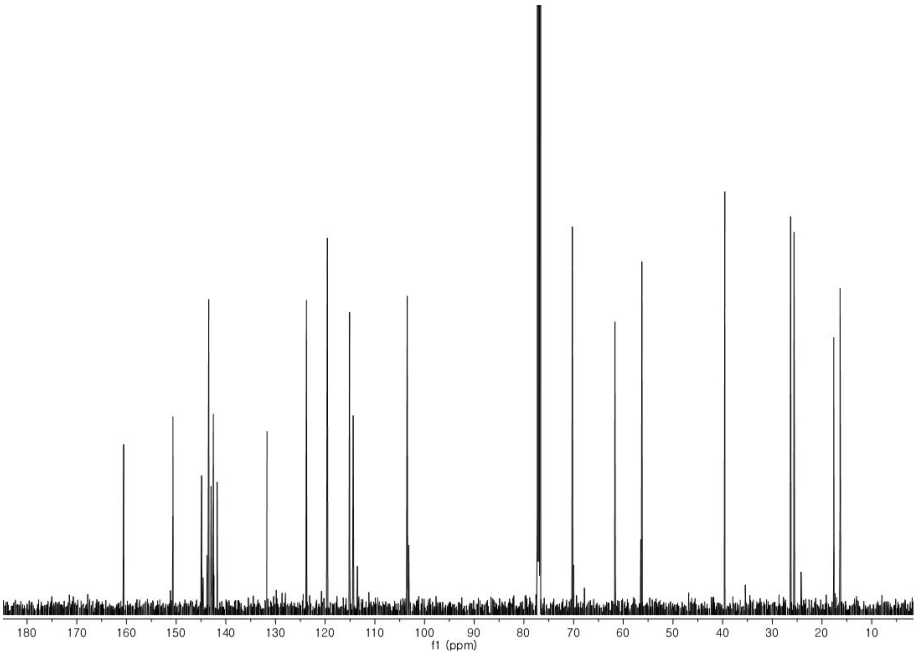

Fig. 17. ^{13}C-NMR spectrum of altissimacoumarin D (**2**)

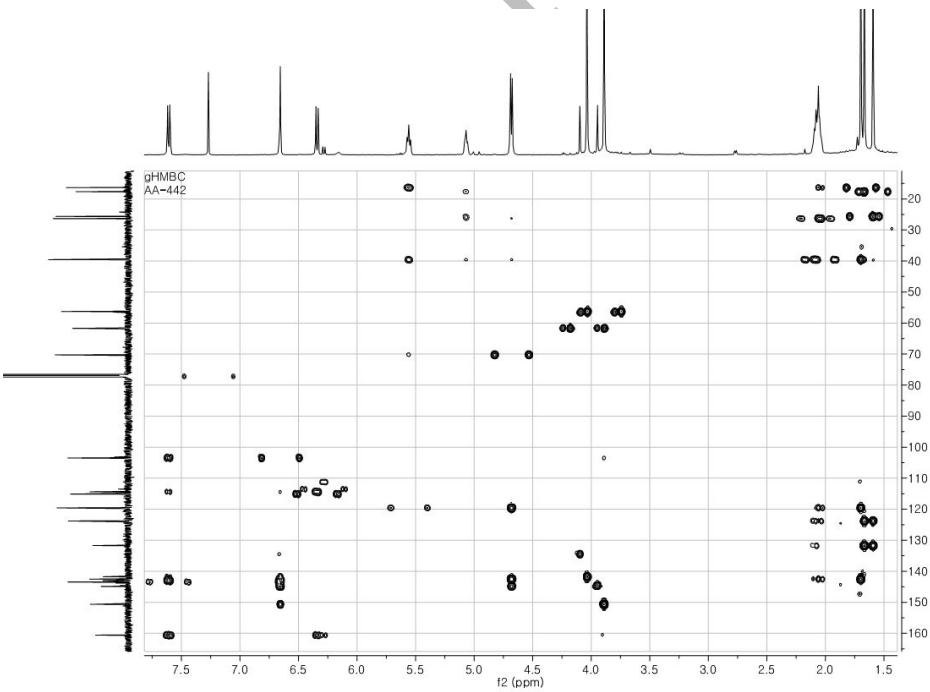

Fig. 18. HMBC spectrum of altissimacoumarin D (**2**)

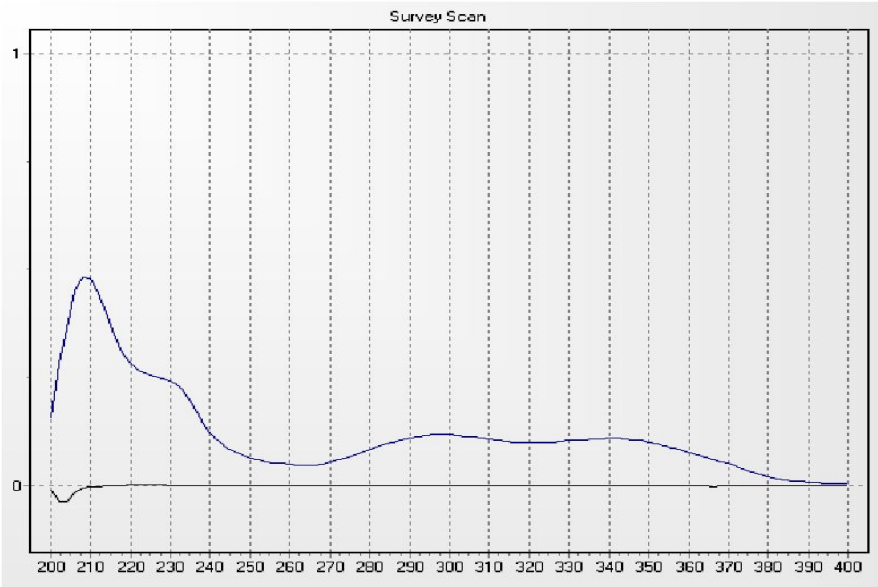

Fig. 19. UV spectrum of altissimacoumarin D (**2**)

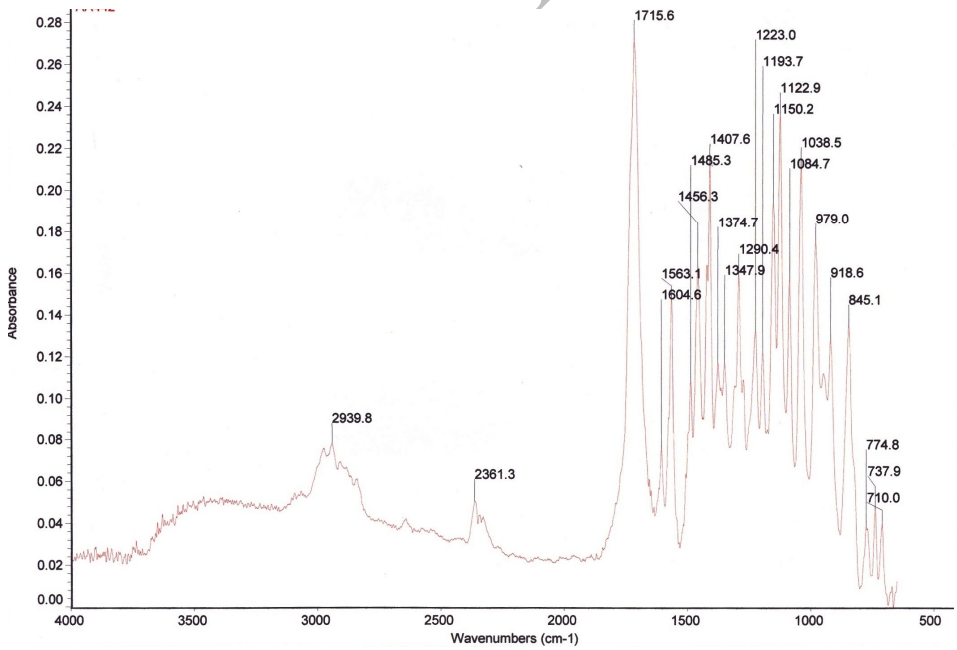

Fig. 20. IR spectrum of altissimacoumarin D (**2**)

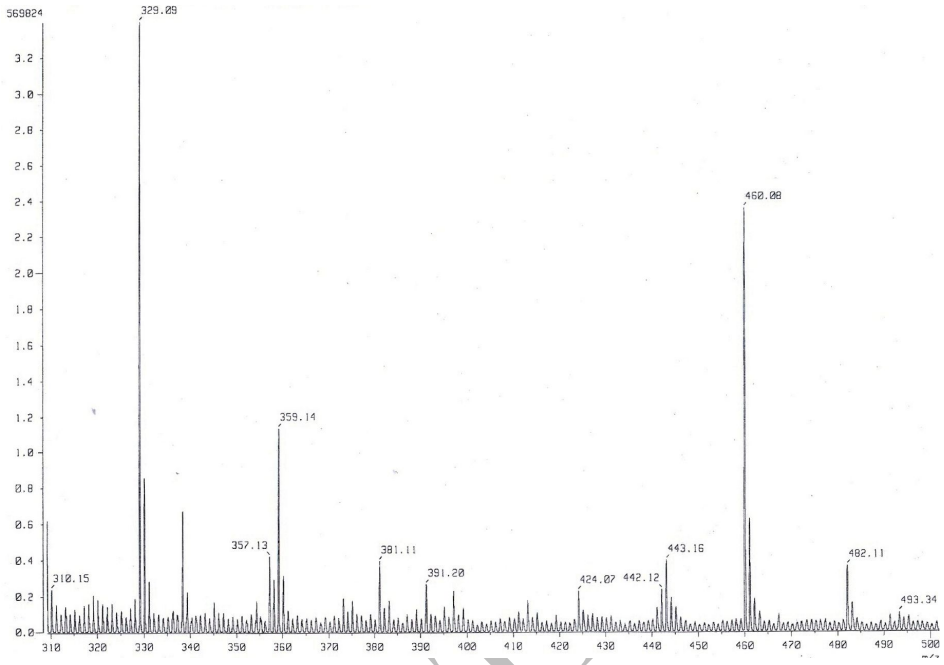

Fig. 21. FABMS spectrum of altissimacoumarin D (**2**)

Table 2. ^{1}H and ^{13}C-NMR data of altissimacoumarin D (**2**)[a] (in $CDCl_3$)

Position	δ_H mult. (*J* in Hz)	δ_C	HMBC (H→C)
2		160.6	
3	6.34 d (10.0)	115.1	C-2, C-4, C-10
4	7.61 d (10.0)	143.5	C-2, C-3, C-5, C-9, C-10
5	6.66 s	103.5	C-4, C-6, C-7, C-9, C-10
6		150.7	
7		144.9	
8		141.8	
9		142.9	
10		114.4	
1′	4.68 d (7.0)	70.3	C-7, C-2′, C-3′
2′	5.56 t (7.0)	119.6	C-1′, C-3′, C-4′
3′		142.5	
4′	2.05 m	39.6	C-2′, C-3′, C-5′, C-9′
5′	2.08 m	26.3	C-4′, C-6′, C-7′
6′	5.06 t (7.0)	123.8	C-5′, C-7′, C-8′
7′		131.7	
8′	1.67 s	25.6	C-6′, C-7′, C-10′
9′	1.69 s	16.4	C-2′, C-3′, C-4′
10′	1.59 s	17.6	C-6′, C-7′, C-8′
OCH_3-6	3.89 s	56.3	C-6
OCH_3-8	4.03 s	61.7	C-8

[a] Assignments were based on HSQC, HMBC experiments.

1.4.3. Structural determination of compound 3

Compound **3** was obtained as a colorless oil with the molecular formula of $C_{21}H_{28}O_8$, which was determined by HREIMS, *m/z* 408.1786 $[M]^+$ (calcd for $C_{21}H_{28}O_8$, 408.1784). The UV and IR spectra of **3** were similar to those of **1**. The ^{1}H and ^{13}C NMR spectra data (**Table 3**) suggested features of a 6,8-dimethoxy-7-terpenylated coumarin, which were almost identical to those of **1**, except for some chemical shift differences due to the position of the epoxy group in the terpenoid chain. Extensive NMR experiments (HMQC, HMBC and NOESY) indicated the epoxy ring at C-6′, C-7′, and two hydroxy groups at C-2′ and C-3′. These assignments were deduced from the HMBC correlations between H-1′/C-2′ and C-3′; H-2′/C-1′, C-3′, C-4′ and C-9′; H-5′/C-3′, C-4′, C-6′ and C-7′; H-6′/C-4′, C-7′, C-8′ and C-10′; and OH-2′/C-2′ (**Fig. 22**). The relative configuration of **3** was then established on the basis of the specific rotation ($[\alpha]_D^{25}$ +13) and NOESY data, which showed NOE correlations between H-2′/H-9′ and H-5′/H-6′, whereas no NOE was observed between H-5′/H-9′ (**Fig. 22**) (Hwang *et al*., 2005; Xin *et al*., 2008). After the reaction with compound **3** and the Mosher ester reagents, (*S*)-MTPA (**3a**) and (*R*)-MTPA (**3b**), respectively, analysis of the ^{1}H NMR data (**Fig. 6**) indicated the *R* configuration at the C-2′ stereocenter in **3**. Thus, the structure of altissimacoumarin E (**3**) was assigned as (2′*R*,3′*R*,6′*R*)-7-(2′,3′-dihydroxy-6′,7′-epoxy-3′,7′-dimethyloctaoxy)-6,8-dimethoxycoumarin.

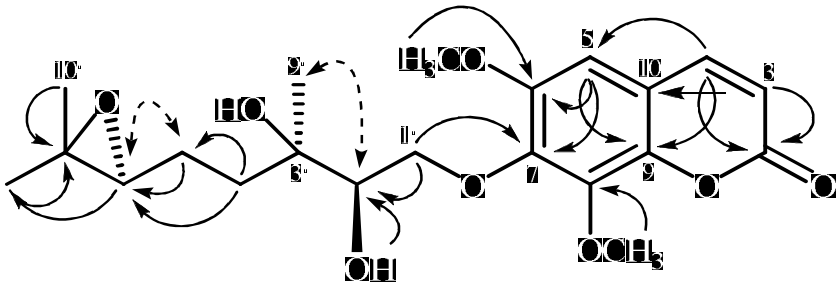

Fig. 22. Key HMBC (H→C) and NOSEY (**↔**) correlations of altissimacoumarin E (**3**)

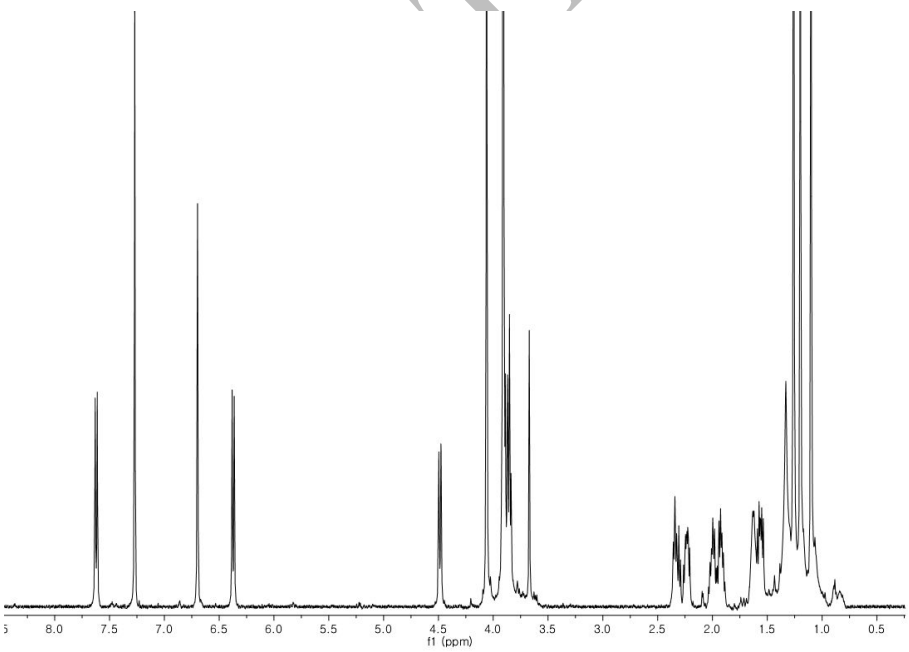

Fig. 23. ^{1}H-NMR spectrum of altissimacoumarin E (**3**)

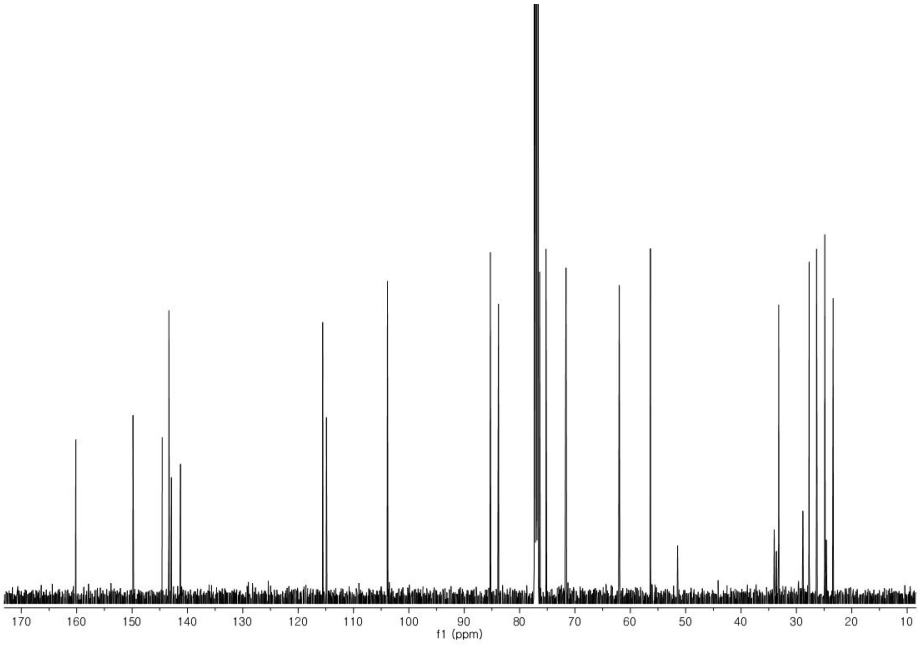

Fig. 24. ^{13}C-NMR spectrum of altissimacoumarin E (**3**)

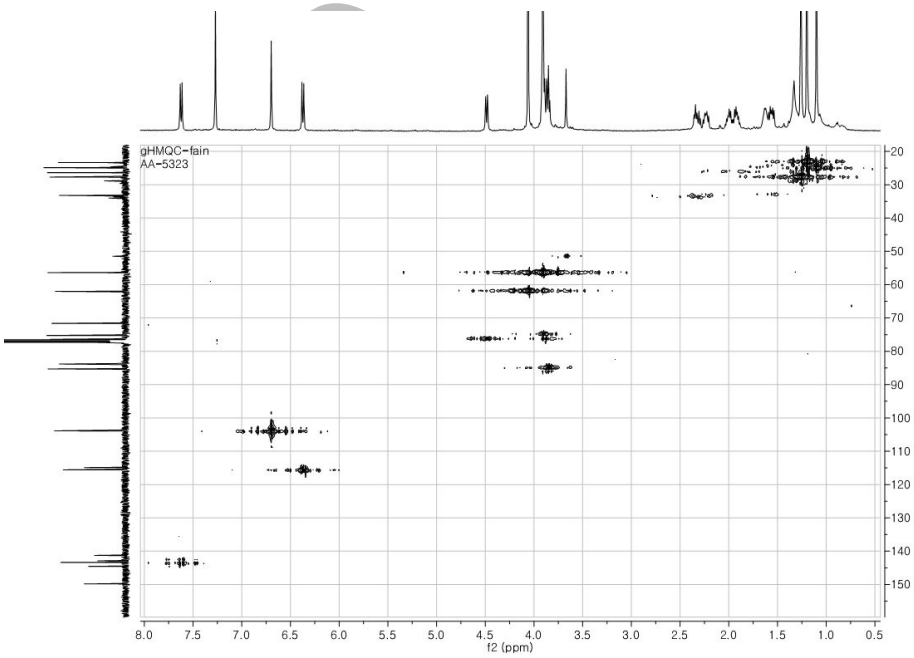

Fig. 25. HSQC spectrum of altissimacoumarin E (**3**)

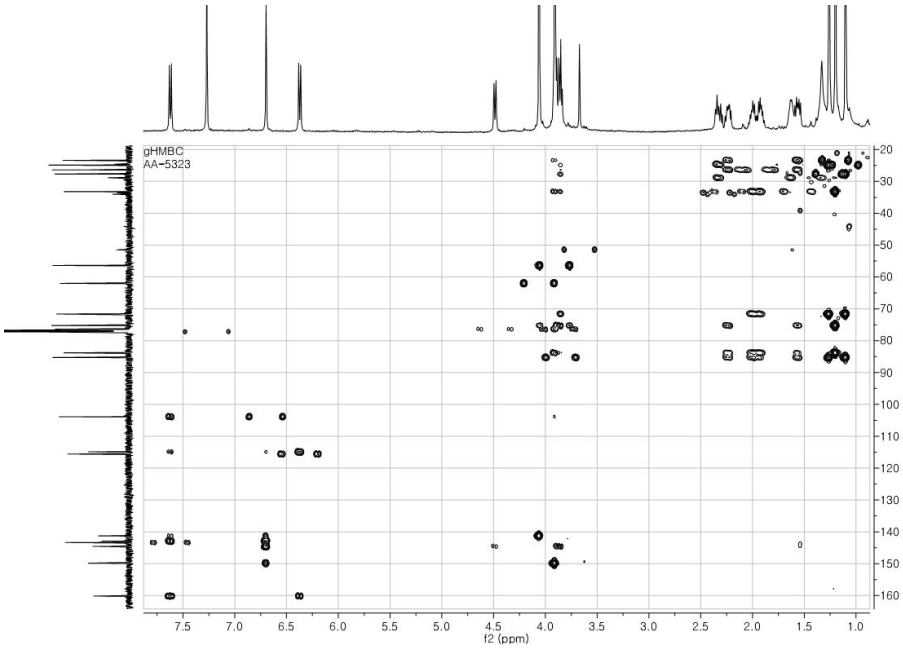

Fig. 26. HMBC spectrum of altissimacoumarin E (**3**)

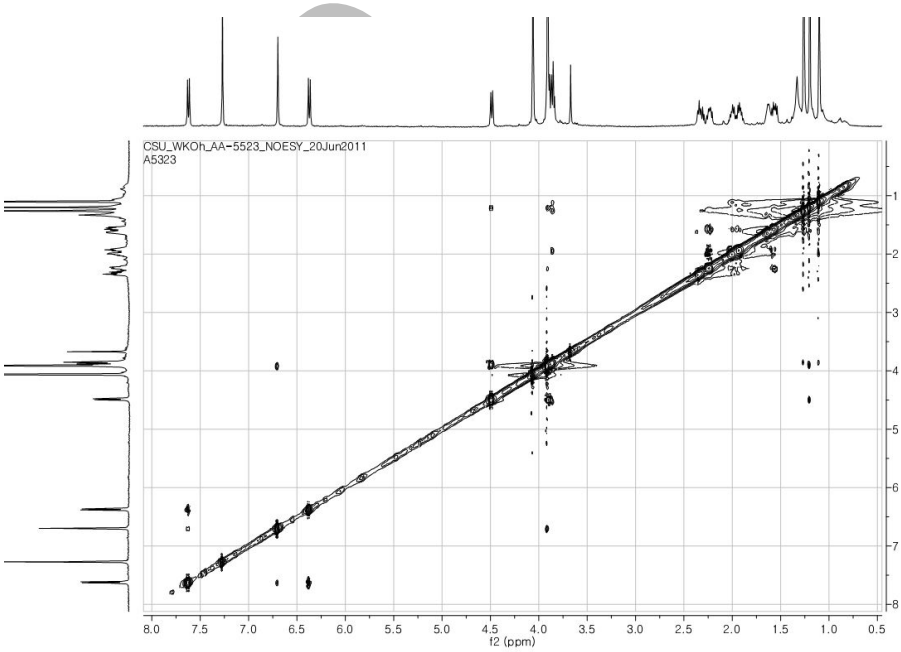

Fig. 27. NOESY spectrum of altissimacoumarin E (**3**)

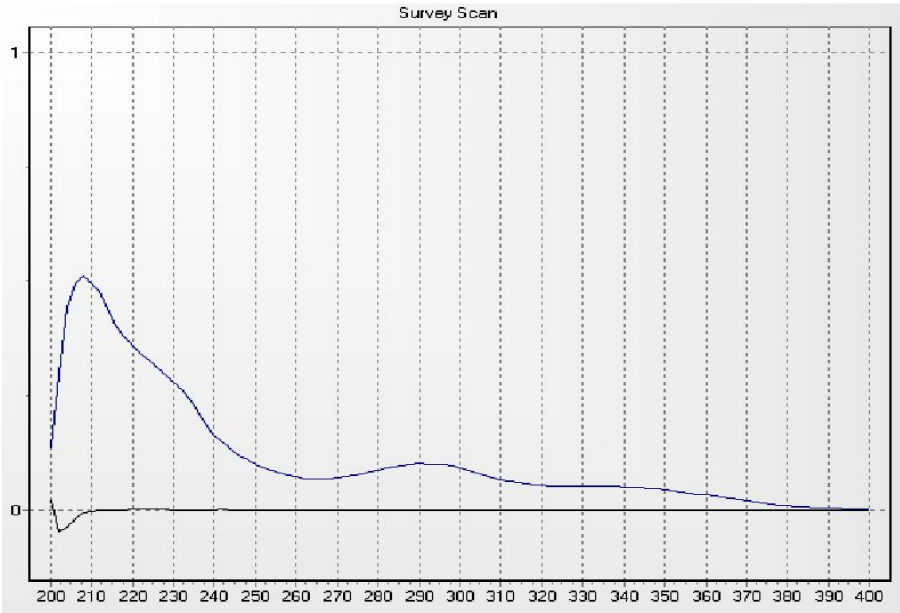

Fig. 28. UV spectrum of altissimacoumarin E (**3**)

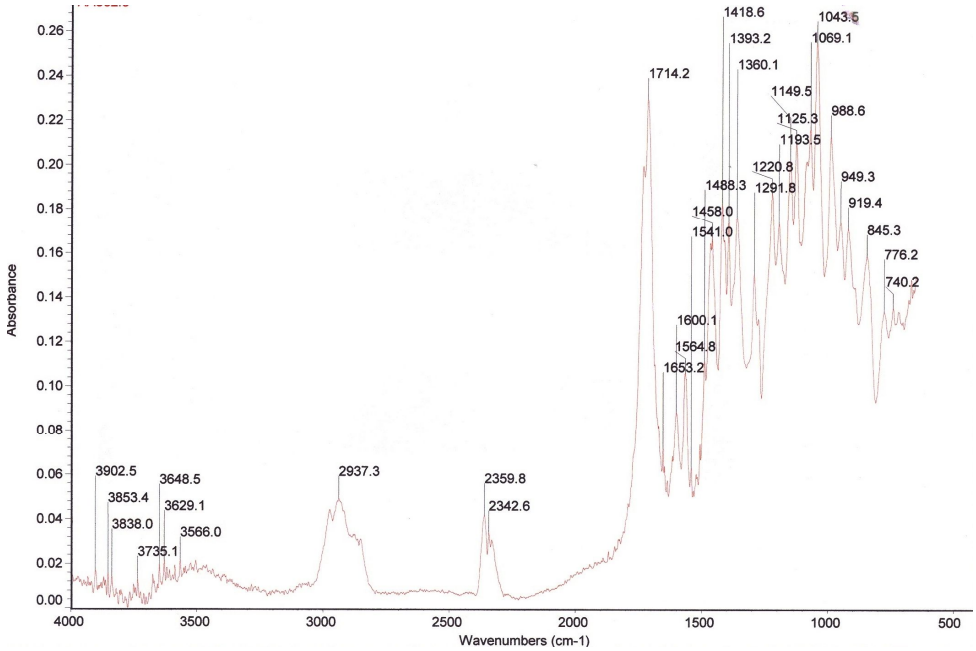

Fig. 29. IR spectrum of altissimacoumarin E (**3**)

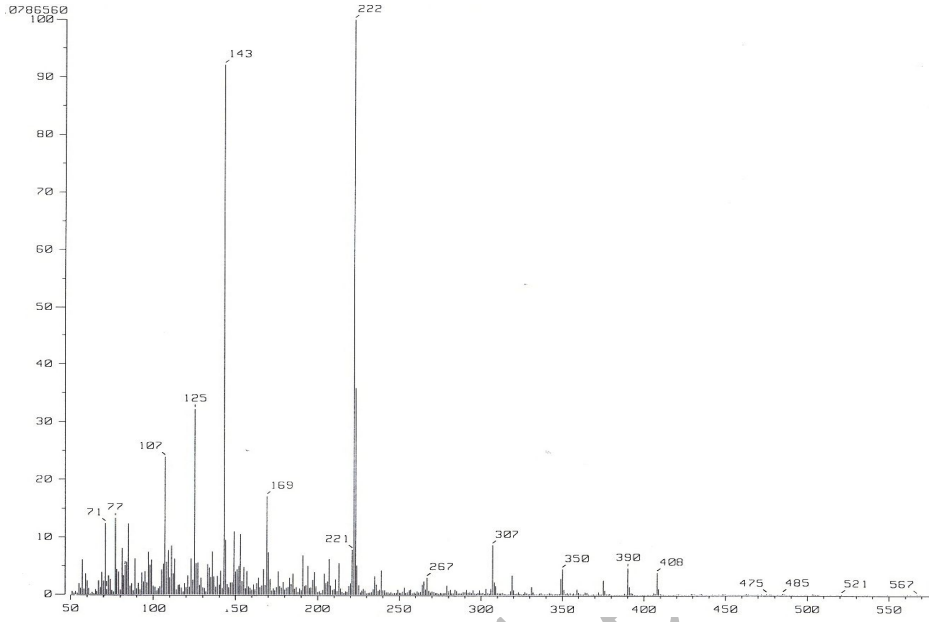

Fig. 30. EIMS spectrum of altissimacoumarin E (**3**)

Table 3. ^{1}H and ^{13}C-NMR data of altissimacoumarin E (**3**)[a] (in $CDCl_3$)

Position	δ_H mult. (*J* in Hz)	δ_C	HMBC (H→C)
2		160.2	
3	6.37 d (9.5)	115.6	C-2, C-4, C-10
4	7.62 d (9.5)	143.4	C-2, C-3, C-5, C-9, C-10
5	6.69 s	103.9	C-4, C-6, C-7, C-9, C-10
6		149.9	
7		144.5	
8		141.2	
9		142.9	
10		114.9	
1′	4.48 dd (10.5, 2.0)	76.4	C-7, C-2′, C-3′
	3.91 dd (10.5, 8.5)		C-7, C-2′, C-3′
2′	3.88 dd (8.5, 2.0)	75.2	C-1′, C-3′, C-4′, C-9′
3′		83.8	
4′	2.23 m	33.2	C-2′, C-3′, C-5′, C-6′, C-9′
	1.55 m		C-3′, C-5′, C-6′, C-9′
5′	1.99 m	26.4	C-3′, C-4′, C-7′
	1.92 m		C-3′, C-4′, C-6′, C-7′
6′	3.85 m	85.3	C-4′, C-7′, C-8′, C-10′
7′		71.6	
8′	1.26 s	27.7	C-6′, C-7′, C-10′
9′	1.19 s	23.4	C-2′, C-3′, C-4′
10′	1.10 s	24.9	C-6′, C-7′, C-8′
OCH_3-6	3.91 s	56.4	C-6
OCH_3-8	4.06 s	62.0	C-8
OH-2′	3.75 s		C-2′

[a] Assignments were based on HSQC, HMBC experiments.

1.4.4. Structural determination of compound 4

Compound **4** was obtained as a colorless oil and its molecular formula, $C_{21}H_{26}O_7$, was established by HREIMS, *m/z* 390.1679 $[M]^+$ (calcd for $C_{21}H_{26}O_7$, 390.1679). The UV and IR absorptions resembled those of **1**–**3**, and the characteristic ^{1}H NMR signals suggested a skeleton of a 6,8-dimethoxy-7-terpenylated coumarin (Hwang *et al.*, 2005). The positions of two methoxy groups were confirmed by the HMBC correlations from the methoxy protons to C-6 (δ_C 149.7) and C-8 (δ_C 141.0), respectively (**Fig. 31**). In addition, analysis of the ^{1}H and ^{13}C NMR spectra, including the HMQC and HMBC data, suggested the presence of a C_{10} terpenyl side-chain at C-7, consisting of three methyl [δ_H 1.72 (3H, s, H-8′), 1.71 (3H, s, H-10′) and 1.47 (3H, s, H-9′)], a methine [δ_H 2.20 (1H, m, H-3′)], three oxymethine [δ_H 4.86 (1H, dd, J = 15.5, 8.5 Hz, H-5′), 4.03 (1H, m, H-4′), 3.99 (1H, dd, J = 8.5, 3.5 Hz, H-2′)], an oxymethylene [δ_H 4.42 (1H, dd, J = 10.0, 3.5 Hz, H-1′a), 4.11 (1H, dd, J = 10.0, 8.0 Hz, H-1′b)], and two olefinic signals [δ_H 5.19 (1H, d, J = 8.5 Hz, H-6′), δ_C 125.3 (C-6′), and δ_C 136.9 (C-7′)]. The observation of mass fragment ions (EIMS) at *m/z* 390 ($[M]^+$), 309 and 222 resulting from cleavage at C-4′/C-5′ and 7-O/C-1′, suggested the presence of an epoxy and a hydroxy group in the terpenoid side-chain. The HMBC correlations of H-2′/C-1′, C-3′ and C-9′; H-3′/C-2′, C-4′ and C-9′; H-4′/C-3′ and C-5′; H-5′/C-3′, C-6′ and C-7′; and H-9′/C-2′, C-3′ and C-4′ confirmed the epoxy ring at C-4′, C-5′, and the hydroxy group at C-2′ position. The *cis* configuration of this epoxy ring was established by the large coupling constant (15.5 Hz) between H-4′ and H-5′, and NOE correlations between H-3′/H-5′, H-4′/H-9′ in the ^{1}H NMR and 2D-NOESY spectra, respectively (**Fig. 31**). Furthermore, the relative configurations of C-2′ and C-3′ in **4** were

deduced from the NOE cross peaks between H-2′/H-3′ and H-1′/H-9′ (**Fig. 31**) (Hwang *et al*., 2005; Xin *et al*., 2008). Finally, the absolute configuration of the stereogenic center at C-2′ was addressed by the Mosher ester method (**Fig. 6**). The *R* configuration of C-2′ in **4** was determined on the interpretation of the data obtained (Phoopichayanun *et al*., 2008; Seco *et al*., 2004). Therefore, the structure of compound **4**, named altissimacoumarin F, was proposed as (2′*R*,3′*R*,4′*S*,5′*S*)-6,8-dimethoxy-7-(3′,7′-dimethyl-4′,5′-epoxy-2′-hydroxyocta-6′-enyloxy)coumarin.

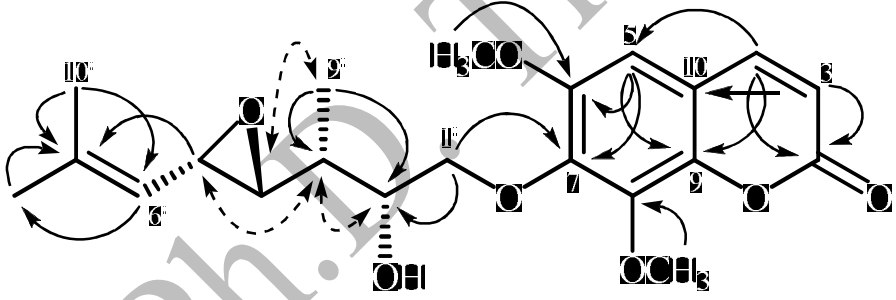

Fig. 31. Key HMBC (H→C) and NOSEY (↔) correlations of altissimacoumarin F (**4**)

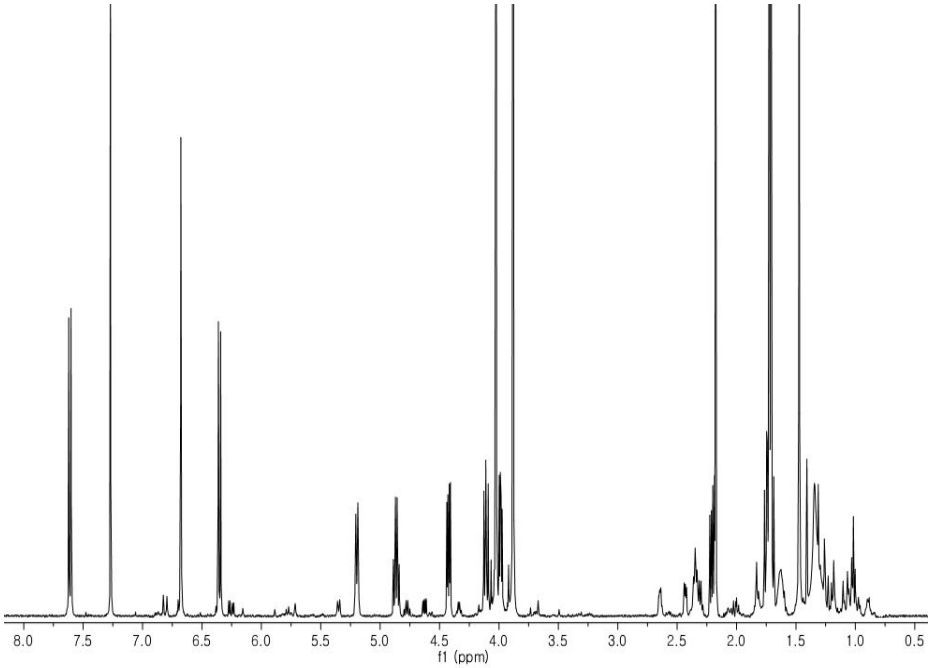

Fig. 32. ^{1}H-NMR spectrum of altissimacoumarin F (**4**)

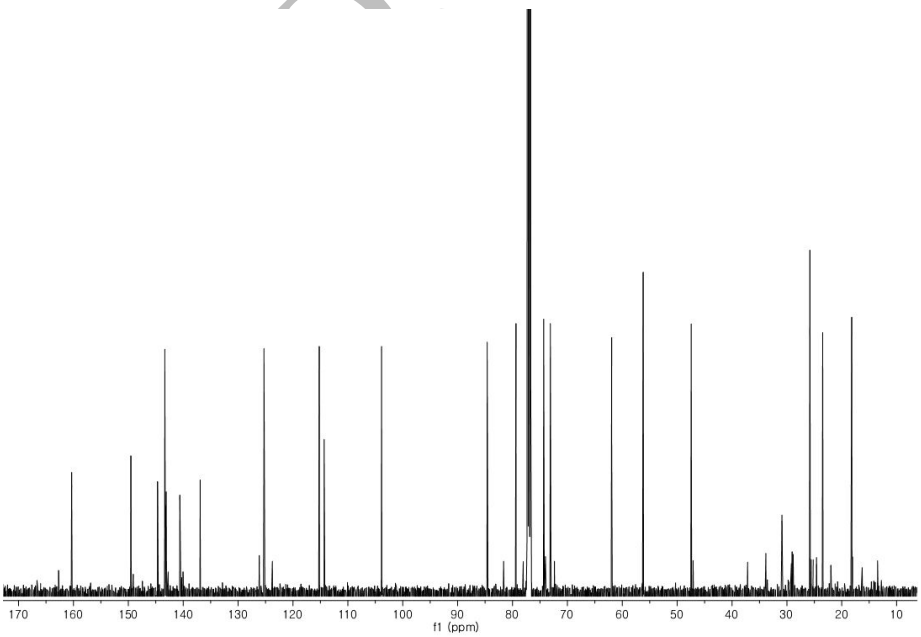

Fig. 33. ^{13}C-NMR spectrum of altissimacoumarin F (**4**)

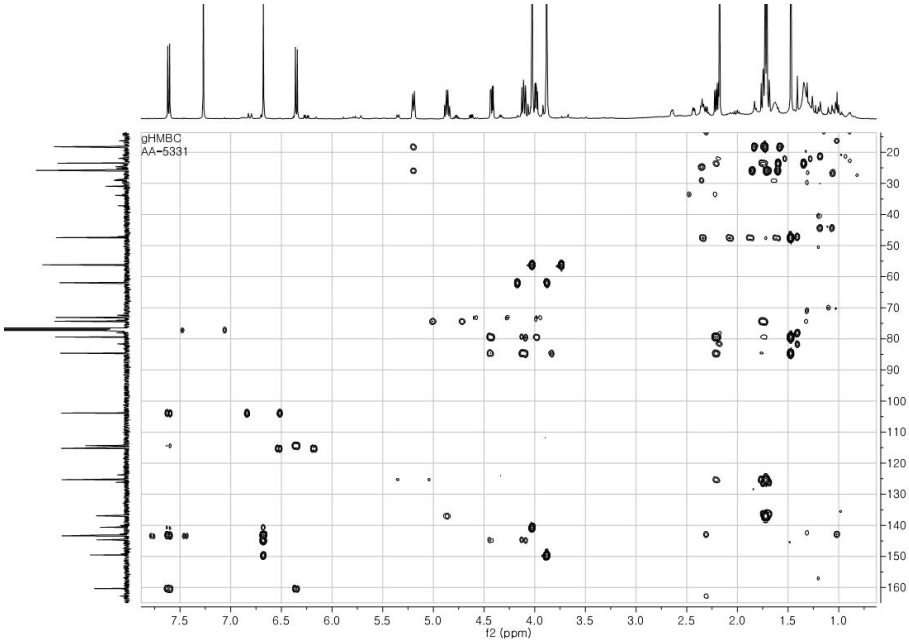

Fig. 34. HMBC spectrum of altissimacoumarin F (**4**)

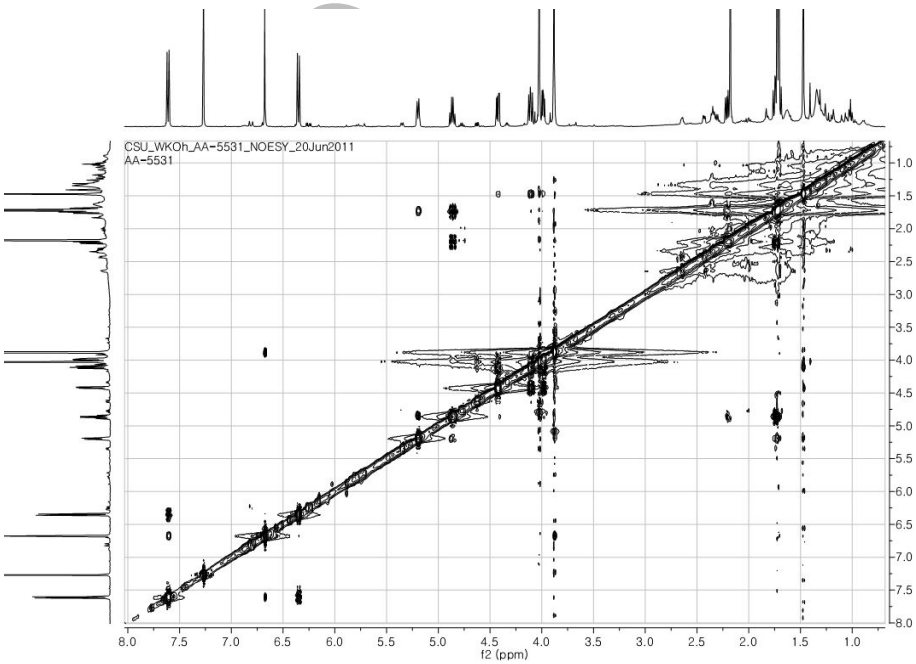

Fig. 35. NOESY spectrum of altissimacoumarin F (**4**)

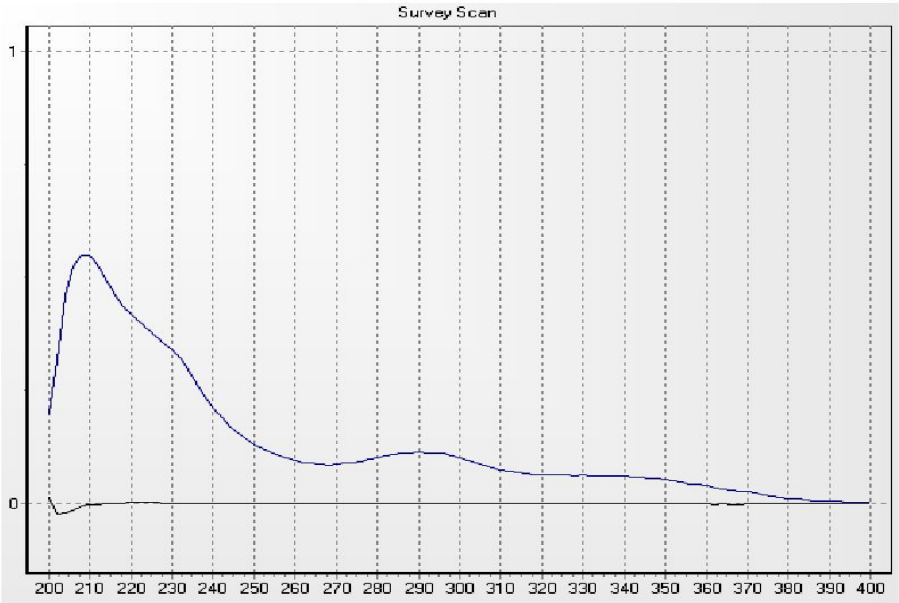

Fig. 36. UV spectrum of altissimacoumarin F (**4**)

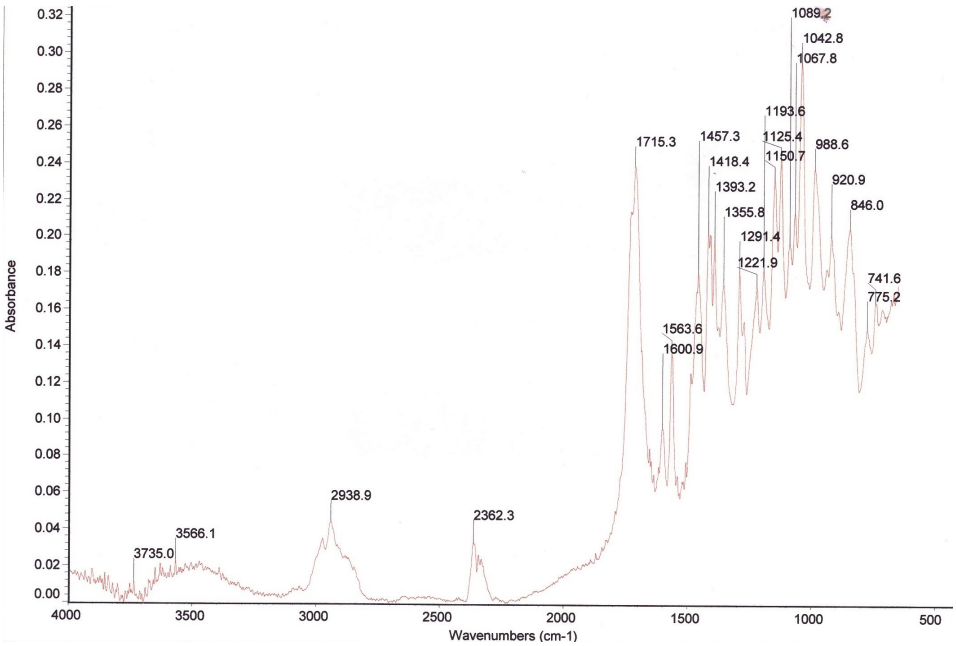

Fig. 37. IR spectrum of altissimacoumarin F (**4**)

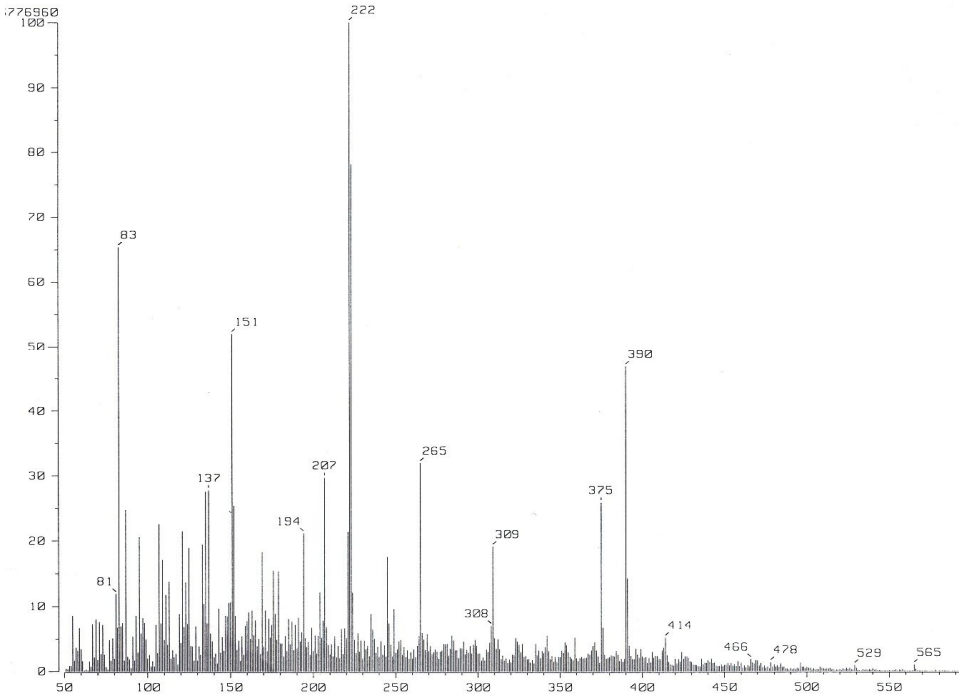

Fig. 38. EIMS spectrum of altissimacoumarin F (**4**)

Table 4. ^{1}H and ^{13}C-NMR data of altissimacoumarin F (**4**)[a] (in $CDCl_3$)

Position	δ_H mult. (*J* in Hz)	δ_C	HMBC (H→C)
2		160.4	
3	6.35 d (9.5)	115.2	C-2, C-4, C-10
4	7.61 d (9.5)	143.4	C-2, C-3, C-5, C-9, C-10
5	6.68 s	103.9	C-4, C-6, C-7, C-9, C-10
6		149.6	
7		144.7	
8		140.6	
9		143.1	
10		114.3	
1′	4.42 dd (10.0, 3.5)	73.1	C-7, C-2′, C-3′
	4.11 dd (10.0, 8.0)		C-7, C-2′, C-3′
2′	3.99 dd (8.0, 3.5)	79.4	C-1′, C-3′, C-9′
3′	2.20 m	47.4	C-2′, C-4′, C-5′, C-9′
4′	4.03 m	84.6	C-2′′, C-3′, C-5′, C-9′
5′	4.86 dd (15.5, 8.5)	74.3	C-3′, C-4′, C-6′, C-7′
6′	5.19 d (8.5)	125.3	C-5′, C-7′, C-8′, C-10′
7′		136.9	
8′	1.72 s	25.8	C-6′, C-7′, C-10′
9′	1.47 s	23.5	C-2′, C-3′, C-4′
10′	1.71 s	18.2	C-6′, C-7′, C-8′
OCH_3-6	3.88 s	56.2	C-6
OCH_3-8	4.02 s	61.9	C-8

[a] Assignments were based on HSQC, HMBC experiments.

1.4.5. Structural determination of compound 5

Compound **5** was obtained as a colorless oil and its molecular formula was determined as $C_{21}H_{26}O_6$ by molecular ion peak at *m/z* 374.1732 $[M]^+$ (calcd for $C_{21}H_{26}O_6$, 374.1729) in HREIMS spectrum. The UV (225, 295 and 340 nm) and IR (1718 cm^{-1} absorptions), and doublets at δ_H 7.62 (1H, d, J = 9.5 Hz, H-4) and 6.35 (1H, d, J = 9.5 Hz, H-3), a singlet at δ_H 6.69 (1H, s, H-5), and two methoxy signals at δ_H 4.06 (3H, s, OCH_3-8) and 3.90 (3H, s, OCH_3-6) in the ^{1}H NMR spectrum (**Table 5**) indicated the presence of a 6,7,8-trioxygenated coumarin skeleton (Hwang *et al*., 2005). The location of two methoxy groups were assigned to C-6 and C-8 by the HMBC correlations between the methoxy protons and C-6 (δ_C 149.9) and C-8 (δ_C 141.4), respectively (**Fig. 39**), and a fragment peak at m/z 222 ($[M–152]^+$) in the EIMS (Banthorpe *et al*., 1989; Hwang *et al*., 2005). The ^{1}H and ^{13}C NMR spectral data were almost identical to those of **1** and altissimarin B (Hwang *et al*., 2005), except for some chemical shift differences due to a 3′,4′-epoxy ring in the terpenyl chain. These assignments were deduced from the HMBC correlations of H-1′/C-2′ and C-3′; H-2′/C-3′ and C-4′; H-4′/C-2′, C-3′ and C-9′; and H-8′/C-6′, C-7′ and C-10′. Finally, the relative stereochemistry of **5** was established on the specific rotation ($[\alpha]_D^{25}$ +11) and NOESY data, which show strong NOE correlation between H-4′/H-9′ (Hwang *et al*., 2005) (**Fig. 39**). Thus, the structure of altissimacoumarin G (**5**) was proposed as (3′*R*,4′*S*)-6,8-dimethoxy-7-(3′,7′-dimethylocta-3′,4′-epoxy-6′-enyloxy)coumarin.

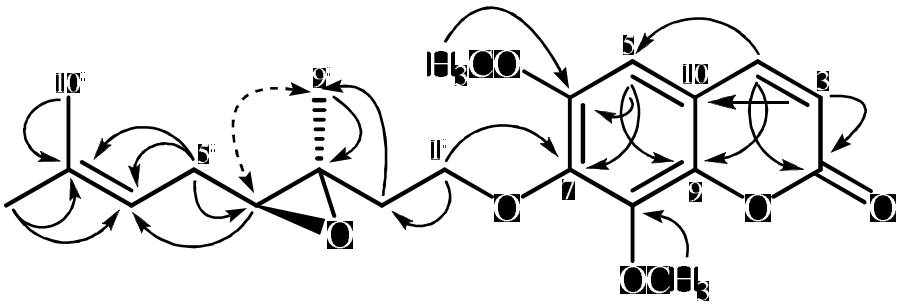

Fig. 39. Key HMBC (H→C) and NOSEY (**↔**) correlations of altissimacoumarin G (**5**)

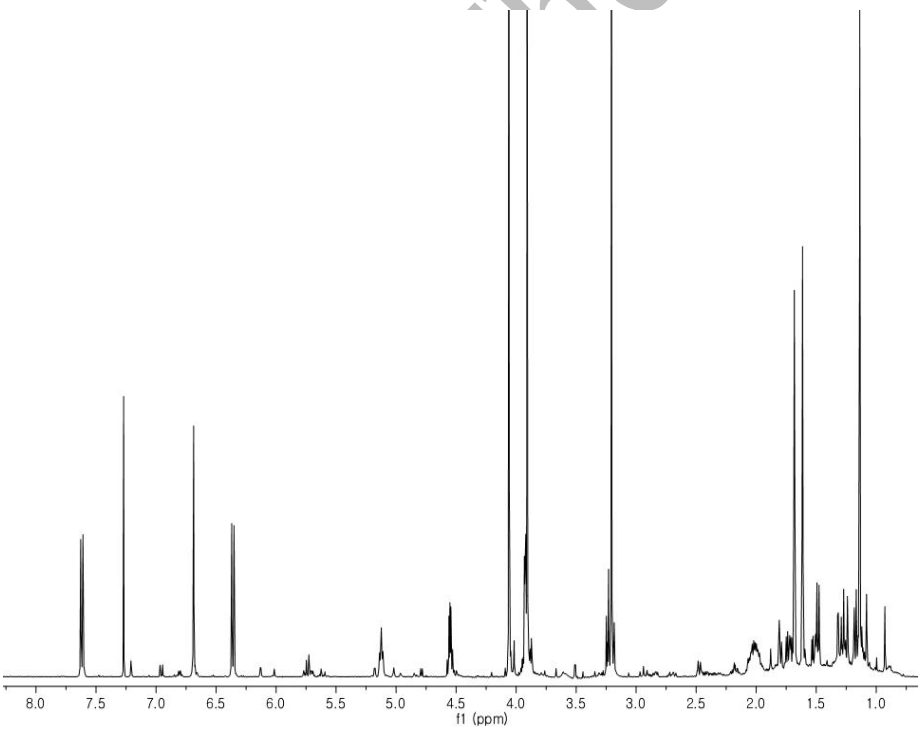

Fig. 40. ^{1}H-NMR spectrum of altissimacoumarin G (**5**)

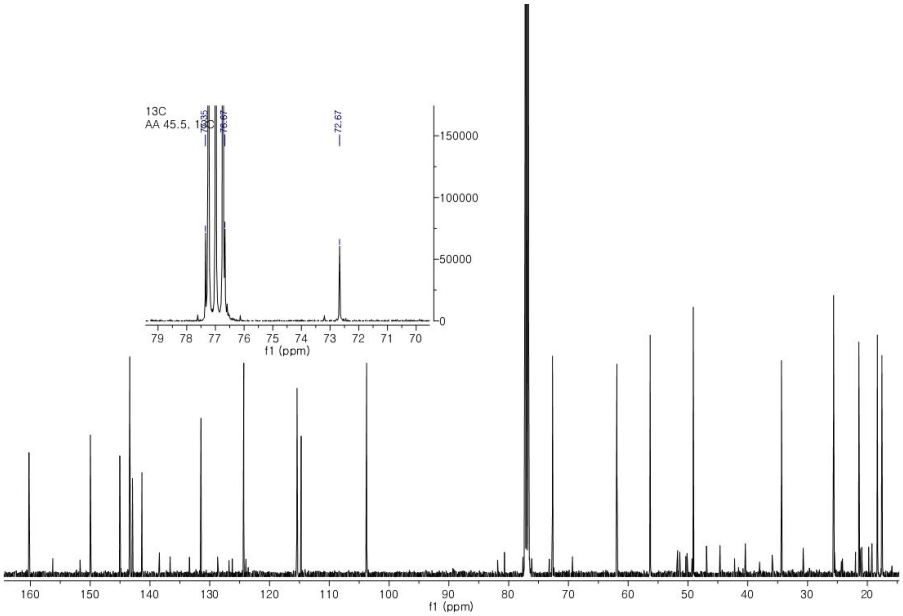

Fig. 41. ^{13}C-NMR spectrum of altissimacoumarin G (**5**)

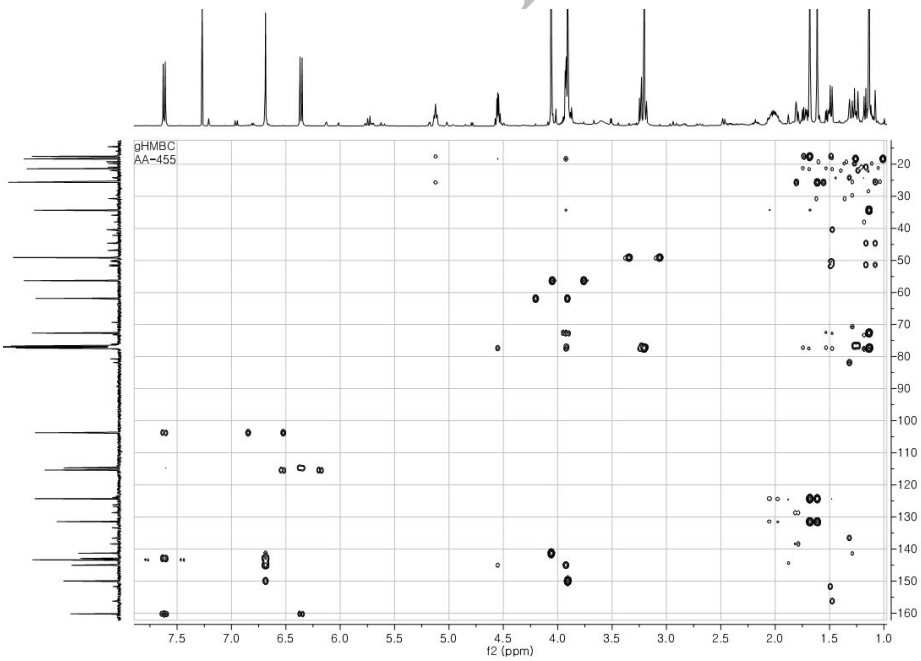

Fig. 42. HMBC spectrum of altissimacoumarin G (**5**)

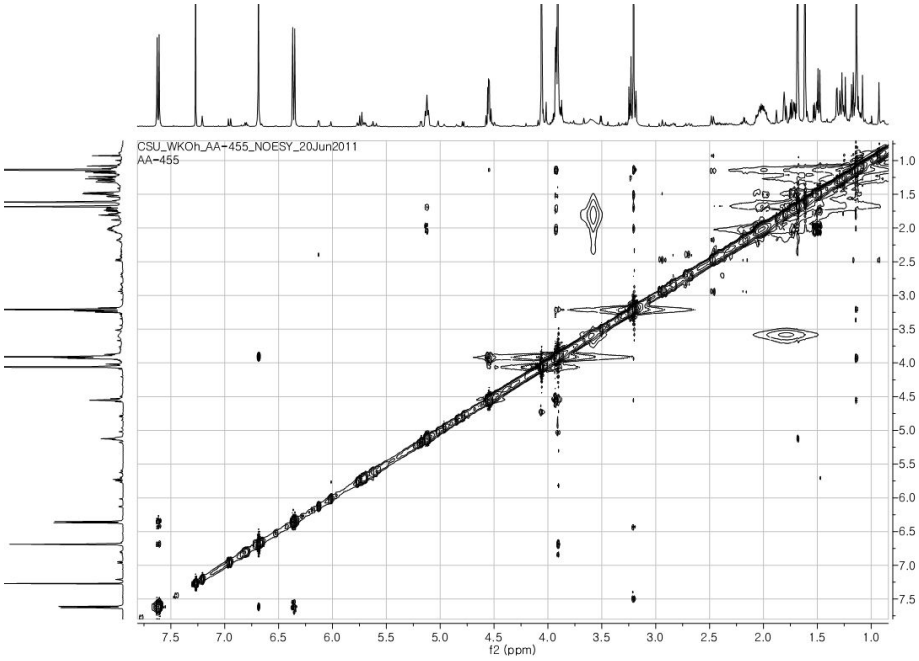

Fig. 43. NOESY spectrum of altissimacoumarin G (**5**)

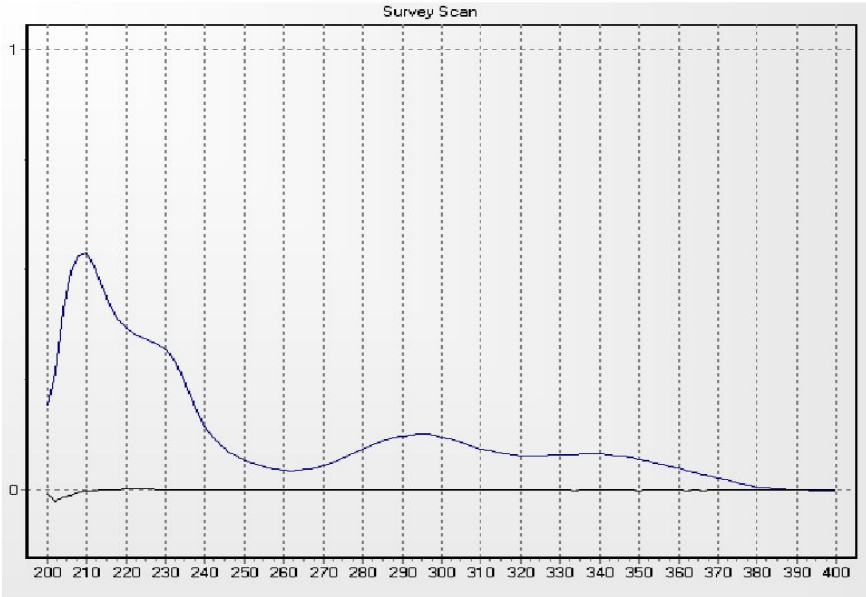

Fig. 44. UV spectrum of altissimacoumarin G (**5**)

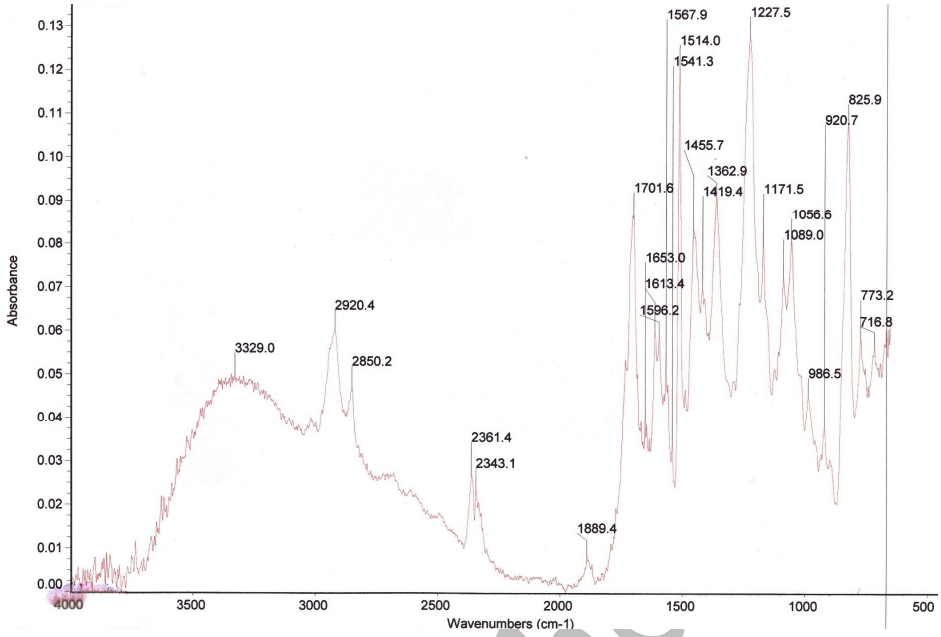

Fig. 45. IR spectrum of altissimacoumarin G (**5**)

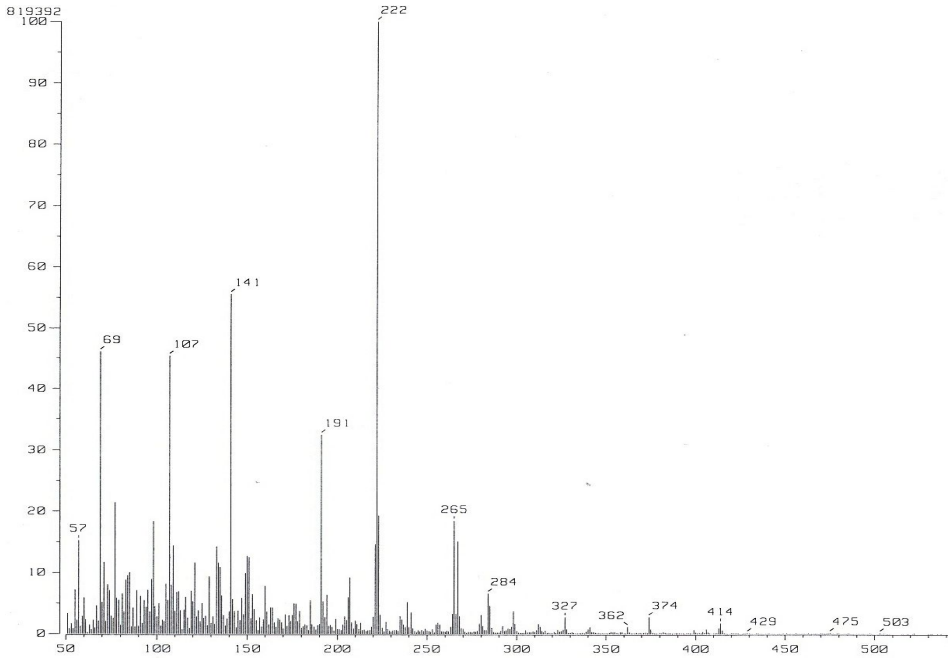

Fig. 46. EIMS spectrum of altissimacoumarin G (**5**)

Table 5. ^{1}H and ^{13}C-NMR data of altissimacoumarin G (**5**)[a] (in $CDCl_3$)

Position	δ_H mult. (*J* in Hz)	δ_C	HMBC (H→C)
2		160.3	
3	6.35 d (9.5)	115.4	C-2, C-4, C-10
4	7.62 d (9.5)	143.4	C-2, C-3, C-5, C-9, C-10
5	6.69 s	103.8	C-4, C-6, C-7, C-9, C-10
6		149.9	
7		145.1	
8		141.4	
9		142.9	
10		114.7	
1′	4.55 m	76.7	C-7, C-2′, C-3′
	3.89 m		C-7, C-2′, C-3′
2′	1.80 m	34.4	C-3′, C-4′, C-9′
	1.50 m		C-3′, C-4′
3′		77.4	
4′	3.90 m	72.8	C-2′, C-3′, C-5′, C-9′
5′	2.09 m	21.4	C-4′, C-6′, C-7′
6′	5.12 t (7.0)	124.3	C-5′, C-7′, C-8′
7′		131.5	
8′	1.68 s	25.7	C-6′, C-7′, C-10′
9′	1.14 s	18.3	C-2′, C-3′
10′	1.61 s	17.6	C-6′, C-7′, C-8′
OCH_3-6	3.90 s	56.3	C-6
OCH_3-8	4.06 s	61.9	C-8

[a] Assignments were based on HSQC, HMBC experiments.

1.4.6. Structural determination of compound 6

Compound **6** was obtained as a colorless oil with the molecular formula of $C_{21}H_{28}O_8$, which was determined by HREIMS, *m/z* 408.1784 $[M]^+$ (calcd for $C_{21}H_{28}O_8$, 408.1784). The UV (230, 295 and 335 nm) and IR (1715 cm^{-1}) absorptions, and the ^1H NMR signals at δ_H 7.62 (1H, d, *J* = 9.5 Hz, H-4), 6.37 (1H, d, *J* = 9.5 Hz, H-3), 6.70 (1H, s, H-5), 4.07 (3H, s, OCH_3-8) and 3.90 (3H, s, OCH_3-6), indicated the presence of 6,8-dimethoxy-7-substituted coumarin nucleus (Hwang *et al.*, 2005). In addition to the coumarin unit, three methyls [δ_H 1.22 (3H, s, H-8′), 1.19 (3H, s, H-9′) and 1.13 (3H, s, H-10′)], two methylenes [δ_H 2.14 (1H, m, H-5′a), 1.87 (1H, m, H-5′b), and 1.74 (1H, m, H-4′a), 1.62 (1H, m, H-4′b)], two oxygenated methine [δ_H 3.85 (1H, dd, *J* = 8.5, 2.0 Hz, H-2′) and 3.79 (1H, t, *J* = 8.5 Hz, H-6′)], and one oxygenated methylene [δ_H 4.53 (1H, dd, *J* = 10.5, 2.0 Hz, H-1′a), 3.91 (1H, dd, *J* = 10.5, 8.5 Hz, H-1′b)] were observed in the ^1H NMR spectrum. These signals were found to correspond to the ^{13}C NMR signals of an oxygenated C_{10} terpenyl side-chain, which was assigned to attach to C-7 by HMBC correlation between the H-1′ protons and carbon C-7 (δ_C 144.9). Furthermore, the observation of significant mass fragment ions (EIMS) at *m/z* 307 and 222 resulting from cleavage at C-4′/C-5′ and 7-O/C-1′, respectively, suggested the terpenyl side-chain comprising of an epoxy and two hydroxy groups. The HMBC correlations of H-2′/C-1′, C-3′, C-4′ and C-9′; H-5′/C-3′, C-4′, C-6′ and C-7′; H-6′/C-7′, C-8′ and C-10′; OH-6′/C-6′; and OH-7′/C-7′ further confirmed the epoxy ring at C-2′, C-3′, and two hydroxy groups at C-6′ and C-7′ position. The relative configuration of **6** was then established on the basis of the specific rotation ($[\alpha]_D^{25}$ +19) and NOESY data, which showed NOE correlations

between H-1′/H-9′ and H-2′/H-4′, whereas no NOE was observed between H-2′/H-9′. After the reaction with compound **6** and the Mosher ester reagents, (*S*)-MTPA (**6a**) and (*R*)-MTPA (**6b**), respectively, analysis of the ^{1}H NMR data (**Fig. 6**) indicated the *R* configuration at the C-6′ stereocenter in **6**. Therefore, the structure of compound **6**, named altissimacoumarin H, was proposed as (2′*R*,3′*R*,6′*R*)-7-(6′,7′-dihydroxy-2′,3′-epoxy-3′,7′-dimethyloctaoxy)-6,8-dimethoxycoumarin.

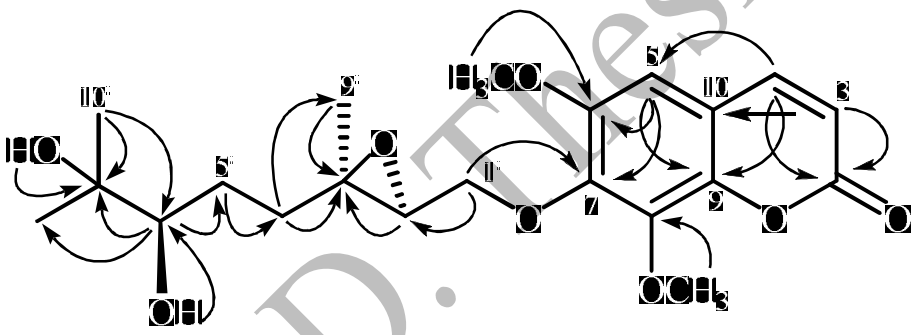

Fig. 47. Key HMBC (H→C) correlations of altissimacoumarin H (**6**)

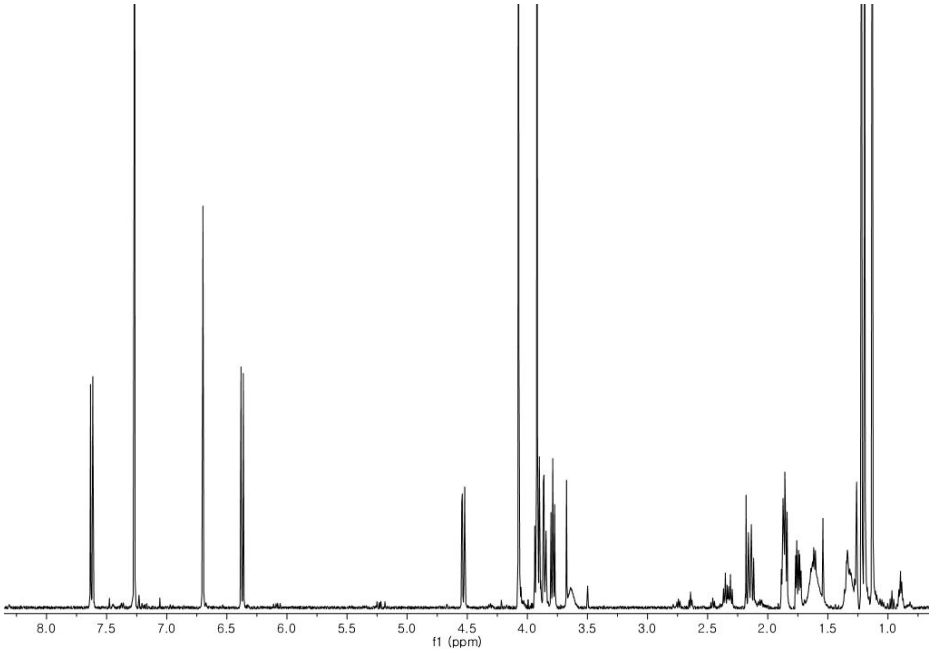

Fig. 48. ^{1}H-NMR spectrum of altissimacoumarin H (**6**)

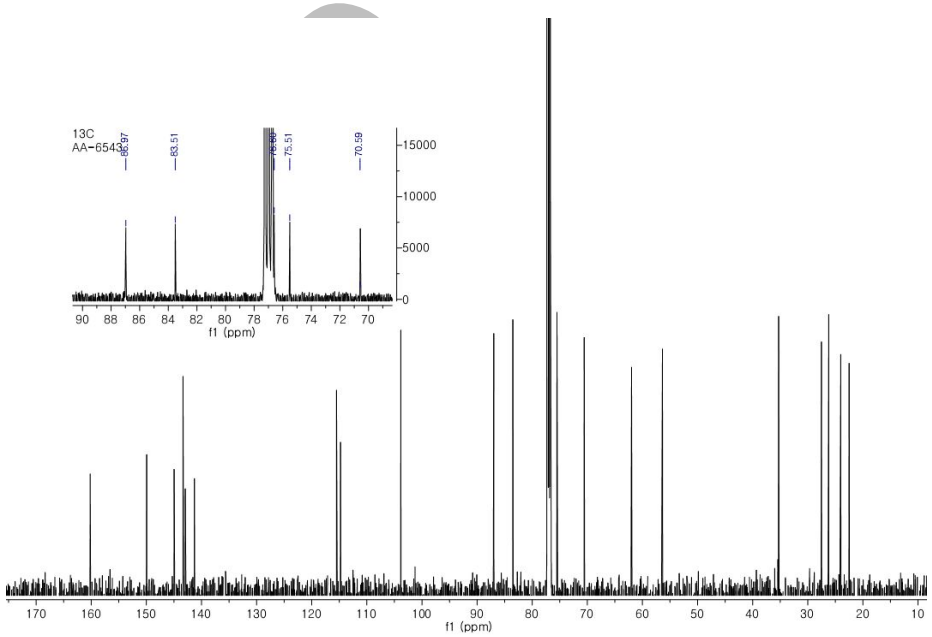

Fig. 49. ^{13}C-NMR spectrum of altissimacoumarin H (**6**)

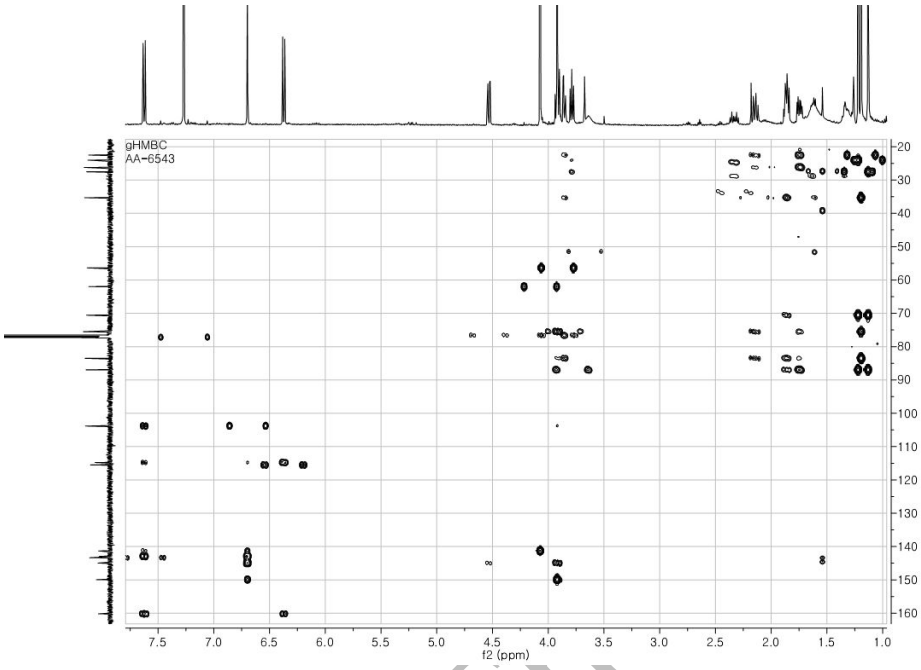

Fig. 50. HMBC spectrum of altissimacoumarin H (**6**)

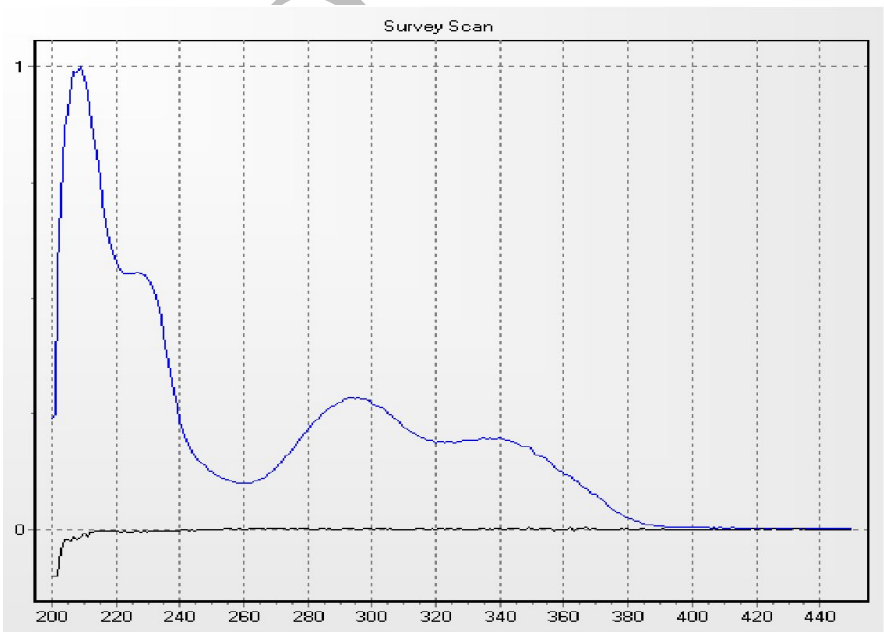

Fig. 51. UV spectrum of altissimacoumarin H (**6**)

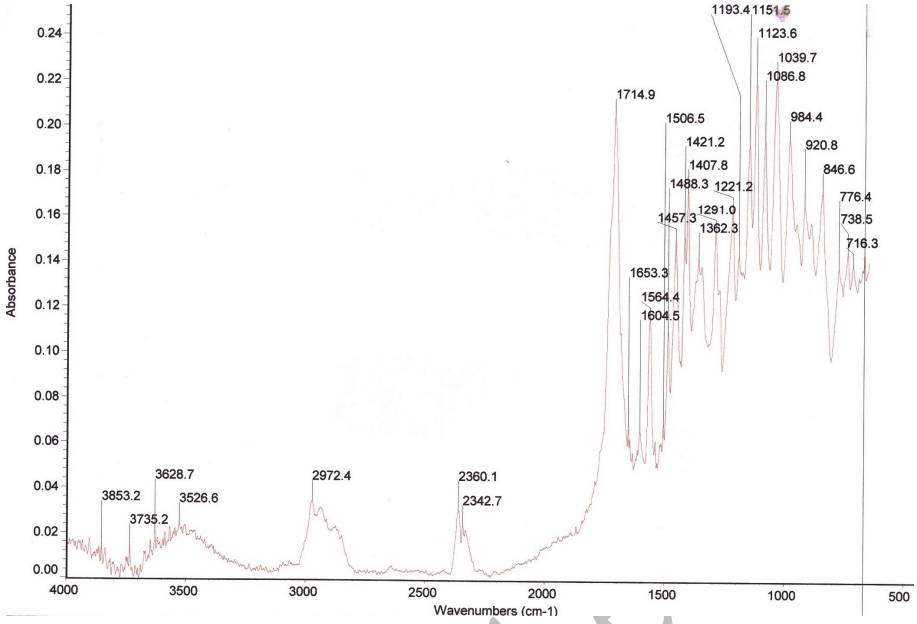

Fig. 52. IR spectrum of altissimacoumarin H (**6**)

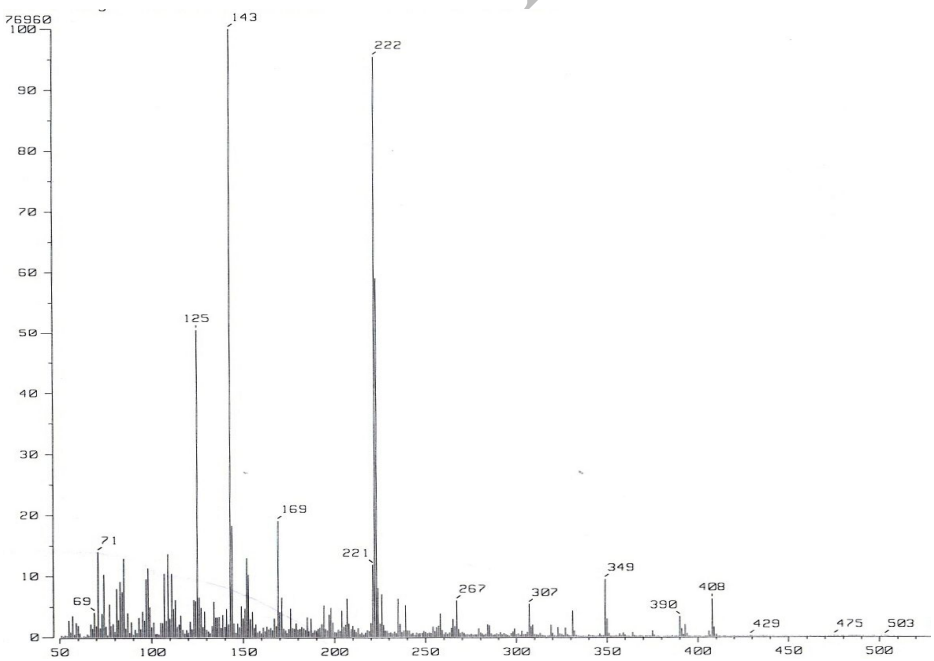

Fig. 53. EIMS spectrum of altissimacoumarin H (**6**)

Table 6. ^{1}H and ^{13}C-NMR data of altissimacoumarin H (**6**) (in $CDCl_3$)

Position	δ_H mult. (*J* in Hz)	δ_C	HMBC (H→C)
2		160.2	
3	6.37 d (9.5)	115.5	C-2, C-4, C-10
4	7.62 d (9.5)	143.4	C-2, C-3, C-5, C-9, C-10
5	6.70 s	103.9	C-4, C-6, C-7, C-9, C-10
6		149.9	
7		144.9	
8		141.3	
9		142.9	
10		114.8	
1′	4.53 dd (10.5, 2.0)	76.6	C-7, C-2′
	3.91 dd (10.5, 8.5)		C-7, C-2′, C-3′
2′	3.85 dd (8.5, 2.0)	75.5	C-1′, C-3′, C-4′, C-9′
3′		83.5	
4′	1.74 m	35.3	C-2′, C-3′, C-5′, C-6′, C-9′
	1.62 m		C-3′, C-5′, C-6′, C-9′
5′	2.14 m	26.2	C-3′, C-4′, C-7′
	1.87 m		C-3′, C-4′, C-6′, C-7′
6′	3.79 t (8.5)	86.9	C-5′, C-7′, C-8′, C-10′
7′		70.6	
8′	1.22 s	27.5	C-6′, C-7′, C-10′
9′	1.19 s	22.5	C-2′, C-3′
10′	1.13 s	24.0	C-6′, C-7′, C-8′
OCH_3-6	3.90 s	56.4	C-6
OCH_3-8	4.07 s	61.9	C-8
OH-6′	3.62 s		C-6′
OH-7′	3.65 s		C-7′

1.4.7. Structural determination of compound 7

Compound **7** was obtained as a colorless oil with the molecular formula of $C_{21}H_{26}O_8$, which was determined by HREIMS, *m/z* 406.1631 $[M]^+$ (calcd for $C_{21}H_{26}O_8$, 406.1628). The UV and IR spectra of **7** were similar to those of **1-6**. The ^1H and ^{13}C NMR spectra data (**Table 7**) suggested features of a 6,8-dimethoxy-7-terpenylated coumarin, which were similar to those of **3** and **6**, except for a presence of an acetal carbon at δ_C 105.8 (C-6′) in the terpenoid chain instead of the oxymethine carbon. Extensive NMR (HMQC, HMBC and NOESY) and EIMS experiments indicated two epoxy rings at C-3′, C-4′ and C-6′, C-7′, and a hydroxy group at C-6′. These assignments were deduced from the HMBC correlations between H-1′/C-2′ and C-3′; H-2′/C-1′, C-3′, C-4′ and C-9′; H-4′/C-3′, C-5′ and C-9′; H-5′/C-3′, C-4′, C-6′ and C-7′ (**Fig. 58**). Attempts to determine the absolute configuration of the stereogenic center at C-6′ using the Mosher method were unsuccessful due to the failure of making Mosher ester derivatives. However, from data of NOESY experiment, which showed strong NOE correlation between H-4′ and H-9′ (**Fig. 54**), the specific rotation ($[\alpha]_D^{25}$ +10), and CD Cotton effects (λ_{max} 325 nm, $\Delta\varepsilon$ = -7.77; λ_{max} 271 nm, $\Delta\varepsilon$ = +1.75), the structure of altissimacoumarin I (**7**) can be assigned as (3′*R*,4′*S*)-7-(2′,3′:6′,7′-diepoxy-6′-hydroxy-3′,7′-dimethyloctaoxy)-6,8-dimethoxycoumarin.

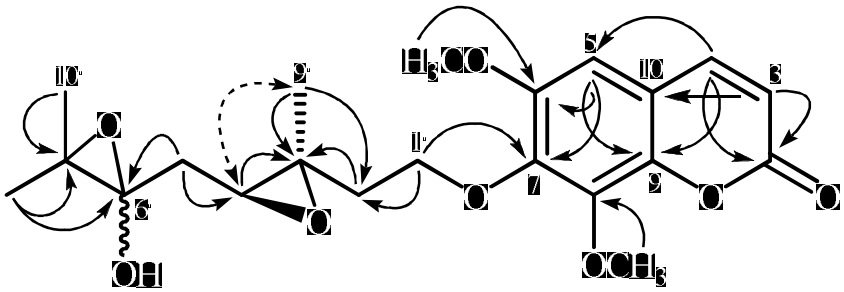

Fig. 54. Key HMBC (H→C) and NOSEY (**↔**) correlations of altissimacoumarin I (**7**)

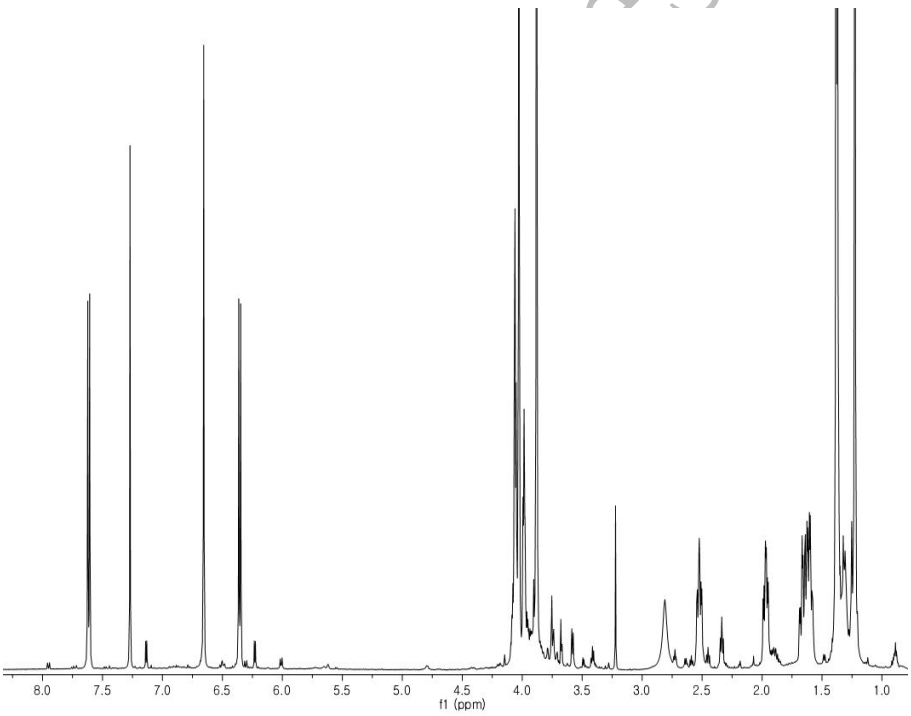

Fig. 55. ^{1}H-NMR spectrum of altissimacoumarin I (**7**)

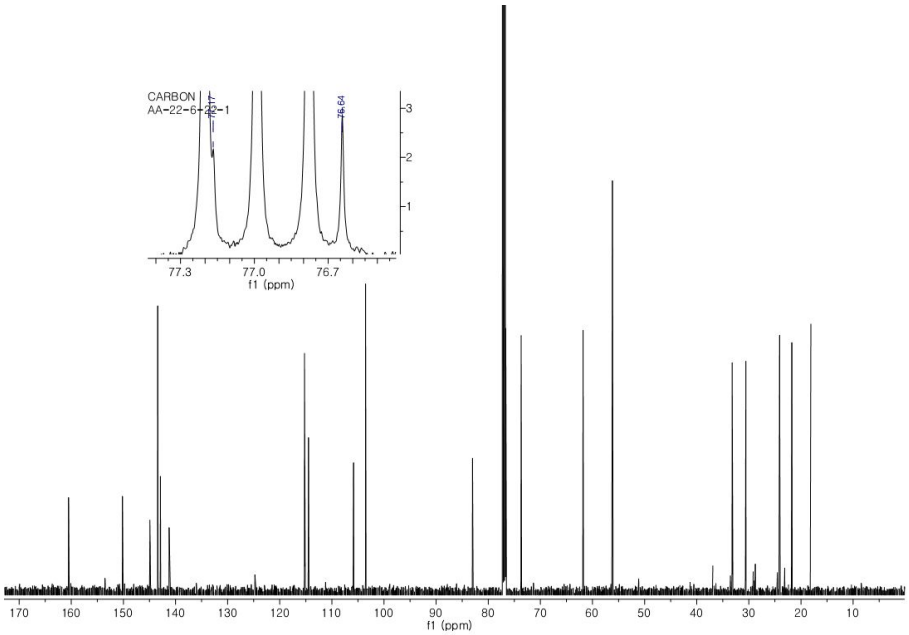

Fig. 56. ^{13}C-NMR spectrum of altissimacoumarin I (**7**)

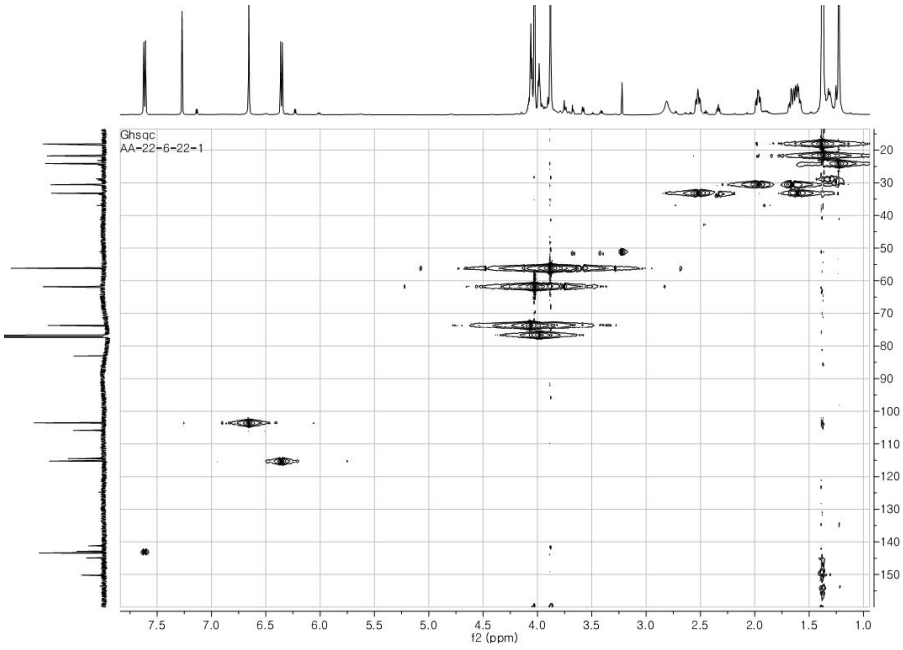

Fig. 57. HSQC spectrum of altissimacoumarin I (**7**)

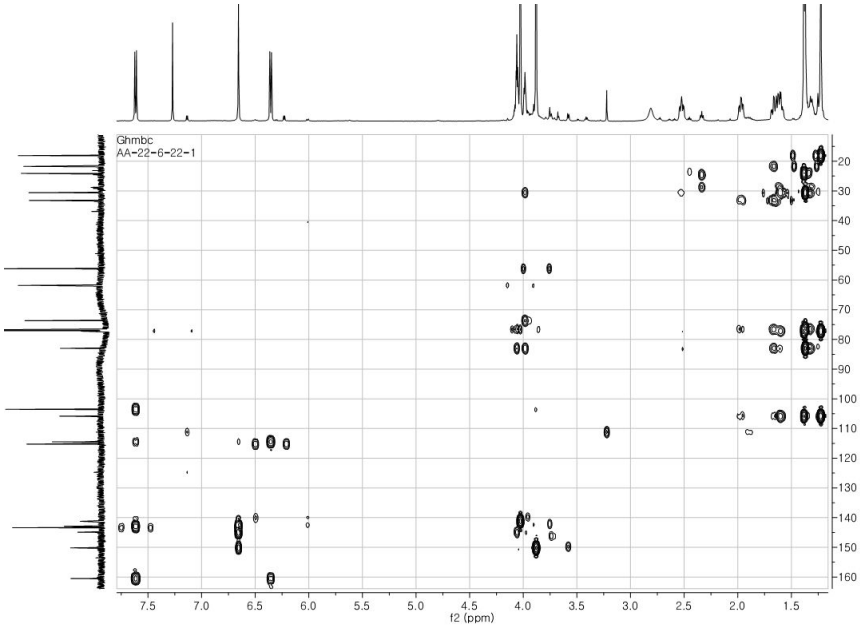

Fig. 58. HMBC spectrum of altissimacoumarin I (**7**)

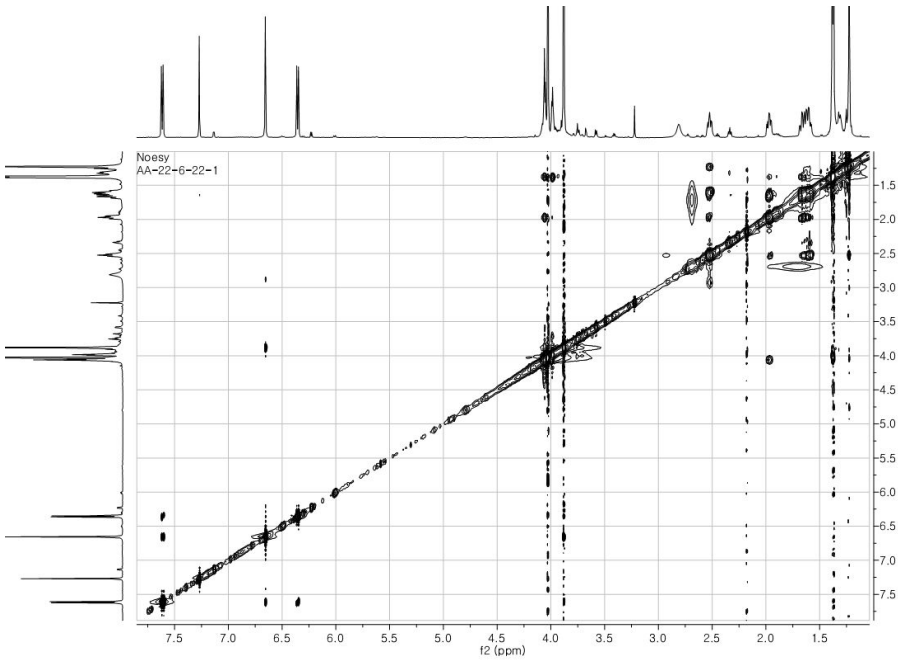

Fig. 59. NOESY spectrum of altissimacoumarin I (**7**)

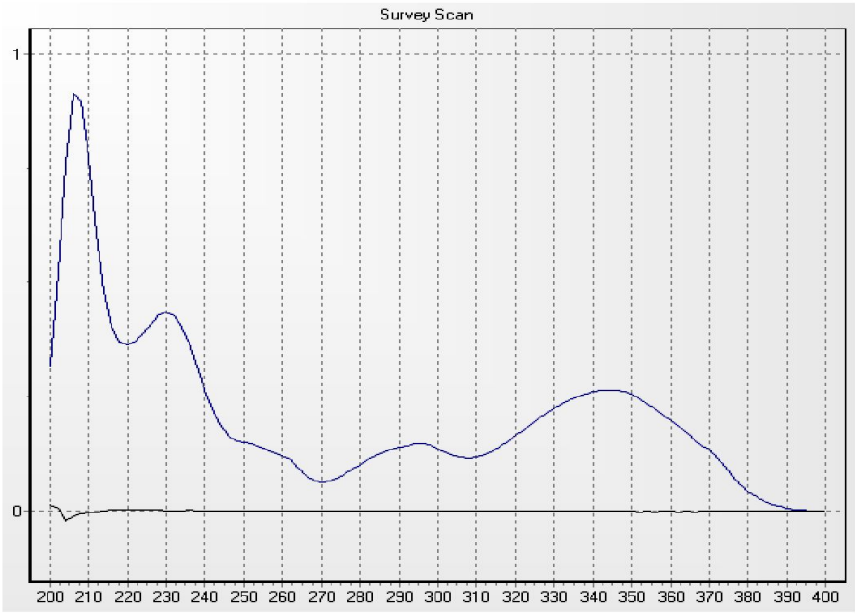

Fig. 60. UV spectrum of altissimacoumarin I (**7**)

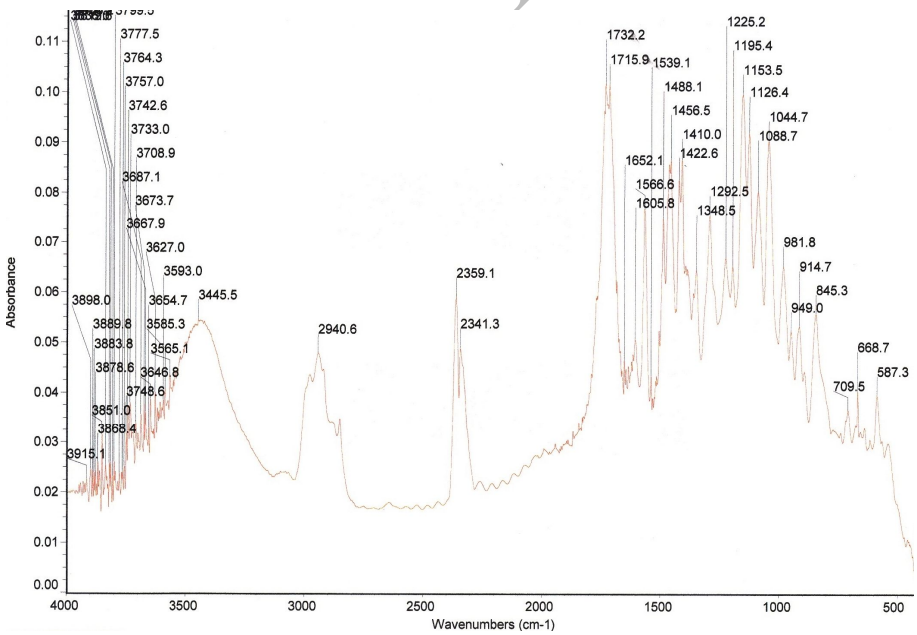

Fig. 61. IR spectrum of altissimacoumarin I (**7**)

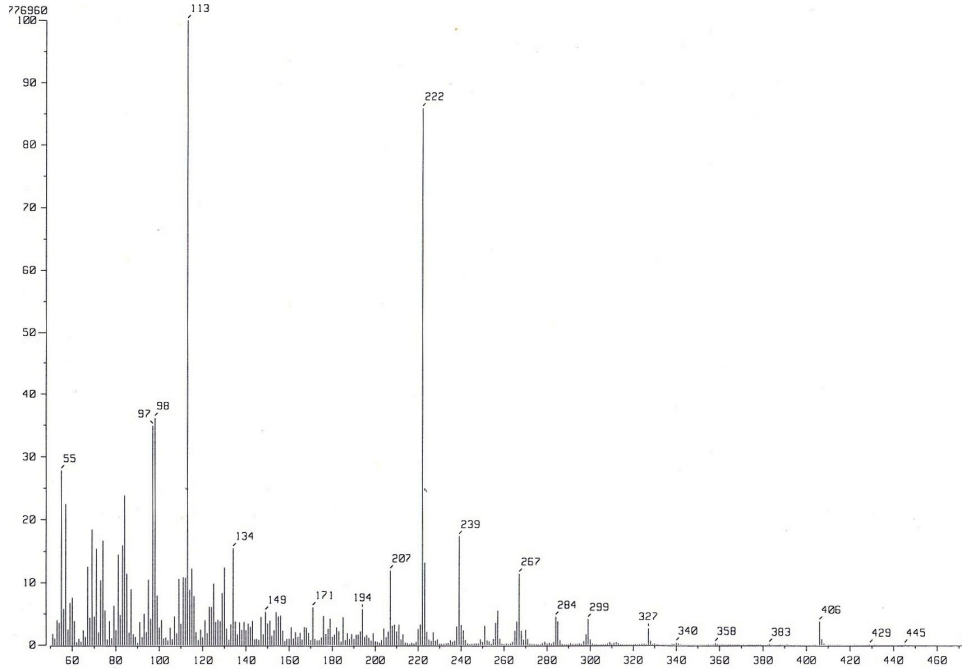

Fig. 62. EIMS spectrum of altissimacoumarin I (**7**)

Table 7. ^{1}H and ^{13}C-NMR data of altissimacoumarin I (**7**)[a] (in $CDCl_3$)

Position	δ_H mult. (*J* in Hz)	δ_C	HMBC (H→C)
2		160.5	
3	6.35 d (9.5)	115.3	C-2, C-4, C-10
4	7.60 d (9.5)	143.4	C-2, C-3, C-5, C-9, C-10
5	6.70 s	103.5	C-4, C-6, C-7, C-9, C-10
6		150.2	
7		144.9	
8		141.2	
9		142.9	
10		114.5	
1′	4.07 m	76.6	C-7, C-2′
	3.91 m		C-7, C-2′, C-3′
2′	1.96 m	30.6	C-1′, C-3′, C-4′, C-9′
	1.64 m		C-1′, C-3′, C-4′, C-9′
3′		83.0	
4′	4.02 m	73.7	C-3′, C-5′, C-9′
5′	2.52 m	33.2	C-3′, C-4′, C-6′, C-7′
	1.60 m		C-3′, C-6′, C-7′
6′		105.8	
7′		77.2	
8′	1.22 s	24.1	C-6′, C-7′, C-10′
9′	1.37 s	21.7	C-2′, C-3′, C-4′
10′	1.38 s	18.1	C-6′, C-7′, C-8′
OCH_3-6	3.87 s	56.2	C-6
OCH_3-8	4.00 s	61.8	C-8

[a] Assignments were based on HSQC, HMBC experiments.

1.4.8. Structural determination of compound 8

Compound **8** was obtained as a colorless oil and its molecular formula, $C_{21}H_{26}O_7$, was established by HREIMS, *m/z* 390.1679 $[M]^+$ (calcd for $C_{21}H_{26}O_7$, 390.1679). The UV and IR absorptions resembled those of **1**–**7**, and the characteristic ^{1}H NMR signals suggested a skeleton of a 6,8-dimethoxy-7-terpenylated coumarin (Hwang *et al.*, 2005). The positions of two methoxy groups were confirmed by the HMBC correlations from the methoxy protons to C-6 (δ_C 149.9) and C-8 (δ_C 141.2), respectively (**Fig. 63**). In addition, analysis of the ^{1}H and ^{13}C NMR spectra, including the HMQC and HMBC data, suggested the presence of a C_{10} terpenyl side-chain at C-7, consisting of two methyl [δ_H 1.68 (3H, s, H-10′) and 1.24 (3H, s, H-9′)], two methylenes [δ_H 2.26 (1H, m, H-4′a), 1.70 (1H, m, H-4′b), and 2.05 (1H, m, H-5′a), 1.62 (1H, m, H-5′b)], two oxymethine [δ_H 4.38 (1H, m, H-6′) and 3.78 (1H, dd, J = 9.0, 2.0 Hz, H-2′)], an oxymethylene [δ_H 4.64 (1H, dd, J = 10.5, 2.0 Hz, H-1′a), 3.97 (1H, dd, J = 10.5, 9.0 Hz, H-1′b)], and two germinal olefinic signals [δ_H 4.97 (1H, s, H-8′a) and 4.78 (1H, s, H-8′b)]. The observation of mass fragment ions (EIMS) at *m/z* 390 $[M]^+$, 290 and 222 resulting from cleavage at C-3′/C-4′ and 7-O/C-1′, suggested the presence of an epoxy and a hydroxy group in the terpenoid side-chain. The HMBC correlations of H-2′/C-1′, C-3′, C-4′ and C-9′; H-6′/C-5', C-7', C-8', C-10' confirmed the epoxy ring at C-2′, C-3′, and the hydroxy group at C-6′ position. The relative configurations of C-2′, C-3′ and C-6′ in **8** were deduced from the NOE cross peak between H-4′/H-6′, H-4′/H-9′and no NOE signal observed between H-2′/H-9′ (**Fig. 68**). (Hwang *et al.*, 2005; Xin *et al.*, 2008). Finally, the absolute configuration of the stereogenic center at C-6′ was addressed by the Mosher ester method (**Fig. 6**). The *R*

configuration of C-6′ in **8** was determined on the interpretation of the data obtained (Seco *et al*., 2004; Phoopichayanun *et al*., 2008). Therefore, the structure of compound **8**, named altissimacoumarin J, was proposed as (2′*R*,3′*R*,6′*S*)-6,8-dimethoxy-7-(6′-hydroxy-2′,3′-epoxy-3′,7′-dimethylocta-7′-enyloxy)coumarin.

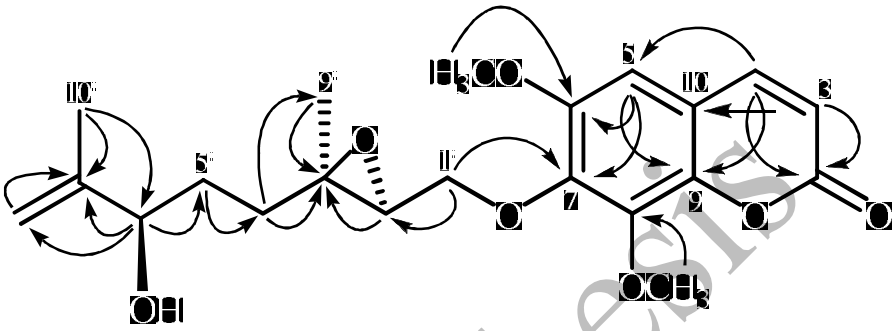

Fig. 63. Key HMBC (H→C) correlation of altissimacoumarin J (**8**)

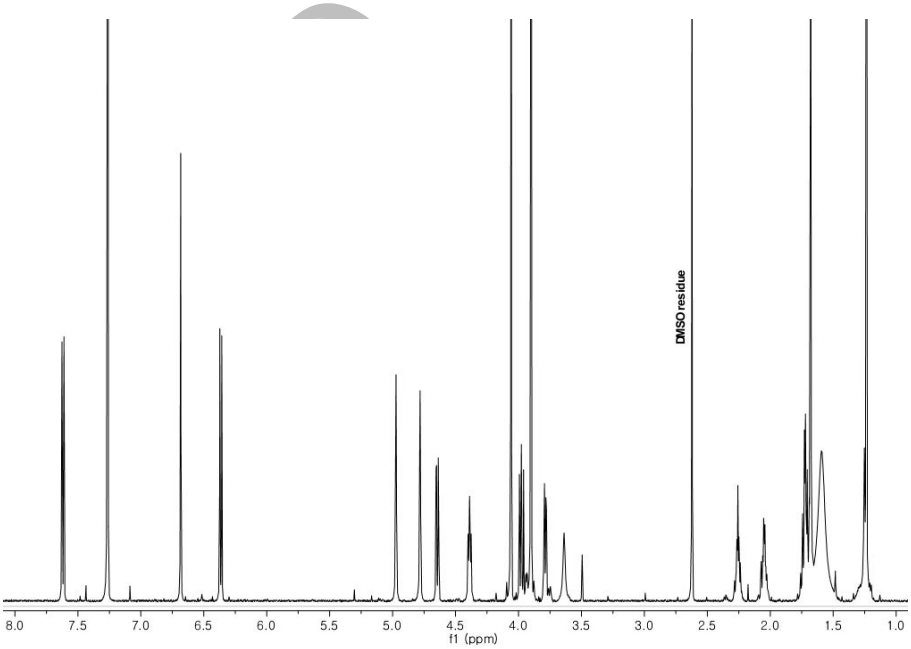

Fig. 64. ^{1}H-NMR spectrum of altissimacoumarin J (**8**)

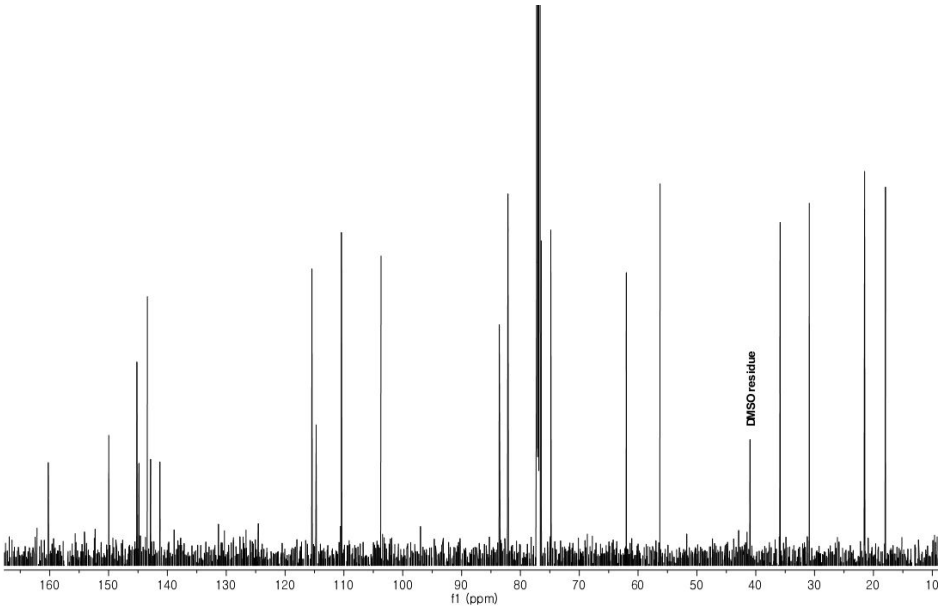

Fig. 65. ^{13}C-NMR spectrum of altissimacoumarin J (**8**)

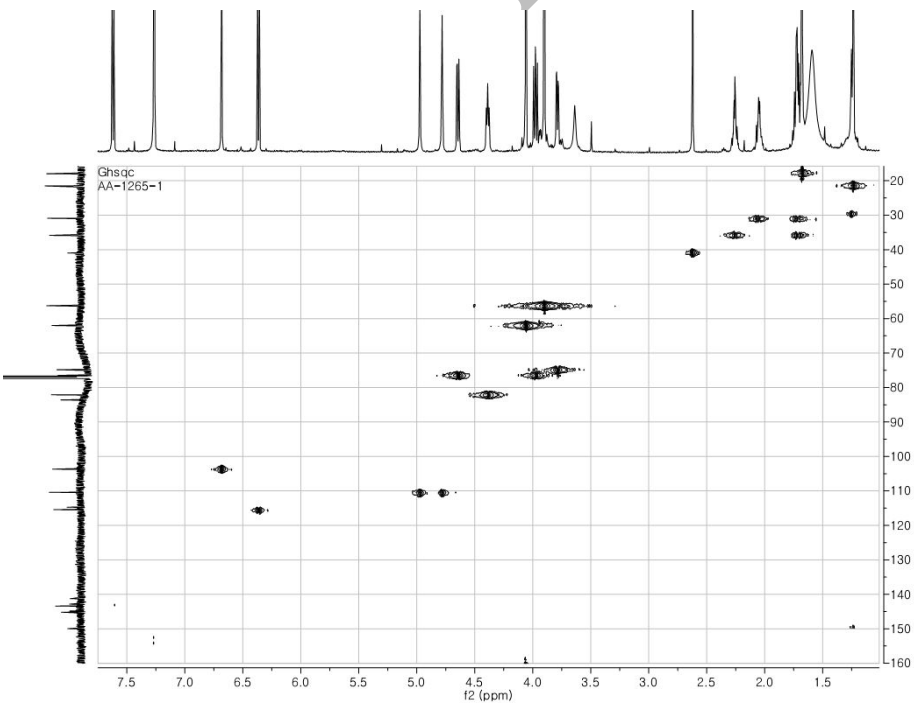

Fig. 66. HSQC spectrum of altissimacoumarin J (**8**)

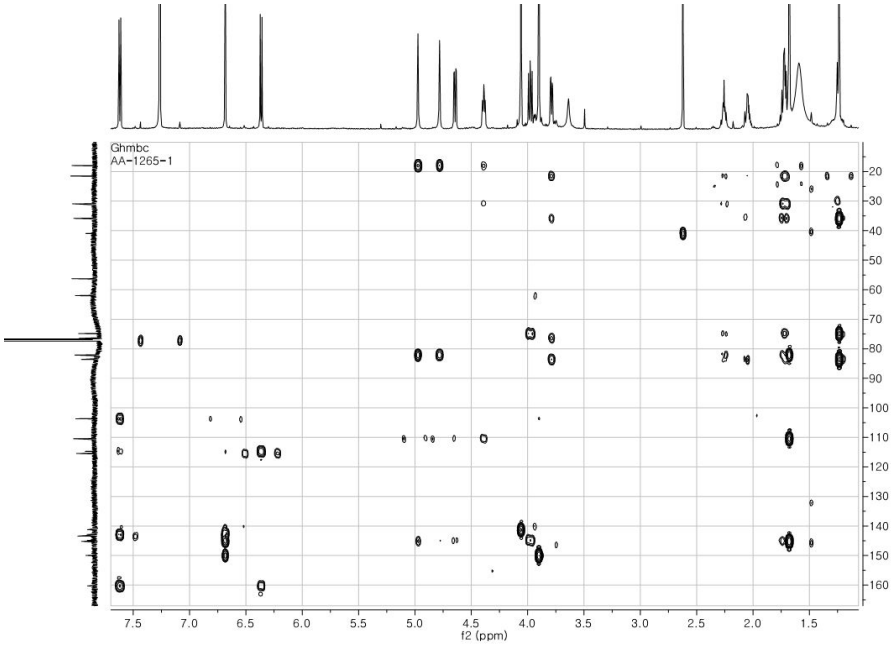

Fig. 67. HMBC spectrum of altissimacoumarin J (**8**)

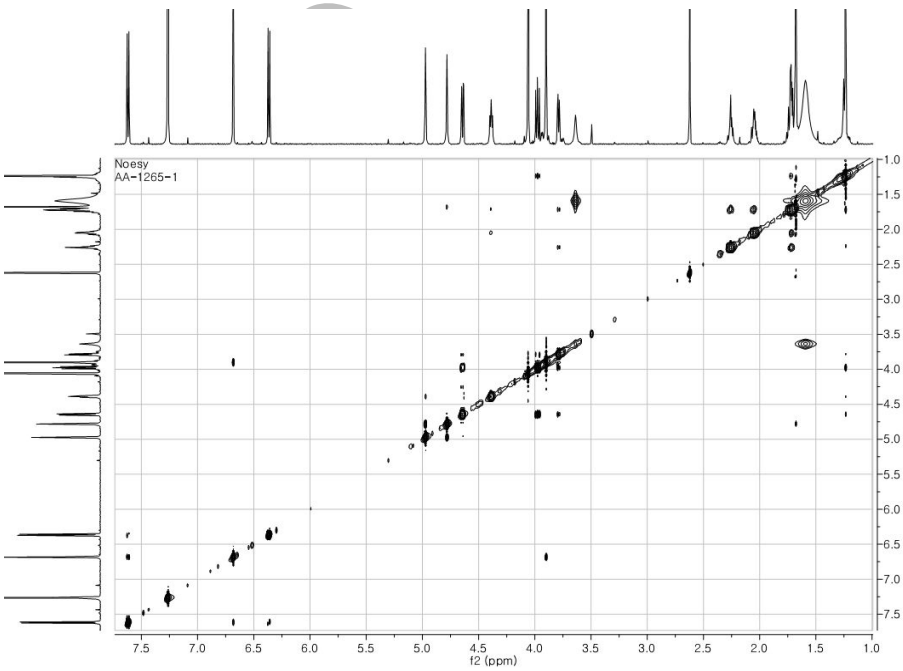

Fig. 68. NOESY spectrum of altissimacoumarin J (**8**)

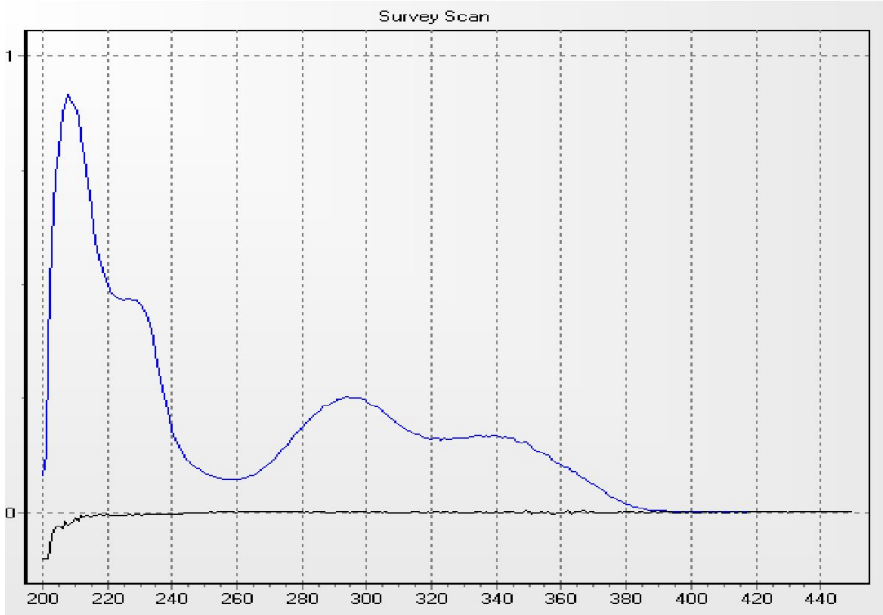

Fig. 69. UV spectrum of altissimacoumarin J (**8**)

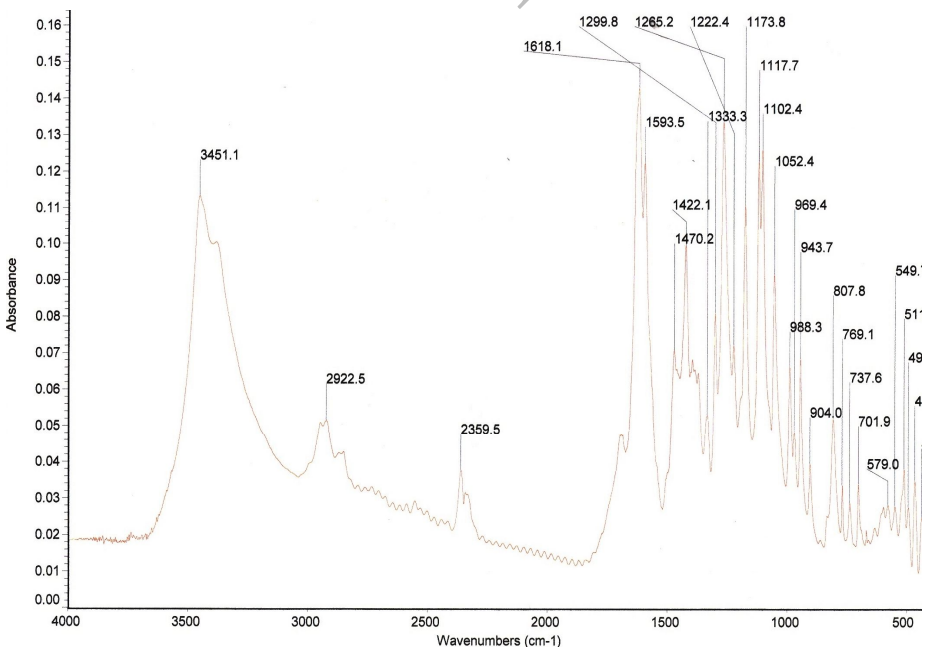

Fig. 70. IR spectrum of altissimacoumarin J (**8**)

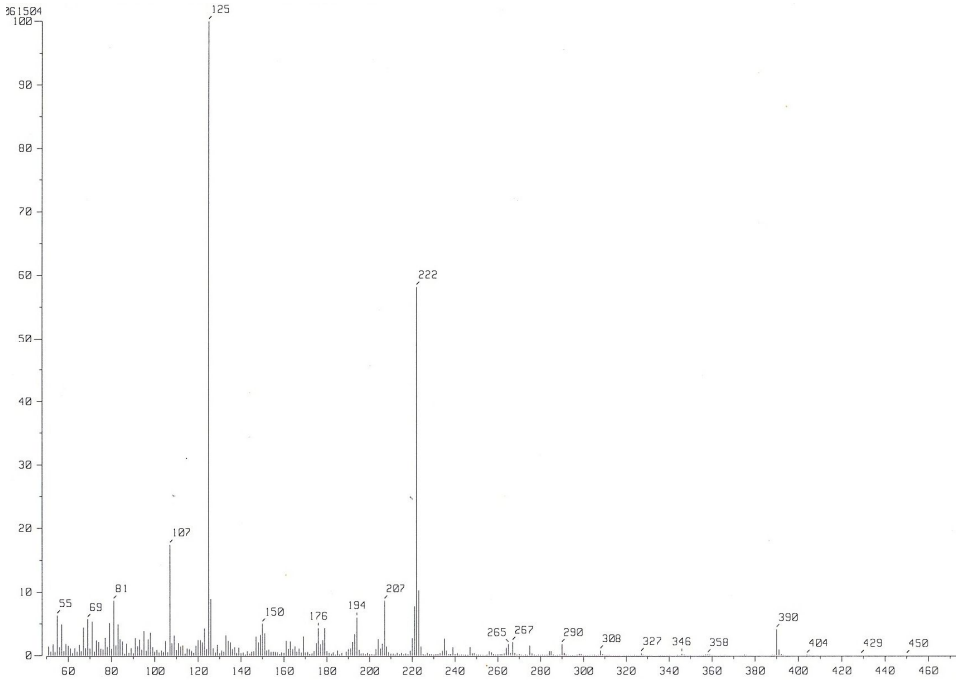

Fig. 71. EIMS spectrum of altissimacoumarin J (**8**)

Table 8. ^{1}H and ^{13}C-NMR data of altissimacoumarin J (**8**)[a] (in $CDCl_3$)

Position	δ_H mult. (*J* in Hz)	δ_C	HMBC (H→C)
2		160.2	
3	6.37 d (9.5)	115.4	C-2, C-4, C-10
4	7.62 d (9.5)	143.4	C-2, C-3, C-5, C-9, C-10
5	6.68 s	103.7	C-4, C-6, C-7, C-9, C-10
6		149.9	
7		144.8	
8		141.2	
9		142.3	
10		114.7	
1′	4.64 dd (10.5, 2.0)	76.5	C-7, C-2′
	3.97 dd (10.5, 9.0)		C-7, C-2′, C-3′
2′	3.78 dd (9.0, 2.0)	74.9	C-1′, C-3′, C-4′, C-9′
3′		83.5	
4′	2.26 m	35.8	C-3′, C-6′, C-9′
	1.70 m		C-2′, C-3′, C-6′, C-9′
5′	2.05 m	30.9	C-3′, C-4′, C-6′
	1.62 m		C-3′, C-4′, C-6′
6′	4.38 m	82.1	C-5′, C-7′, C-8′, C-10′
7′		145.2	
8′	4.97 s	110.4	C-6′, C-7′, C-10′
	4.78 s		C-6′, C-7′, C-10′
9′	1.24 s	21.5	C-2′, C-3′, C-4′
10′	1.68 s	17.8	C-6′, C-7′, C-8′
OCH_3-6	3.90 s	56.3	C-6
OCH_3-8	4.06 s	62.0	C-8

[a] Assignments were based on HSQC, HMBC experiments.

1.4.9. Structural determination of compound 9

Compound **9** was obtained as a colorless oil with the molecular formula of $C_{21}H_{28}O_8$, which was determined by a dehydrated molecular ion peak at *m/z* 390.1677 $[M-H_2O]^+$ in HREIMS spectrum (calcd for $C_{21}H_{26}O_7$, 390.1679). The UV and IR spectra of **9** were similar to those of **1**–**8**. The ^1H and ^{13}C NMR spectra data (**Table 9**) suggested features of a 6,8-dimethoxy-7-terpenylated coumarin, which were almost identical to those of **8**, except for some chemical shift differences due to the opening of the epoxy ring in the terpenoid chain. Extensive NMR experiments (HMQC, HMBC and NOESY) indicated three hydroxy groups attached at C-2′, C-3′ and C-6′. These assignments were deduced from the HMBC correlations between H-1′/C-2′ and C-3′; H-2′/C-1′, C-3′ and C-9′; H-6′/C-5', C-7', C-8' and C-10' and OH-2′/C-2′ (**Fig. 72**). The relative configuration of **9** was then established by NOESY experiments, which showed strong NOE correlations between H-2′/H-9′, H-4′/H-9′ and no NOE signal observed between H-4′/H-6′. The configuration of **9** was then established on the basis of the specific rotation ($[\alpha]_D^{25}$ +14), CD Cotton effects (λ_{max} 325 nm, $\Delta\varepsilon$ = -3.86; λ_{max} 270 nm, $\Delta\varepsilon$ = +2.38), and NOESY data, which showed strong NOE correlations between H-2′/H-9′, H-4′/H-9′ and H-4′/H-6′ (**Fig. 77**) (Hwang *et al.*, 2005; Xin *et al.*, 2008). Consequently, the structure of compound **9**, named altissimacoumarin K, was proposed as (2′*R*,3′*R*,6′*S*)-6,8-dimethoxy-7-(2′,3′6′-trihydroxy-3′,7′-dimethylocta-7′-enyloxy)coumarin.

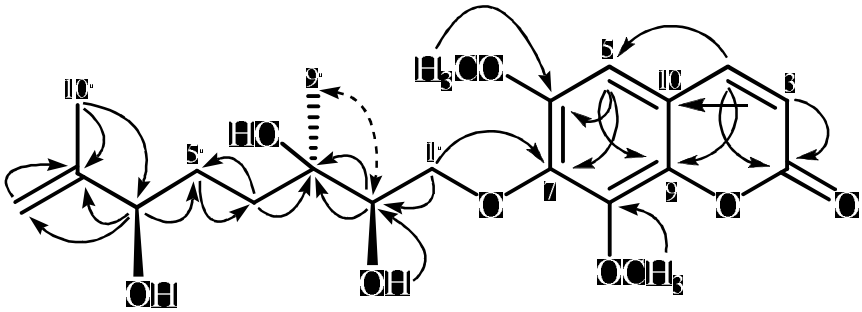

Fig. 72. Key HMBC (H→C) and NOSEY (**↔**) correlations of altissimacoumarin K (**9**)

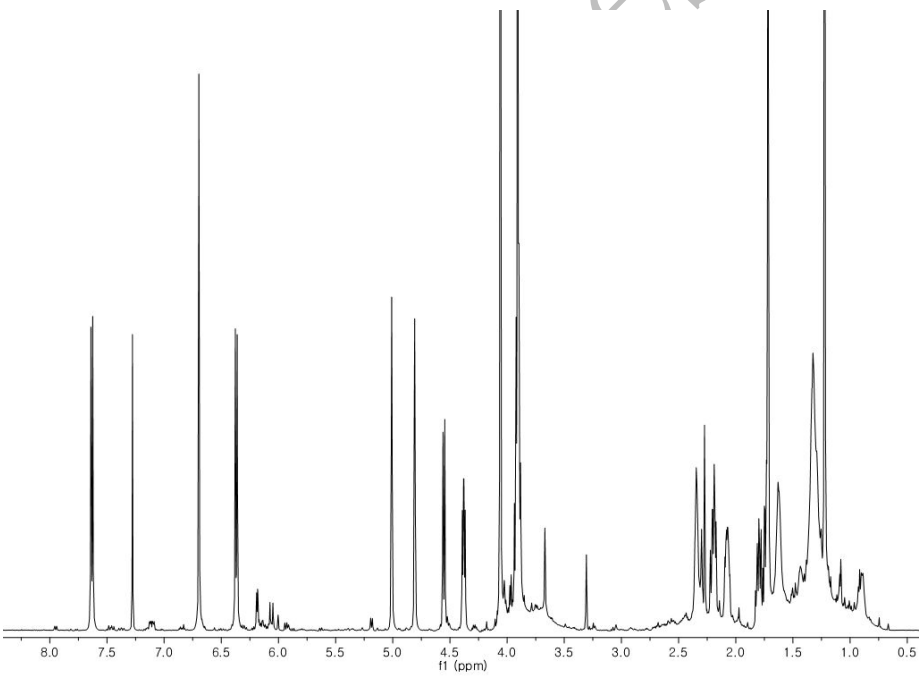

Fig. 73. ^{1}H-NMR spectrum of altissimacoumarin K (**9**)

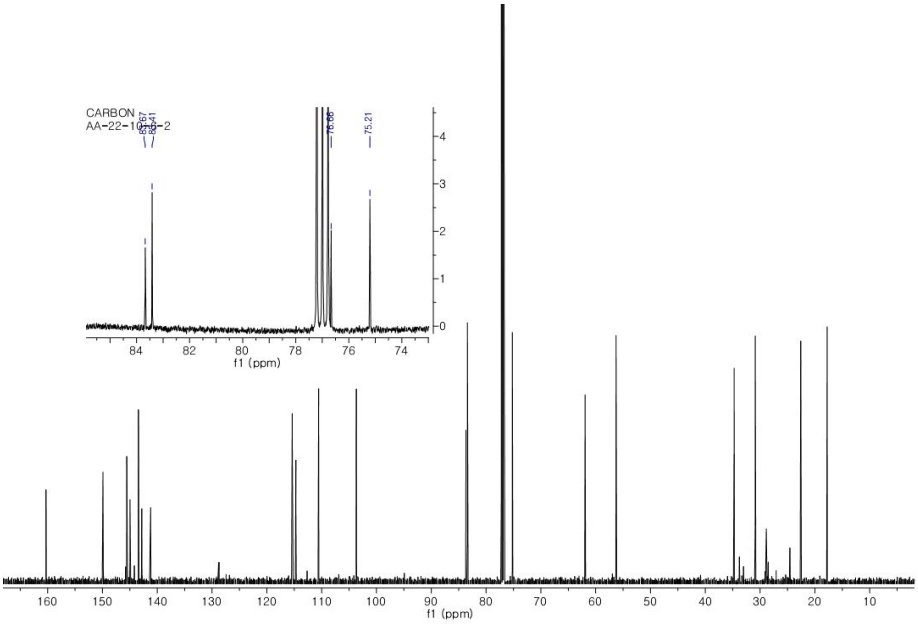

Fig. 74. ^{13}C-NMR spectrum of altissimacoumarin K (**9**)

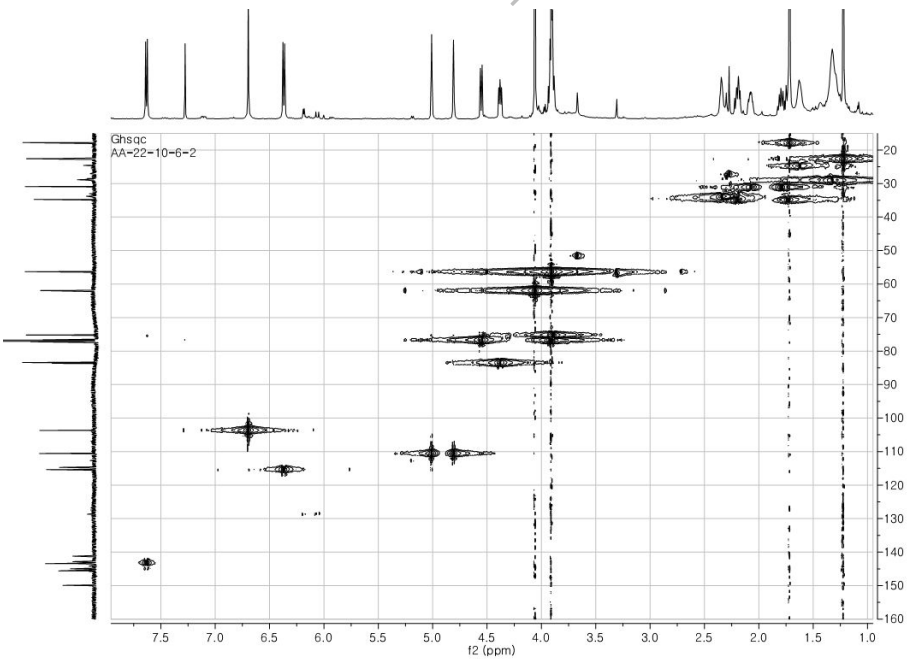

Fig. 75. HSQC spectrum of altissimacoumarin K (**9**)

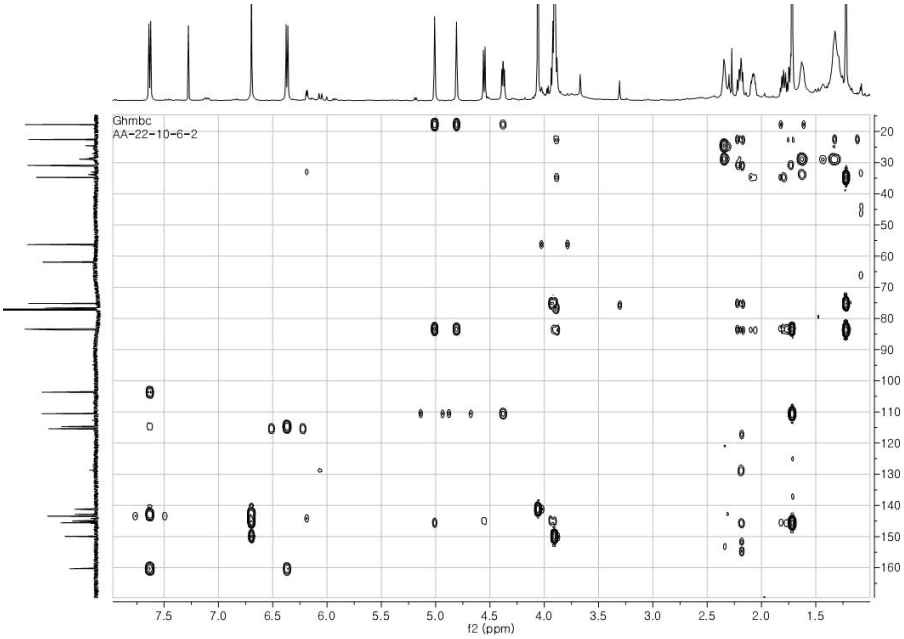

Fig. 76. HMBC spectrum of altissimacoumarin K (**9**)

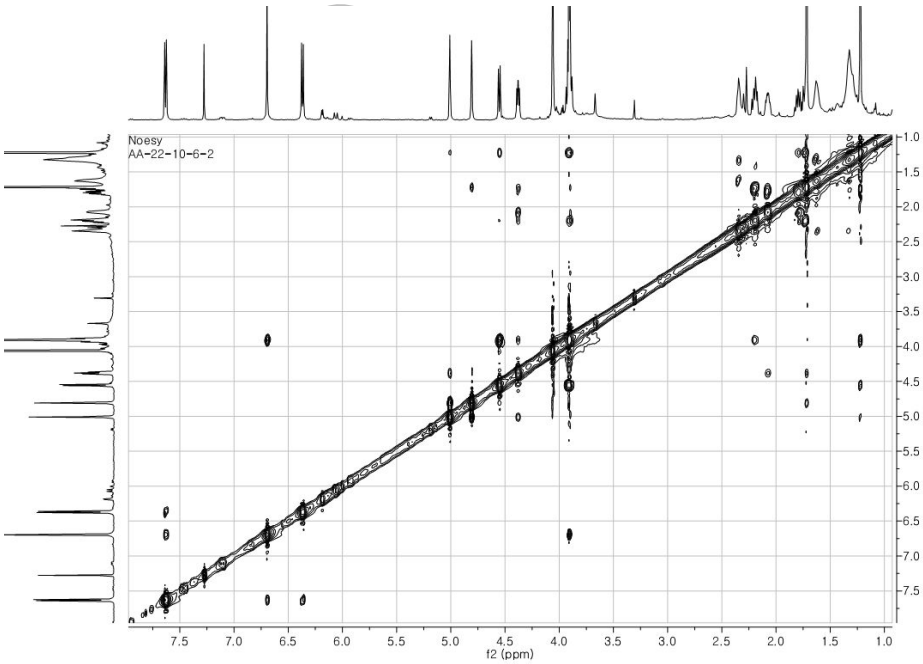

Fig. 77. NOESY spectrum of altissimacoumarin K (**9**)

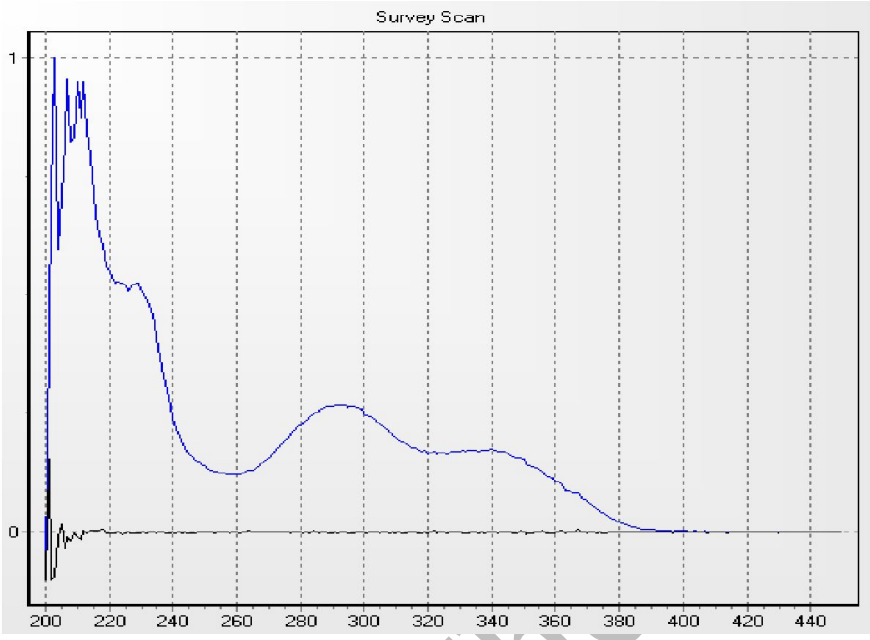

Fig. 78. UV spectrum of altissimacoumarin K (**9**)

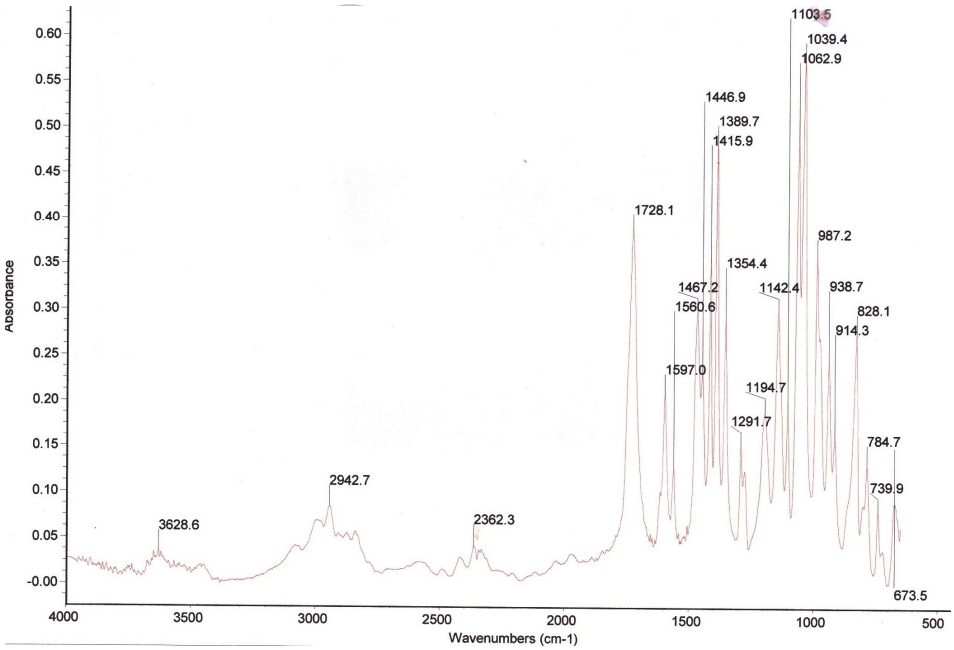

Fig. 79. IR spectrum of altissimacoumarin K (**9**)

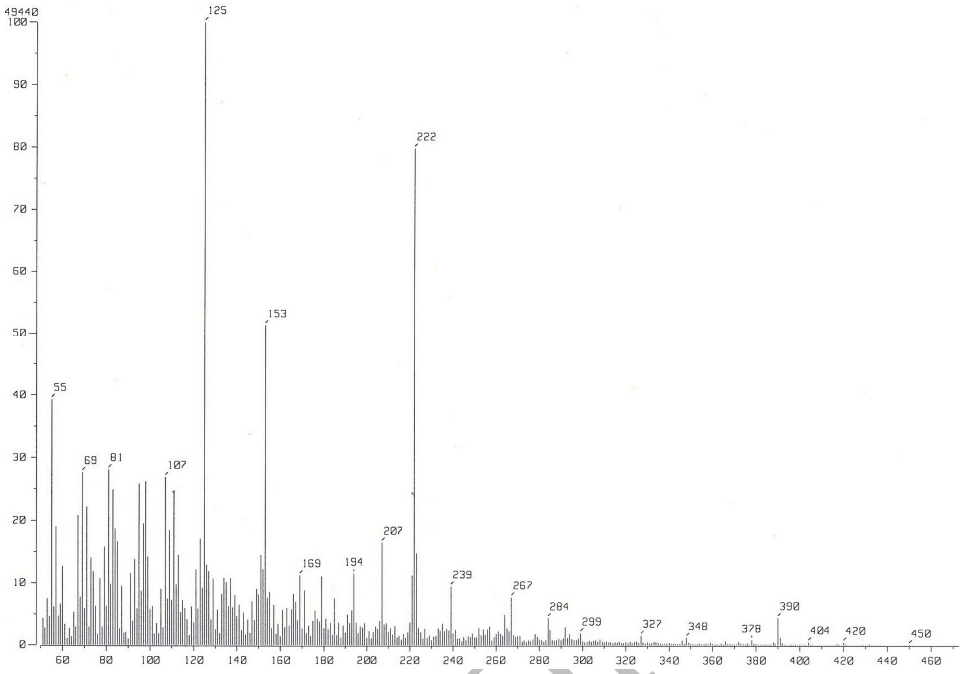

Fig. 80. EIMS spectrum of altissimacoumarin K (**9**)

Table 9. ^{1}H and ^{13}C-NMR data of altissimacoumarin K (**9**)[a] (in $CDCl_3$)

Position	δ_H mult. (*J* in Hz)	δ_C	HMBC (H→C)
		160.3	
3	6.37 d (9.5)	115.4	C-2, C-4, C-10
4	7.63 d (9.5)	143.4	C-2, C-3, C-5, C-9, C-10
5	6.70 s	103.7	C-4, C-6, C-7, C-9, C-10
6		149.9	
7		144.9	
8		141.2	
9		142.8	
10		114.7	
1′	4.56 dd (10.0, 3.0)	76.6	C-7, C-2′
	3.92 dd (10.0, 8.0)		C-7, C-2′, C-3′
2′	3.87 m	75.2	C-1′, C-3′, C-9′
3′		83.7	
4′	2.20 m	34.7	C-3′, C-6′, C-9′
	1.75 m		C-3′, C-5′, C-6′, C-9′
5′	2.10 m	30.9	C-3′, C-4′, C-6′, C-7′
	1.78 m		C-3′, C-4′, C-6′
6′	4.38 dd (8.5, 6.0)	83.4	C-5′, C-7′, C-8′, C-10′
7′		145.6	
8′	5.01 s	110.6	C-6′, C-7′, C-10′
	4.81 s		C-6′, C-7′, C-10′
9′	1.22 s	22.6	C-2′, C-3′, C-4′
10′	1.71 s	17.8	C-6′, C-7′, C-8′
OCH_3-6	3.91 s	56.3	C-6
OCH_3-8	4.06 s	61.9	C-8
OH-2′	3.31 s		C-2′

[a] Assignments were based on HSQC, HMBC experiments.

1.5. Stimulatory effects of the isolated compounds on SIRT1 activity

SIRT1, a mammalian ortholog of yeast Sir2, binds to and deacetylates p53 at the K382 residue, thereby negatively regulating p53-mediated transcriptional activation, which prevents the cellular senescence and apoptosis caused by DNA damage and stress (Langley *et al*., 2002; Kim *et al*., 2007). To evaluate the effects of the isolated compounds on SIRT1, the in vitro enzymatic deacetylation and the p53 transcription activities were determined. In a bioluminescence assay that measures deacetylated peptide signals via the consumption of NAD^+ (Liu *et al*., 2008), all tested compounds increased the observation of deacetylated substrate, except for compound **10**, a non-terpenylated coumarin (**Fig. 81**). Moreover, after co-transfection with p53-luc and SIRT1 into HEK293 cells, treatment with compounds **1**–**4** or resveratrol (10 μM) strongly decreased p53 transcriptional activity compared to the control (**Fig. 82**).

Since these compounds induced an increase in SIRT1 enzymatic activity and a decrease in p53 transcriptional activity, their direct effects on SIRT1 deacetylation activity were confirmed by determining the actual level of substrate used in the SIRT1 reaction using a NAD/NADH assay. As shown in **Fig. 83A** and **83B**, the SIRT1 deacetylation activity was increased in a dose-dependent manner in both in vitro and in vivo assays. Interestingly, these compounds also increased the NAD-to-NADH ratio by more than 50% (**Fig. 83C**), further supporting the catalytic activity of SIRT1 in vivo (Houtkooper *et al*., 2009; Um *et al*., 2010).

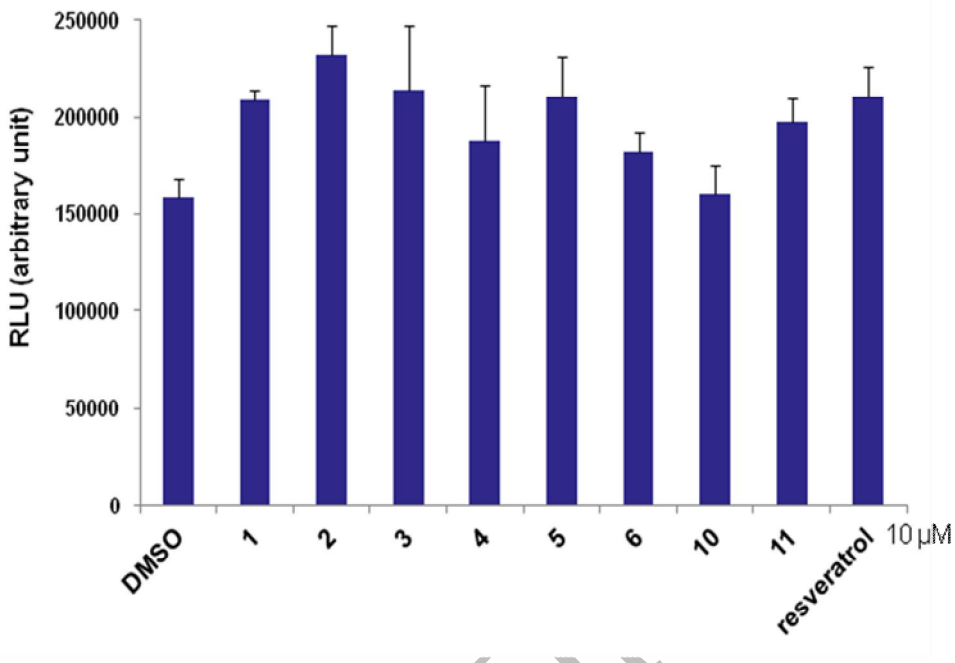

Fig. 81. The effects of isolated compounds on SIRT1 enzymatic activity with p53 peptide substrate determined by a bioluminescence assay.

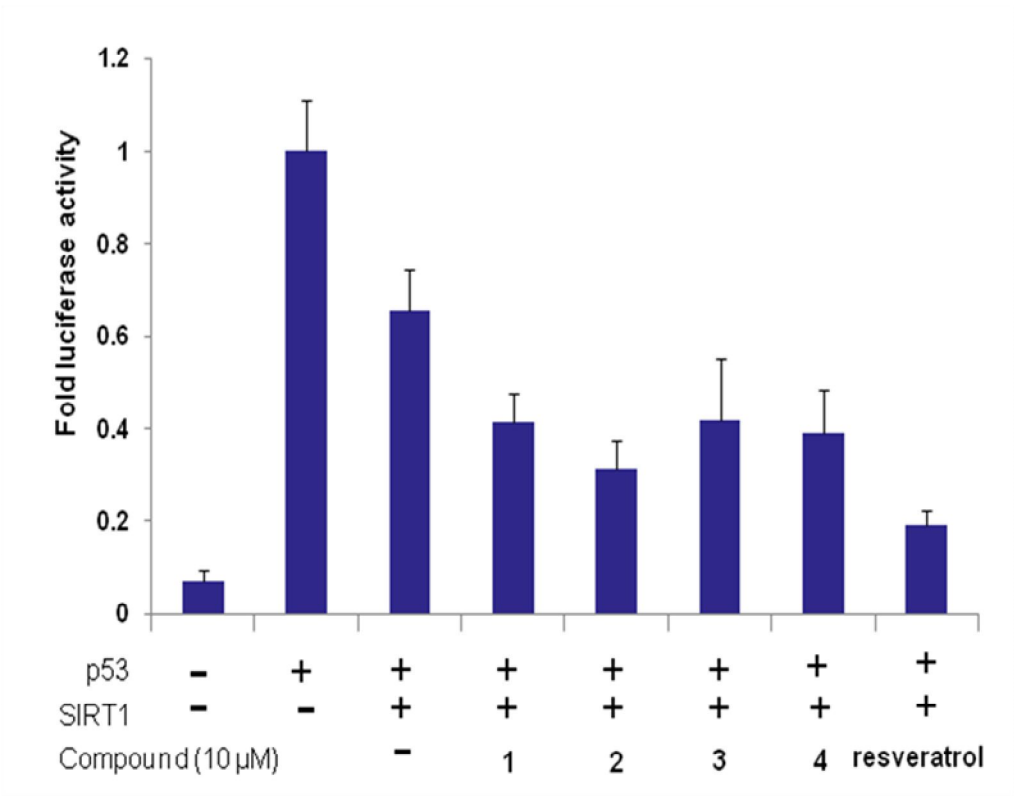

Fig. 82. The effects of **1**–**4** on the transcription activity of p53 in HEK293 cells. The cells were transfected with p53-luc, myc-p53, flag-SIRT1 and *β*–gal vectors. After 1 day, cells were treated with the compounds and resveratrol for 12 h. Data are presented as means ± standard deviation of triplicate experiments.

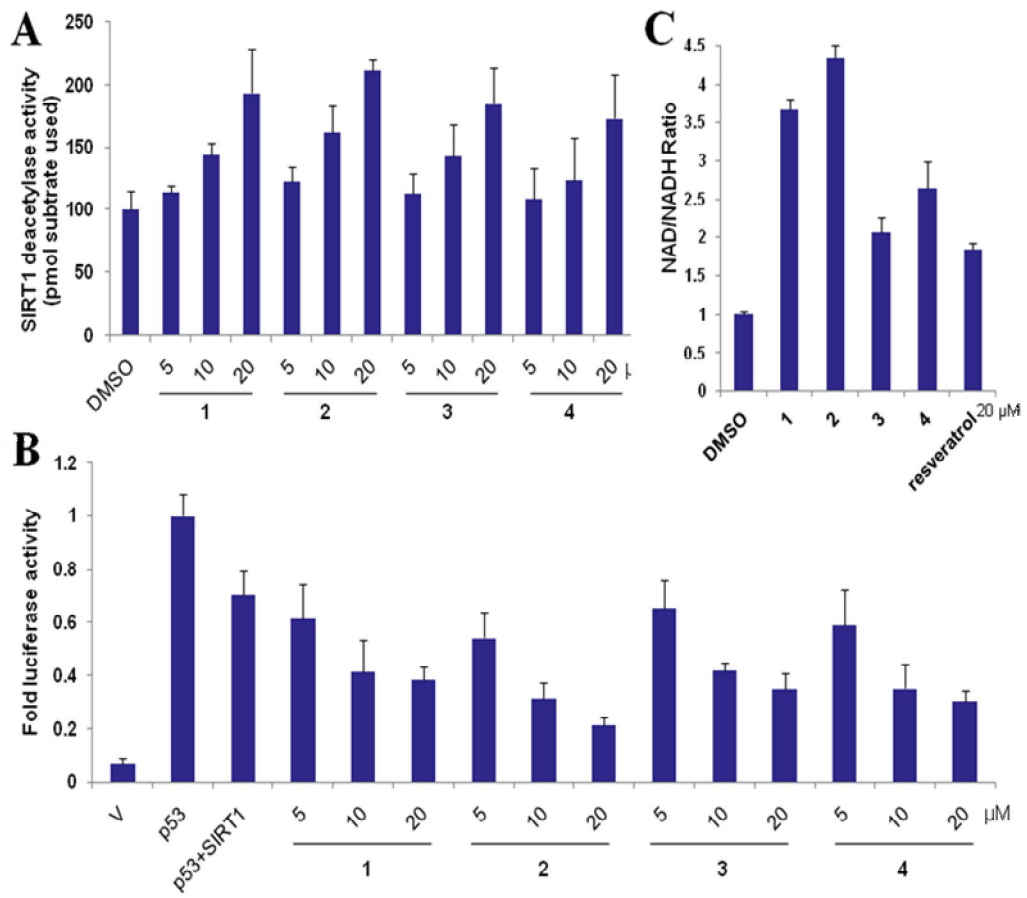

Fig. 83. Compounds **1**–**4** increased the SIRT1 deacetylation activity (A and B), and the intracellular NAD-to-NADH ratio in HEK293 cells (C) in a dose-dependent manner.

2. Isolation of SIRT1 activators from *Curcuma longa*

2.1. Introduction

C. longa is a plant belonging to Zingiberaceae family, which is found in south and southeast tropical Asia (Ammon & Wahl, 1991). Its rhizome is used as a spice (main ingredient of curry), a pigment dye of textiles, and in traditional medicine. Two fundamental groups of compounds from this plant are curcuminoids and sesquiterpenes (Nishiyama *et al*., 2005), in which curcuminoids with several pharmacological activities including cardiovascular protection, antitumor, antioxidant, anti-inflammatory, anti-Alzheimer, anti-hepatotoxic, and antiviral have been reported (Chen *et al*., 2010; Miriyala *et al*., 2007; Park & Kim, 2002; Simon *et al*., 1998; Masuda *et al*., 1993).

2.2. Plant material

The rhizomes of *C. longa* were purchased from Kangwon Herbal Medicine Company (Kangwon-do, Republic of Korea), in August 2010 and botanically identified by Prof. Y. H. Moon. A voucher specimen (CU2010–06) has been deposited at the Herbarium of Chosun University, Gwangju, Republic of Korea.

2.3. Extraction and isolation

The dried rhizomes of *C. longa* (4.0 kg) were extracted with MeOH (15.0 L × 3 times) at room temperature for a week. The combined MeOH extract was then concentrated to yield a dry residue (420.0 g). This crude extract was suspended in H_2O (2.5 L) and partitioned successively with *n*-hexane (3 × 2.0 L), EtOAc (3 × 2.0 L), and BuOH (3 × 2.0 L). The EtOAc and BuOH soluble fractions, which exhibited strong SIRT1 activity, were combined (160.0 g) and chromatographed over a silica gel column (15 × 30 cm; 63–200 μm particle size) eluting with gradient solvent chloroform/acetone (19:1, 18:2…1:19, each 2.5 L), to yield seven fractions (F1: 20.6 g; F2: 16.4 g; F3: 8.3 g; F4: 13.8 g; F5: 14.5 g; F6: 18.6 g; F7: 27.8 mg) based on the TLC profile. The crystallization of fraction F3 from *n*-hexane/EtOAc afforded compound **13** (curcumin, 5.8 g). Fraction F4 was further applied to a normal-phase silica gel column (7 × 40 cm; 40–63 μm particle size) with a stepwise gradient of chloroform/MeCN (9:1, 8:2…1:9, each 2.0 L) to afford five subfractions (F4.1–F4.5). Crystallization of subfractions F4.2 and F4.3 from chloroform gave compound **4** (demethoxycurcumin, 1.7 g) and compound **5** (bisdemethoxycurcumin, 2.9 g), respectively. Fraction F4.4 (150.0 mg) was separated by HPLC [Optima Pak C_{18} column (10 × 250 mm, 10 μm particle size, RS Tech, Korea);

mobile phase MeCN in H_2O containing 0.1% HCO_2H (0–40 min: 45% MeCN, 40–45 min: 100% MeCN, 45–55 min: 100% MeCN); flow rate 2 mL/min; UV detection at 205 and 254 nm] to give compound **8** (t_R = 30.0 min, 7.5 mg) and compound **10** (t_R = 34.0 min, 16.0 mg). Fraction F5 was chromatographed over a Sephadex LH-20 column (7 × 40 cm) using MeOH as the eluting solvent to afford three subfractions (F5.1–F5.3). Subfraction F5.2 (7.5 g) was further chromatographed over a silica gel column (5 × 40 cm; 40–63 μm particle size) with a gradient solvent of chloroform/MeCN (9:1, 8:2…1:9, each 2.5 L) to yield eight fractions (F5.2.1–F5.2.8). Subfraction F5.2.2 (190.0 mg) was purified by HPLC (0–45 min: 60% MeCN, 45–50 min: 100% MeCN) to yield compound **9** (t_R = 35.0 min, 13.5 mg) and compound **11** (t_R = 38.5 min, 15.0 mg). Further separation of F5.2.3 (160.0 mg) by HPLC (0–65 min: 57% MeCN, 65–70 min: 100% MeCN) resulted in the isolation of compound **6** (t_R = 42.0 min, 12.5 mg), compound **7** (t_R = 58.0 min, 8.0 mg), and compound **14** (t_R = 61.0 min, 7.0 mg). Compound **1** (t_R = 46.0 min, 7.5 mg), compound **2** (t_R = 48.5 min, 6.0 mg), and compound **12** (t_R = 52.0 min, 8.5 mg) were obtained from subfraction F5.2.4 (120.0 mg) by HPLC (0–60 min: 35% MeCN, 60–65 min: 100% MeCN). Finally, compound **3** (t_R = 38.0 min, 15.5 mg) was purified from subfraction F5.2.5 (140.0 mg) by HPLC (0–45 min: 30% MeCN, 45–50 min: 100% MeCN).

*Curcumalongin A (**1**):* yellow amorphous powder; UV (MeOH) λ_{max} nm (log ε) 295 (3.53), 398 (4.06); IR (KBr) ν_{max} 3415 (OH), 1665 (C=O), 1598, 1547, 1511, 1489, 1273 cm^{-1}; ^1H (500 MHz) and ^{13}C (125 MHz) NMR data, see **Table 10**; EIMS *m/z*: 352 ($[M]^+$, 100), 322 (59), 278 (22), 267 (20), 191 (52), 180 (28), 150 (27); HRFABMS *m/z* 353.1022 $[M+H]^+$ (calcd for $C_{20}H_{17}O_6$, 353.1025).

*Curcumalongin B (**2**):* yellow amorphous powder; UV (MeOH) λ_{max} nm (log

ε) 290 (3.76), 410 (4.12); IR (KBr) ν_{max} 3416 (OH), 1665 (C=O), 1588, 1547, 1512, 1490, 1284 cm^{-1}; ^{1}H (500 MHz) and ^{13}C (125 MHz) NMR data, see **Table 11**; EIMS *m/z*: 382 ($[M]^+$, 100), 352 (20), 322 (8), 308 (10), 278 (6), 267 (9), 245 (12), 191 (10), 180 (24); HREIMS *m/z* 382.1054 $[M]^+$ (calcd for $C_{21}H_{18}O_7$, 382.1053).

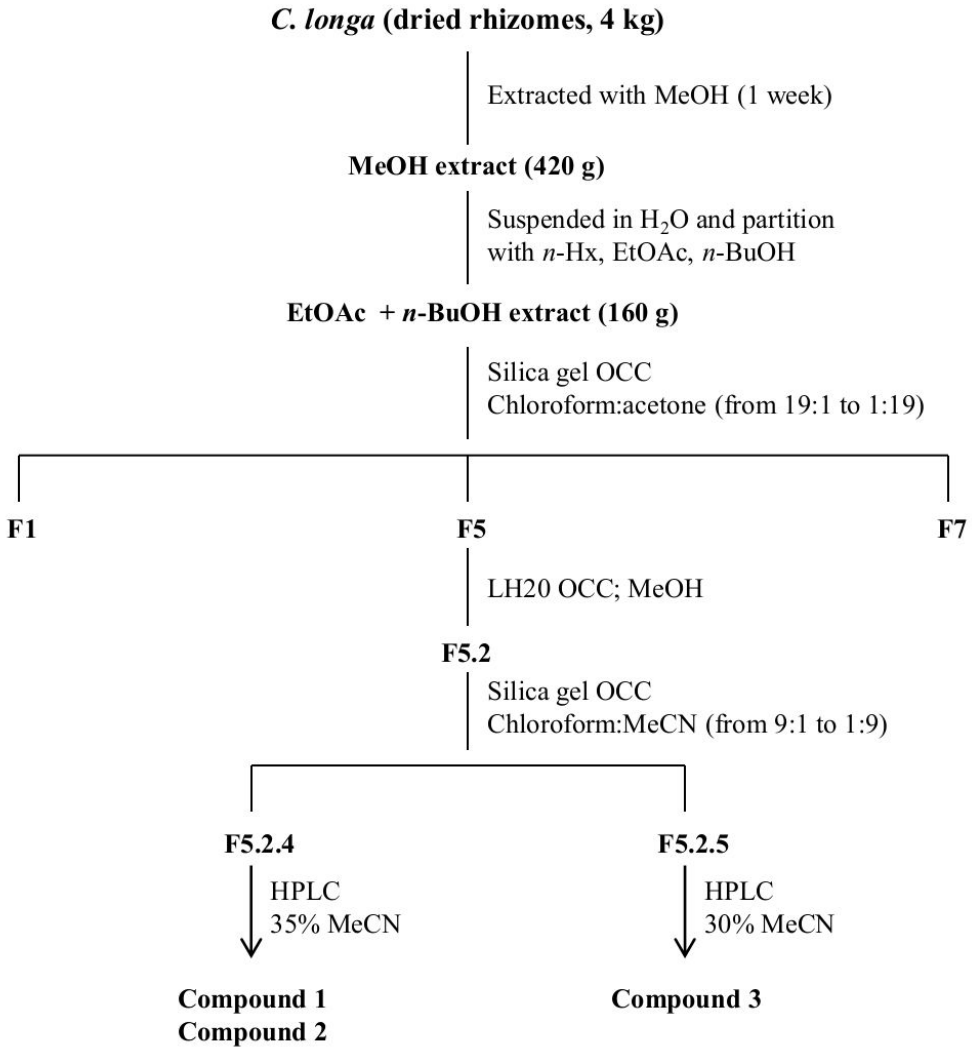

Scheme 2. Isolation of new compounds (**1**–**3**) from *C. longa*

Curcumalongin D (3): Yellow amorphous powder; $[\alpha]_D^{25}$ +13 (*c* 0.1, MeOH); UV (MeOH) λ_{max} nm (log ε) 280 (3.83), 390 (4.06); IR (KBr) ν_{max} 3418 (OH), 2937, 1610, 1516, 1271, 1083 cm^{-1}; CD (MeOH, Δε) λ_{max} 218 (-12.41), 208 (+6.57); ^1H (500 MHz) and ^{13}C (125 MHz) NMR data, see **Table 12**; EIMS *m/z*: 390 ($[M-H_2O]^+$, 10), 327 (3), 284 (9), 267 (14), 239 (5), 192 (8), 137 (100); HREIMS *m/z* 390.1678 $[M-H_2O]^+$ (Calcd for $C_{21}H_{26}O_7$, 390.1679).

Fig. 84. Chemical structures of known compounds isolated from *C. longa*

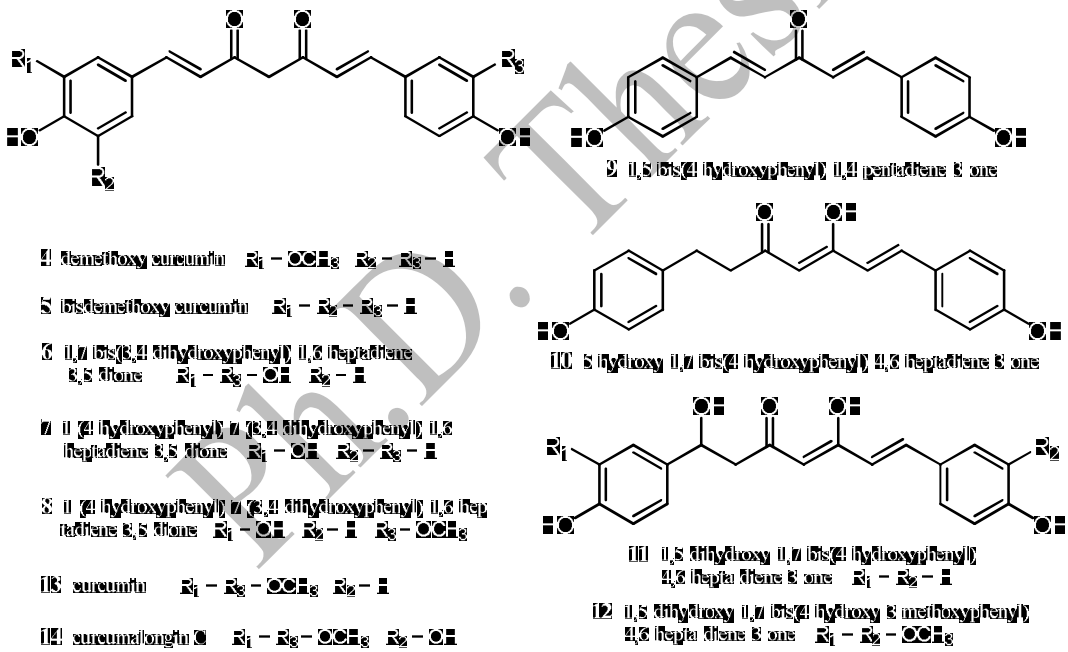

2.4. Structural determination of new compounds isolated from *C. longa*

In order to isolate the compounds with stimulating SIRT1 activity, the methanol extract of *C. longa* was subjected to a succession of chromatographic procedures including silica gel chromatography, Shephadex LH-20, RP-C18, and HPLC to afford

fourteen compounds, including 3 new (**1**–**3**) and 11 known (**4**–**14**) curcumin derivatives (Jayaprakasha *et al*., 2002; Venkateswarlu *et al*., 2005; Li *et al*., 2009; Masuda *et al*., 1993; Dao *et al*., 2012) (**Fig. 84**).

2.4.1. Structural determination of compound 1

Compound **1** was obtained as a yellow amorphous powder. The ^{1}H NMR spectrum (**Table 10**) showed a 1,3,4,5-tetrasubstituted benzene ring [δ_H 7.23 (1H, d, J = 1.8 Hz, H-2′) and 7.21 (1H, d, J = 1.8 Hz, H-6′)], a set of A_2B_2 aromatic protons [δ_H 7.63 (2H, d, J = 8.4 Hz, H-2", H-6") and 6.94 (2H, d, J = 8.4 Hz, H-3", H-5")], a pair of *trans*-olefinic protons [δ_H 7.67 (1H, d, J = 15.6 Hz, H-7") and 7.08 (1H, d, J = 15.6 Hz, H-8")], a methoxy group [δ_H 3.99 (3H, s, 3′-OCH_3)], an alkene proton [δ_H 6.52 (1H, s, H-7′)], and a proton on the central carbon of *β*-diketone in their enol form δ_H 5.92 (1H, s, H-4). Consistent with the above ^{1}H NMR analysis, the ^{13}C NMR spectrum displayed signals corresponding to the methoxy group at δ_C 56.5, four olefinic carbons at δ_C 146.7, 139.3, 113.3 and 112.2, a conjugated ketone at δ_C 186.6, a hydroxylated olefinic carbon at δ_C 176.1, the central carbon of *β*-diketone at δ_C 105.4, and twelve carbons of two aromatic rings. These protonated carbons and their bonded protons, which were determined unambiguously by the HMQC experiment, showed the presence of 20 carbons of a curcuminoid skeleton (Li *et al*., 2009). In addition, the deshielding of both the two olefinic carbons at δ_C 146.7 (C-2) and 176.1 (C-5) indicated their linkage to an oxygen atom. These observations with the presence of characteristic absorption bands in the IR (1665, 1598 cm^{-1}) and UV (398, 295 nm) spectra, suggested the existence of a 3(2*H*)-furanone moiety instead of a linkage fragment (-C=CH-CO-CH=C(OH)-CH=CH-) like in curcuminoid

derivatives (Comte *et al.*, 1996; Gershenzon & Mabry, 1984). This was confirmed by HMBC correlations between H-4/C-2, C-3 and C-5 (**Fig. 85**), and further supported by the quasi-molecular ion peak at *m/z* 353.1022 [M+H] in the HRFABMS, which indicated the molecular formula of $C_{20}H_{16}O_6$. The HMBC correlations from H-7′ to C-2, C-3, C-2′, and C-6′, and from H-2′ and H-6′ to C-7′ suggested that the 1,3,4,5-tetrasubstituted aromatic ring was linked to C-2 of the furanone ring through olefinic carbon C-7′. Finally, the substituted pattern of two benzen rings at C-7′ and C-7" were deduced from full assignments based on HMQC and key HMBC correlations as shown in **Fig. 85**. Thus, the structure of compound **1** was identified as 2-(4,5-dihydroxy-3-methoxyphenyl)methenyl-5-(4-hydroxyphenyl)ethenyl-3(2*H*)-furanone, and it was named as curcumalongin A.

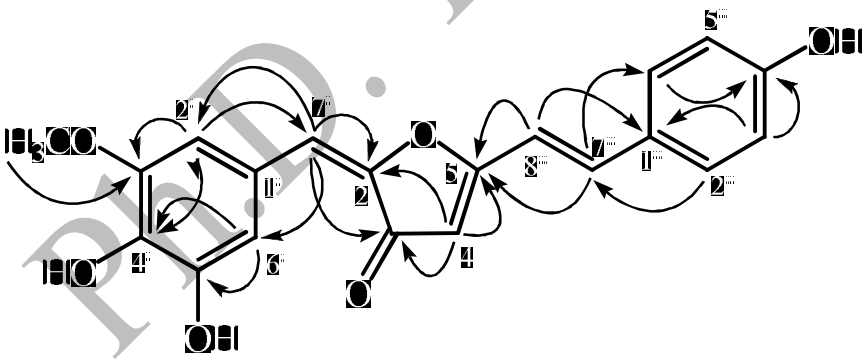

Fig. 85. Key HMBC (H→C) correlations of curcumalongin A (**1**)

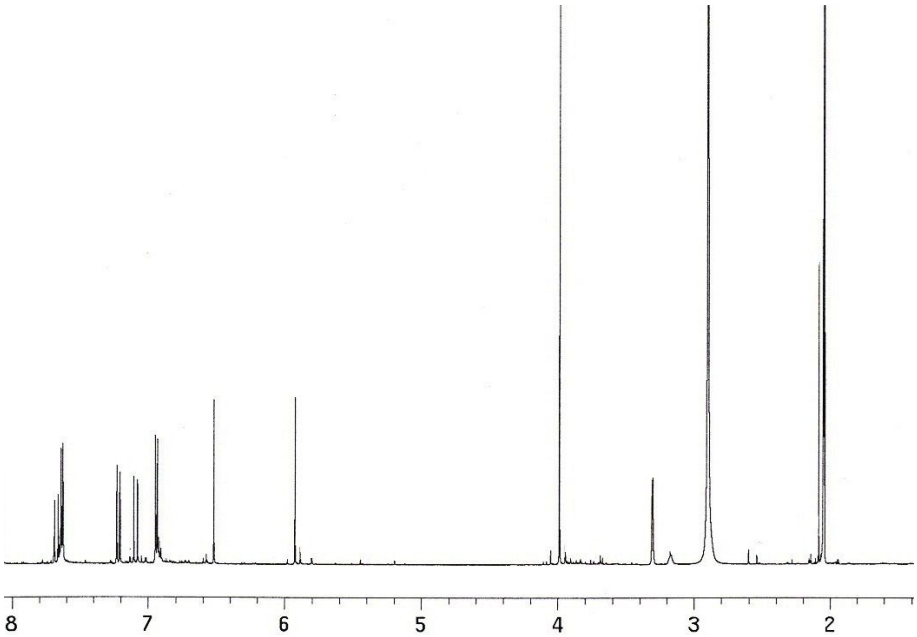

Fig. 86. ^{1}H-NMR spectrum of curcumalongin A (**1**)

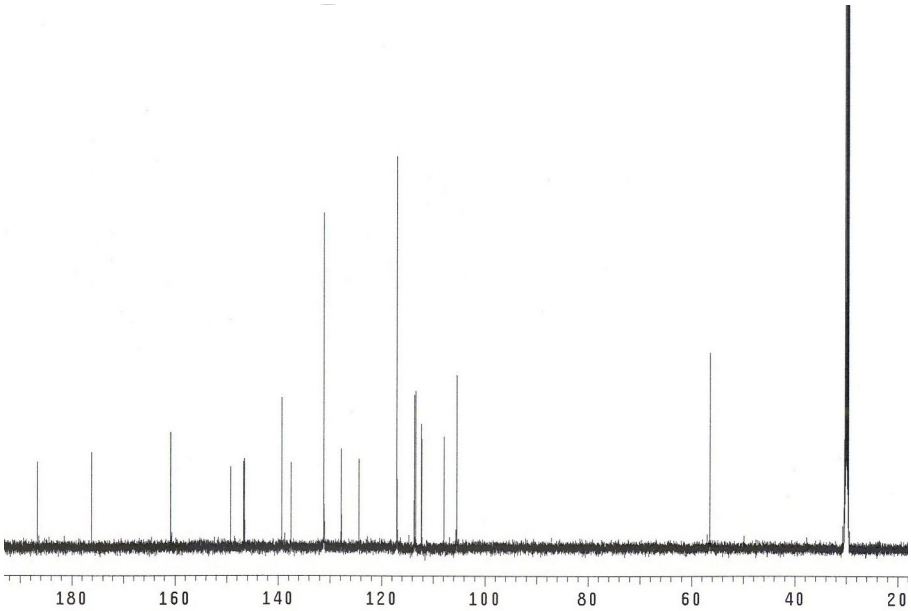

Fig. 87. ^{13}C-NMR spectrum of curcumalongin A (**1**)

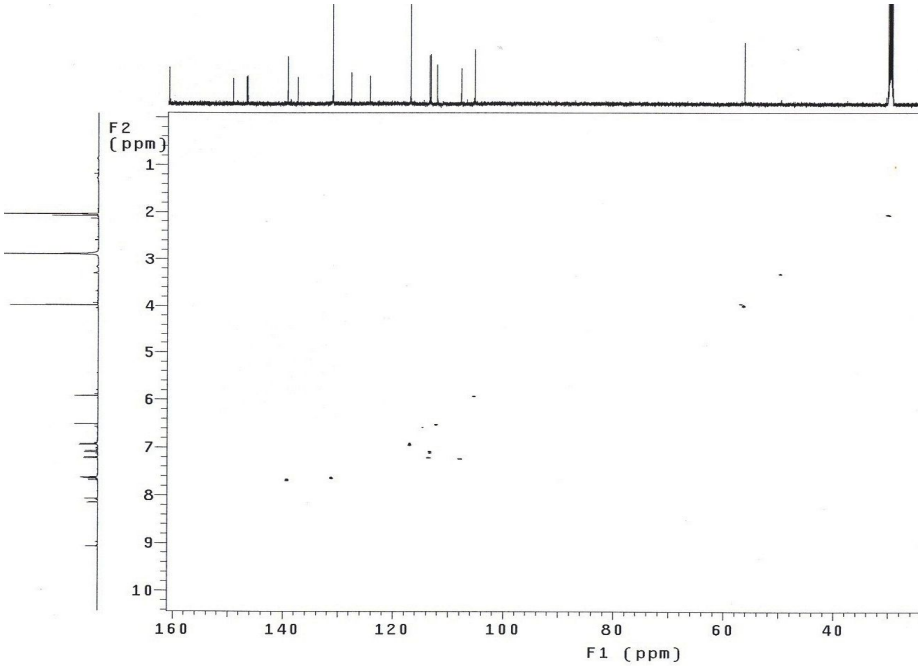

Fig. 88. HSQC spectrum of curcumalongin A (**1**)

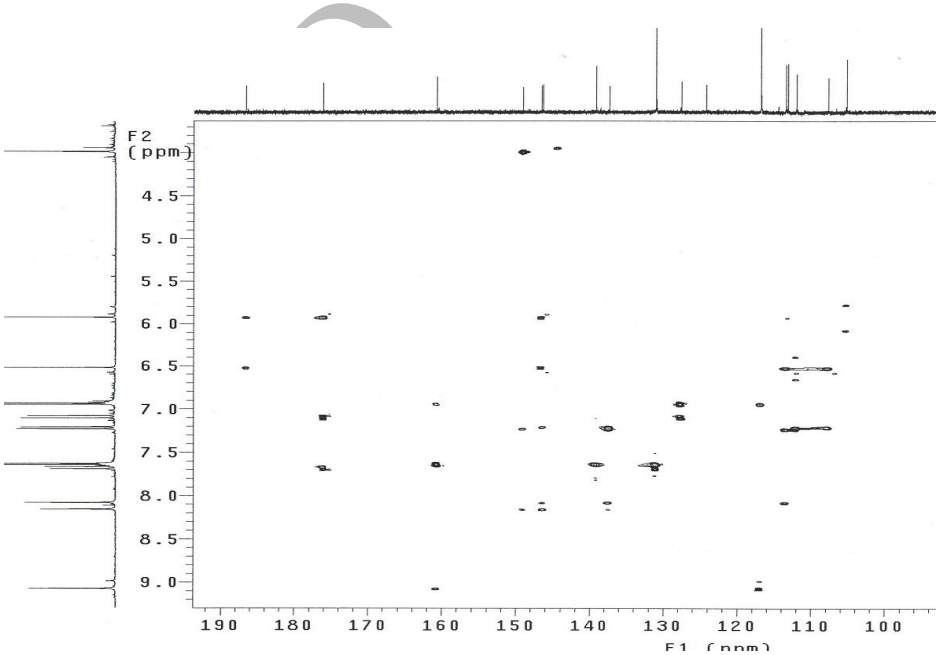

Fig. 89. HMBC spectrum of curcumalongin A (**1**)

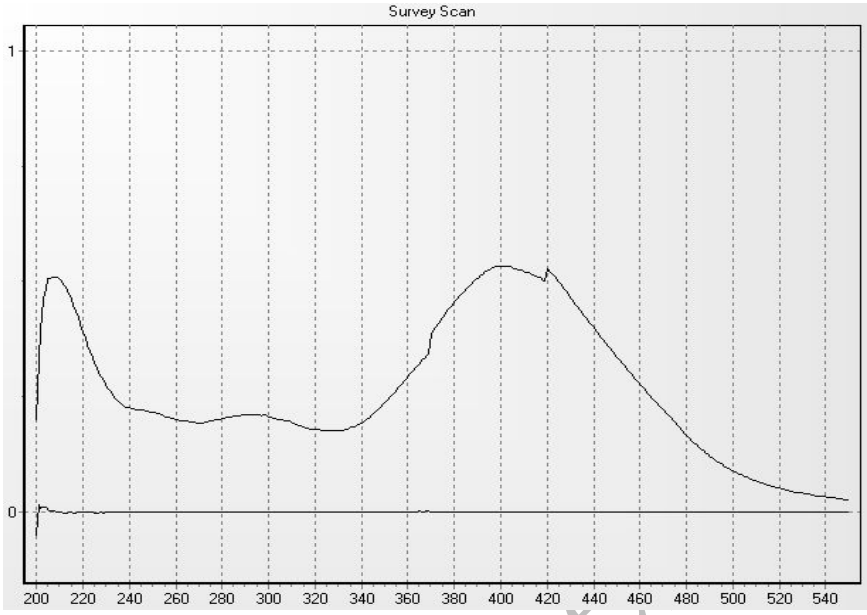

Fig. 90. UV spectrum of curcumalongin A (**1**)

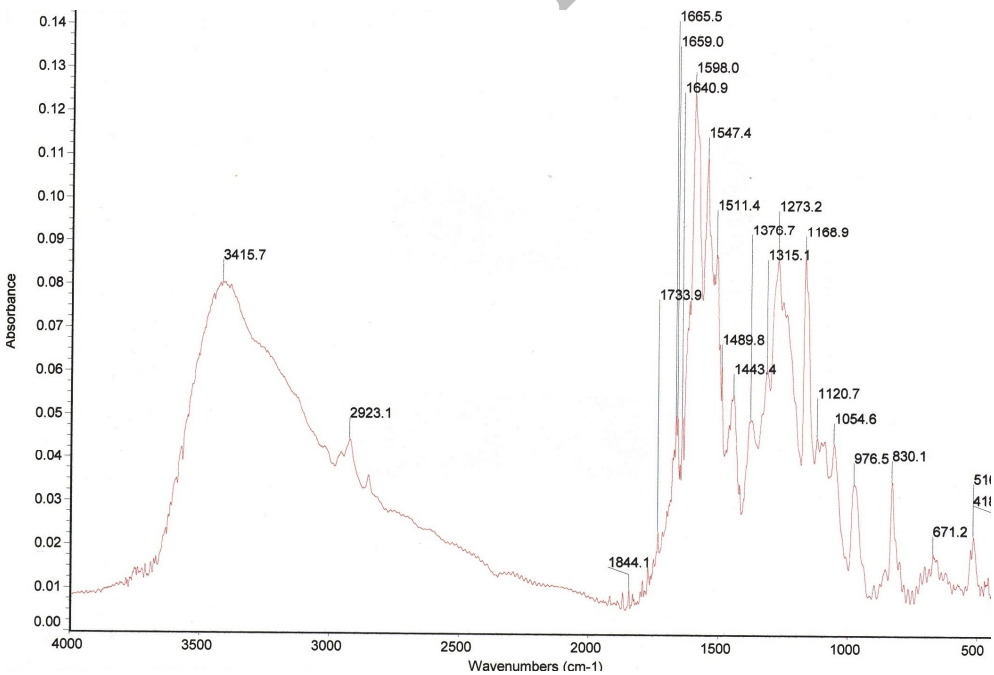

Fig. 91. IR spectrum of curcumalongin A (**1**)

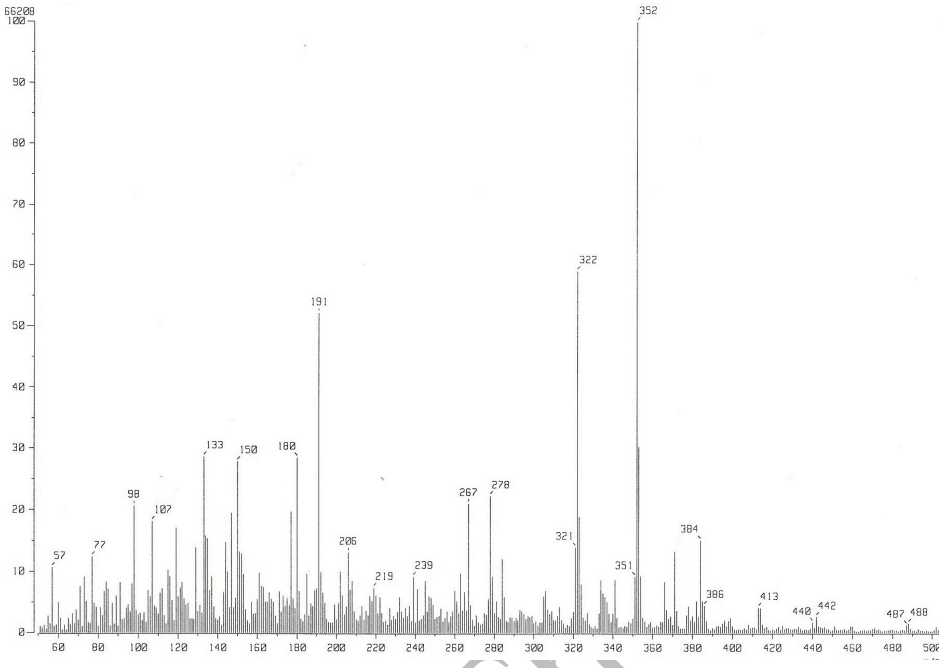

Fig. 92. EIMS spectrum of curcumalongin A (**1**)

Table 10. ^{1}H and ^{13}C-NMR data of curcumalongin A (**1**)[a] (in CD_3COCD_3)

Position	δ_H mult. (*J* in Hz)	δ_C	HMBC (H→C)
2		146.7	
3		186.6	
4	5.92 s	105.4	C-2, C-3, C-5
5		176.1	
6			
7			
1′		124.4	
2′	7.23 d (1.8)	107.9	C-1′, C-3′, C-4′, C-6′, C-7′
3′		149.2	
4′		137.5	
5′		146.5	
6′	7.21 d (1.8)	113.6	C-1′, C-4′, C-5′, C-7′
7′	6.52 s	112.2	C-2, C-3, C-1′, C-2′, C-6′
1"		127.7	
2"	7.63 d (8.4)	131.2	C-1", C-3", C-4", C-7"
3"	6.94 d (8.4)	117.0	C-1", C-2", C-4"
4"		160.8	
5"	6.94 d (8.4)	117.0	C-1", C-4", C-6"
6"	7.63 d (8.4)	131.2	C-1", C-4", C-5", C-7"
7"	7.67 d (15.6)	139.3	C-5, C-1", C-2", C-6", C-8"
8"	7.08 d (15.6)	113.3	C-4, C-5, C-1", C-7"
3′-OCH_3	3.99 s	56.5	C-3′

[a] Assignments were based on HSQC, HMBC experiments.

2.4.2. Structural determination of compound 2

Compound **2** was obtained as a yellow amorphous powder. A molecular formula of $C_{21}H_{18}O_7$ was determined from the molecular ion peak at *m/z* 382.1051 $[M]^+$ (calcd for $C_{21}H_{18}O_7$, 382.1053) in HREIMS. Its IR spectrum revealed the presence of a hydroxy group (3416 cm^{-1}), conjugated carbonyl group (1665 cm^{-1}), and aromatic ring (1588, 1547, 1512, and 1490 cm^{-1}). The ^1H and ^{13}C NMR spectra data of **2** (**Table 11**) were similar to those of **1**, except for signals due to an additional methoxy group at δ_H 3.99 (3H, s, 3"-OCH_3) and an ABX spin system [δ_H 7.43 (1H, d, *J* = 1.8 Hz, H-2"), 7.20 (1H, dd, *J* = 8.4, 1.8 Hz, H-6") and 6.91 (1H, d, *J* = 8.4 Hz, H-5")] instead of the A_2B_2 aromatic protons on benzene ring of **1**. The HMBC correlations from the methoxy proton and aromatic protons (H-2" and 5") to carbon C-3" (δ_C 149.2) indicated that the additional methoxy group was attached to C-3". Therefore, the structure of compound **2**, curcumalongin B, was determined to be 2-(4,5-dihydroxy-3-methoxyphenyl)methenyl-5-(4-hydroxy-3-methoxyphenyl)ethenyl-3(2*H*)-furanone.

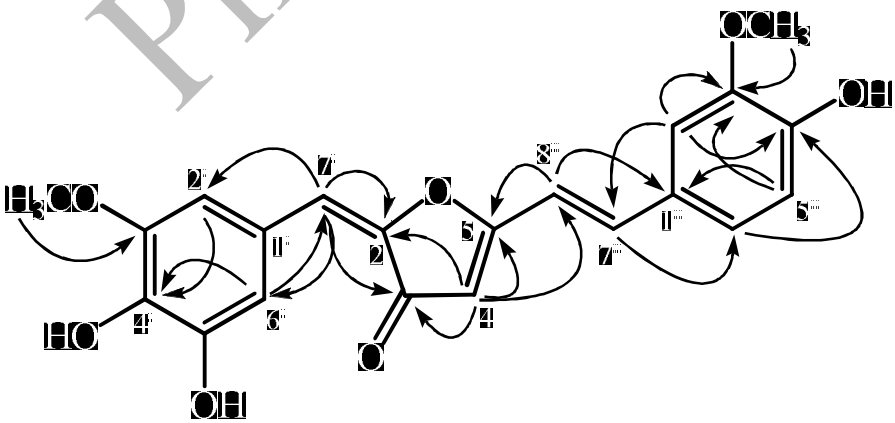

Fig. 93. Key HMBC (H→C) correlations of curcumalongin B (**2**)

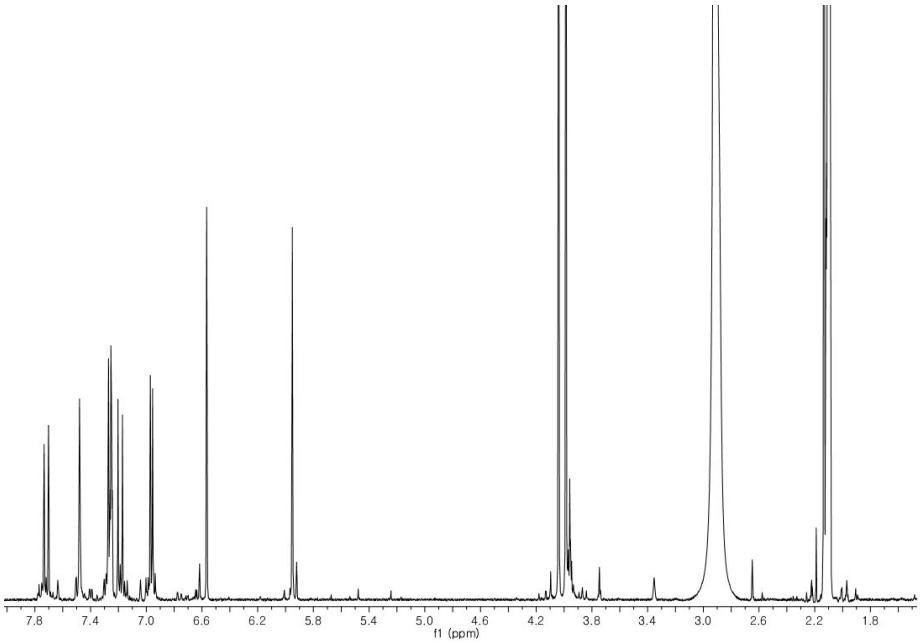

Fig. 94. ^{1}H-NMR spectrum of curcumalongin B (**2**)

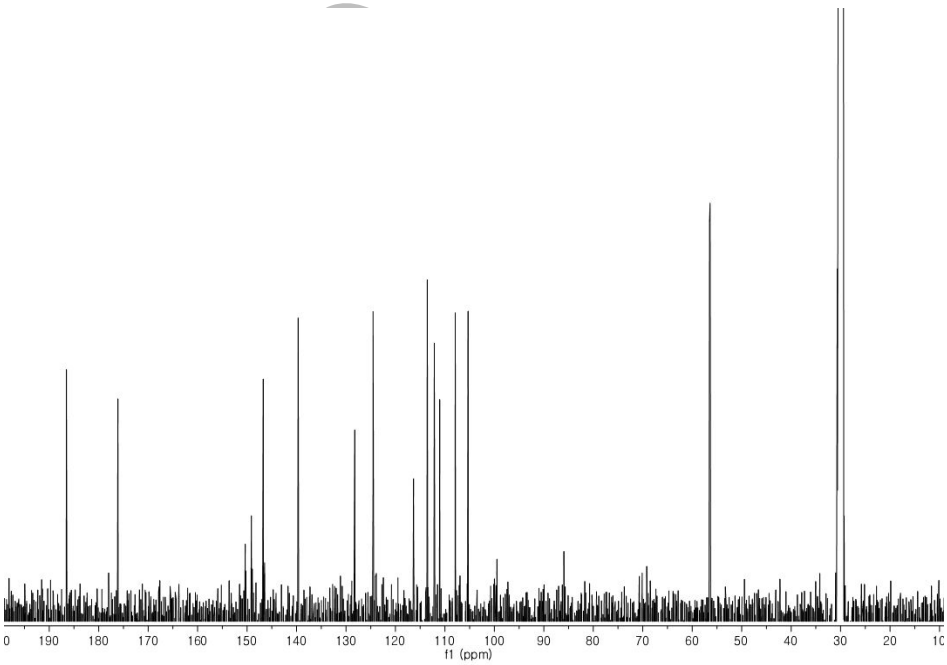

Fig. 95. ^{13}C-NMR spectrum of curcumalongin B (**2**)

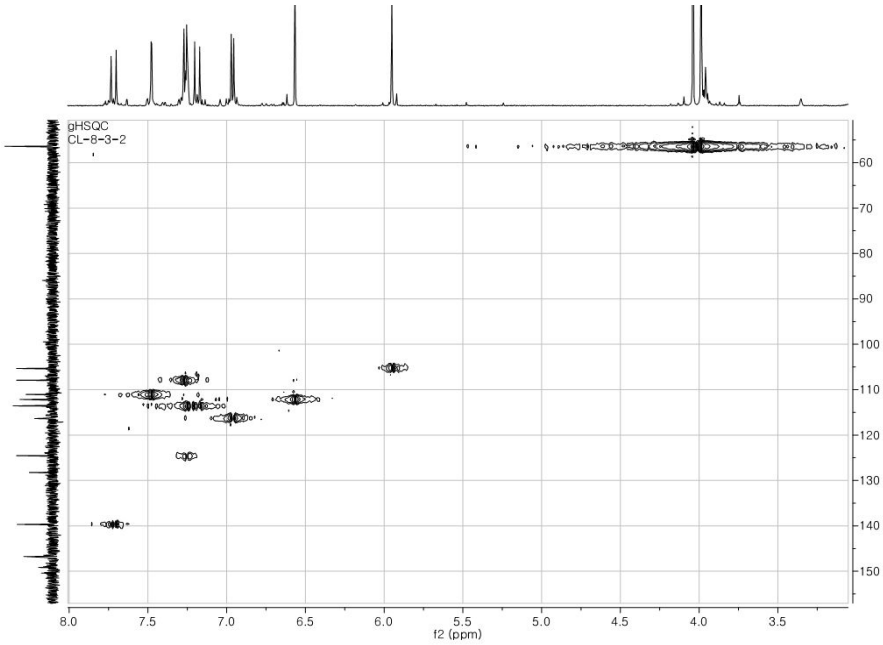

Fig. 96. HSQC spectrum of curcumalongin B (**2**)

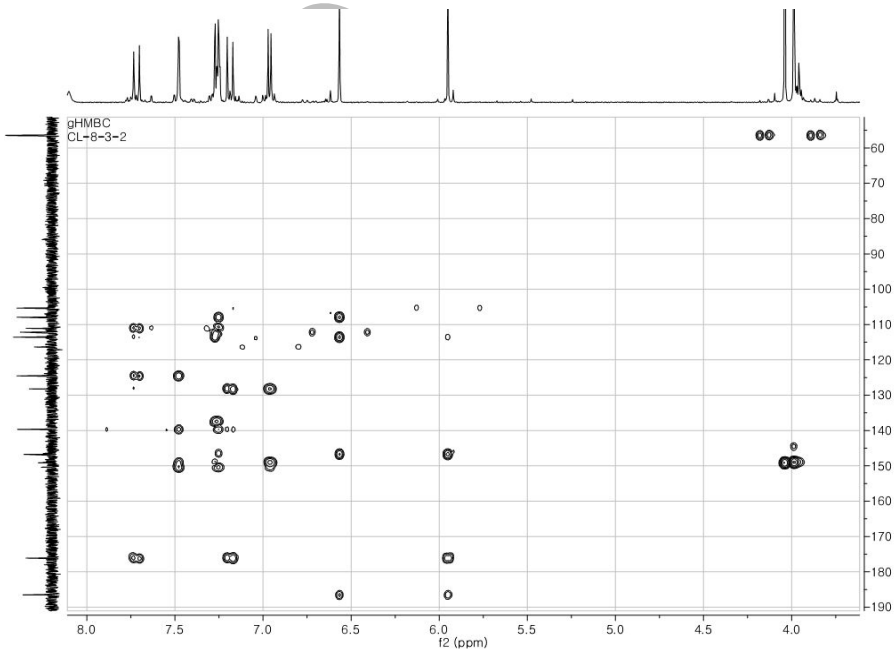

Fig. 97. HMBC spectrum of curcumalongin B (**2**)

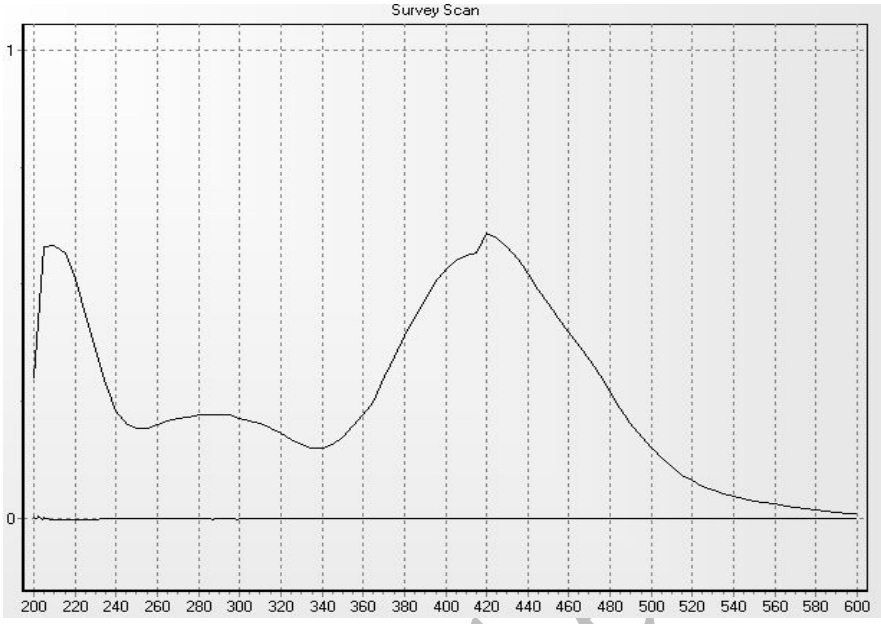

Fig. 98. UV spectrum of curcumalongin B (**2**)

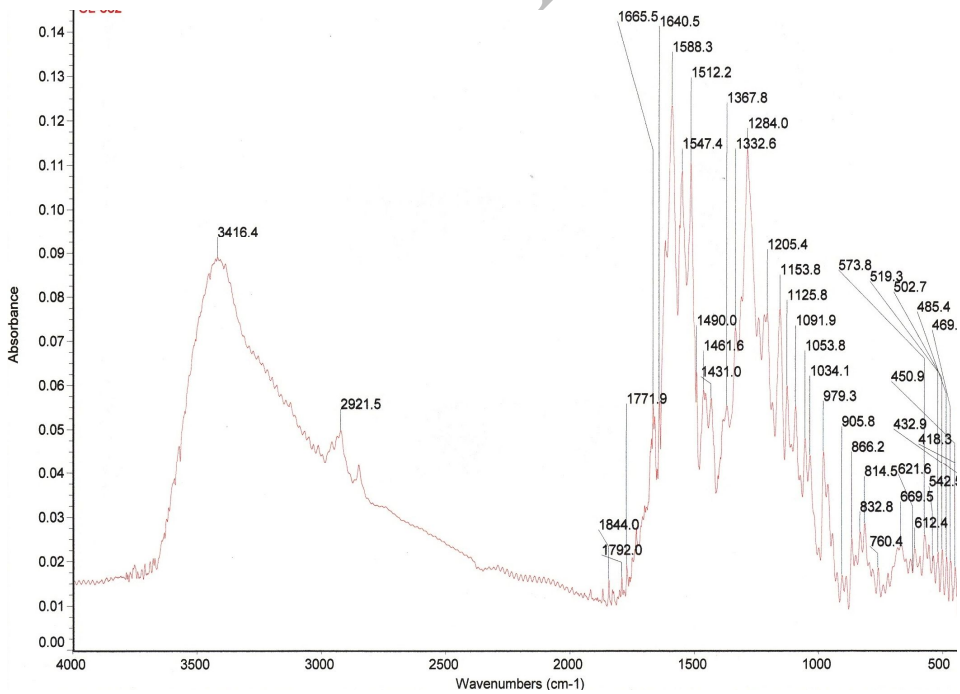

Fig. 99. IR spectrum of curcumalongin B (**2**)

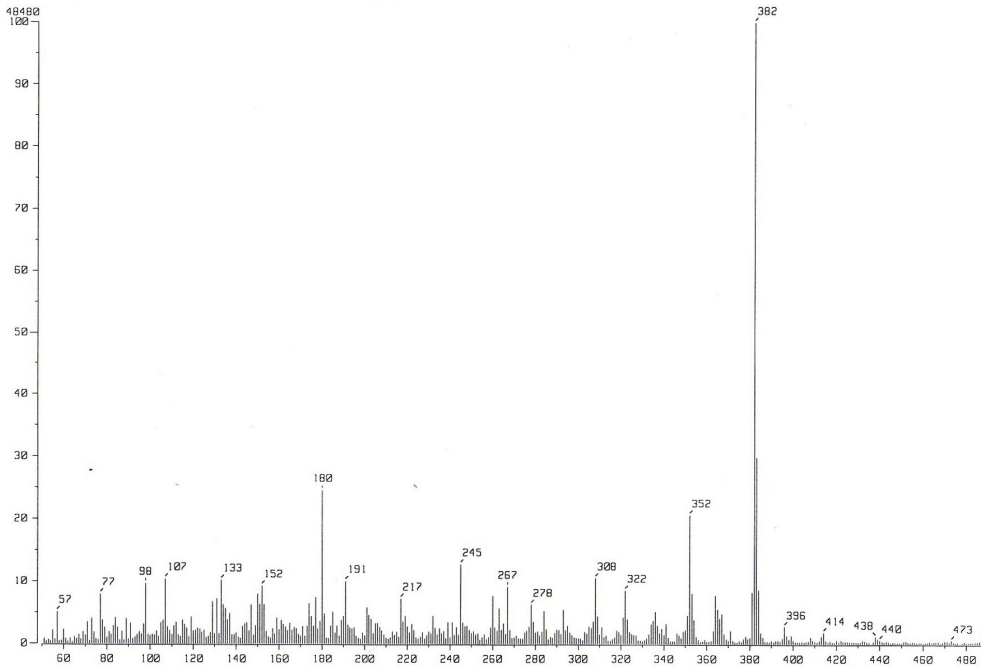

Fig. 100. EIMS spectrum of curcumalongin B (**2**)

Table 11. ^{1}H and ^{13}C-NMR data of curcumalongin B (**2**)[a] (in CD_3COCD_3)

Position	δ_H mult. (*J* in Hz)	δ_C	HMBC (H→C)
2		146.7	
3		186.6	
4	5.91 s	105.3	C-2, C-3, C-5, C-8'
5		176.1	
6			
7			
1′		124.4	
2′	7.23 d (1.8)	107.9	C-1′, C-3′, C-4′, C-6′, C-7′
3′		149.0	
4′		137.4	
5′		146.5	
6′	7.21 d (1.8)	113.6	C-1′, C-4′, C-5′, C-7′
7′	6.52 s	112.2	C-2, C-3, C-1′, C-2′, C-6′
1"		128.2	
2"	7.43 d (1.8)	111.0	C-1", C-3", C-4", C-7"
3"		149.2	
4"		150.4	
5"	6.91 d (8.4)	116.4	C-1", C-3", C-4", C-6"
6"	7.20 dd (8.4, 1.8)	124.6	C-1", C-4", C-5", C-7"
7"	7.67 d (15.6)	139.7	C-5, C-1", C-2", C-6", C-8"
8"	7.14 d (15.6)	113.5	C-4, C-5, C-1", C-7"
3′-OCH_3	3.94 s	56.4	C-3′
3"-OCH_3	3.99 s	56.5	C-3"

[a] Assignments were based on HSQC, HMBC experiments.

2.4.3. Structural determination of compound 3

Compound **3** was obtained as a yellow amorphous powder, and its HREIMS spectrum showed an $[M-H_2O]^+$ ion at *m/z* 390.1678, indicating a dehydrated molecular formula of $C_{21}H_{26}O_7$ (calcd for 390.1679). The IR spectrum showed a strong and broad hydroxy absorption at 3418 cm^{-1}. In the ^1H NMR spectrum (**Table 12**), the signals of a 1,3,4-trisubstituted benzene ring [δ_H 6.77 (1H, d, J = 2.0 Hz, H-2″), 6.67 (1H, d, J = 8.5 Hz, H-5″), and 6.62 (1H, dd, J = 8.5, 2.0 Hz, H-6″], a 1,3,4,5-tetrasubstituted benzene ring [δ_H 6.54 (1H, s, H-6′) and 6.50 (1H, s, H-2′)], and two methoxy groups [δ_H 3.77 (3H, s, 3′-OCH_3) and 3.75 (3H, s, 3″-OCH_3)] were observed. These findings and the base peaks at *m/z* 137 and 153 in the MS suggested the presence of 4-hydroxy-3-methoxyphenyl and 4,5-dihydroxy-3-methoxyphenyl groups (Dao *et al.*, 2012). In addition, the ^1H NMR spectrum showed seven more signals due to four methylenes [δ_H 2.63 (1H, m, H-7a), 2.56 (1H, m, H-7b); 1.81 (1H, d, J = 10.5 Hz, H-2a), 1.61 (1H, m, H-2b); 1.74 (1H, m, H-6a), 1.60 (1H, m, H-6b); and 1.64 (1H, m, H-4a), 1.46 (1H, m, H-4b)], and three oxymethines [δ_H 4.66 (1H, d, J = 10.5 Hz, H-1), 4.19 (1H, m, H-5), and 3.87 (1H, m, H-3)]. Base on the observed HMQC correlations, these signals correspond to the ^{13}C NMR signals for a C_7 linkage fragment (-CH(OH)-CH_2-CH(OH)-CH_2-CH(OH)-CH_2-CH_2-) of diarylheptanoid (Hashimoto *et al.*, 1986). The ^1H and ^{13}C NMR spectra of compound **3** were similar to those of (3*S*,5*S*)-3,5-dihydroxy-1,7-bis(4-hydroxy-3-methoxyphenyl)heptane (Kikuzaki *et al.*, 2012) except for two additional hydroxy groups attached to carbon C-5′ of the aromatic ring and carbon C-1. The HMBC correlations from H-2″, H-5″ and H-6″/C-4″, H-2″ and H-5″/C-3″, H-2′/C-3′ and C-4′, H-6′/C-4′ and C-5′, 3′-OCH_3/C-3′, and 3″-OCH_3/C-3″

suggested the location of each substituted groups on the two aromatic rings. Three hydroxy groups attached to C-1, C-3 and C-5 on C_7 linkage were confirmed by the HMBC correlations between H-1/C-2, C-3, C-4′ and C-6′, H-3/C-1, C-2, C-4 and C-5, and H-5/C-3 (**Fig. 101**). The configuration of **3** was then established upon the basis of the specific rotation ($[\alpha]_D^{25}$ +13) and NOESY data, which showed NOE correlations between H-1/H-3, whereas NOE was not observed between H-3/H-5 (**Fig. 101**) (Hashimoto *et al*., 1986). Thus, the structure of compound **3** was identified as (1*R*,3*R*,5*S*)-trihydroxy-1-(4,5-dihydroxy-3-methoxyphenyl)-7-(4-hydroxy-3-methoxyphenyl)heptane, and it was named as curcumalongin D.

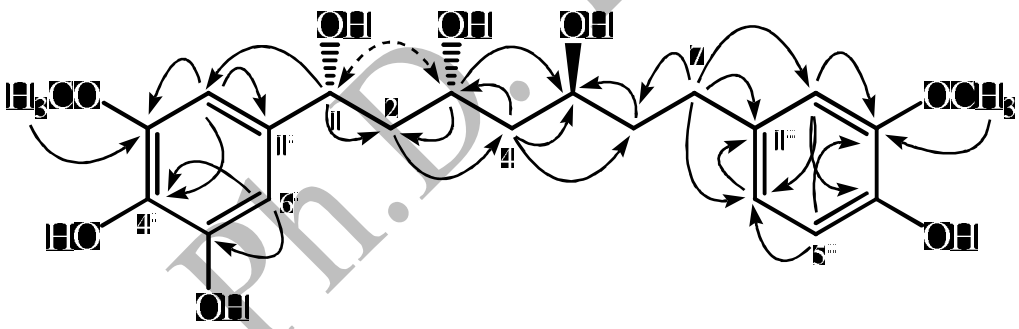

Fig. 101. Key HMBC (H→C) and NOSEY (↔) correlations of curcumalongin D (**3**)

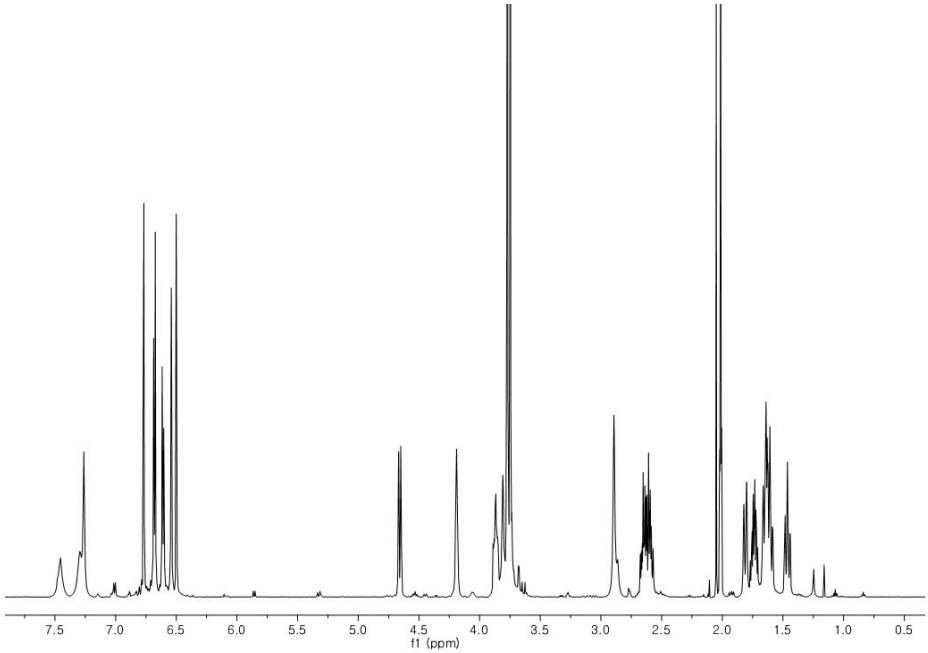

Fig. 102. ^{1}H-NMR spectrum of curcumalongin D (**3**)

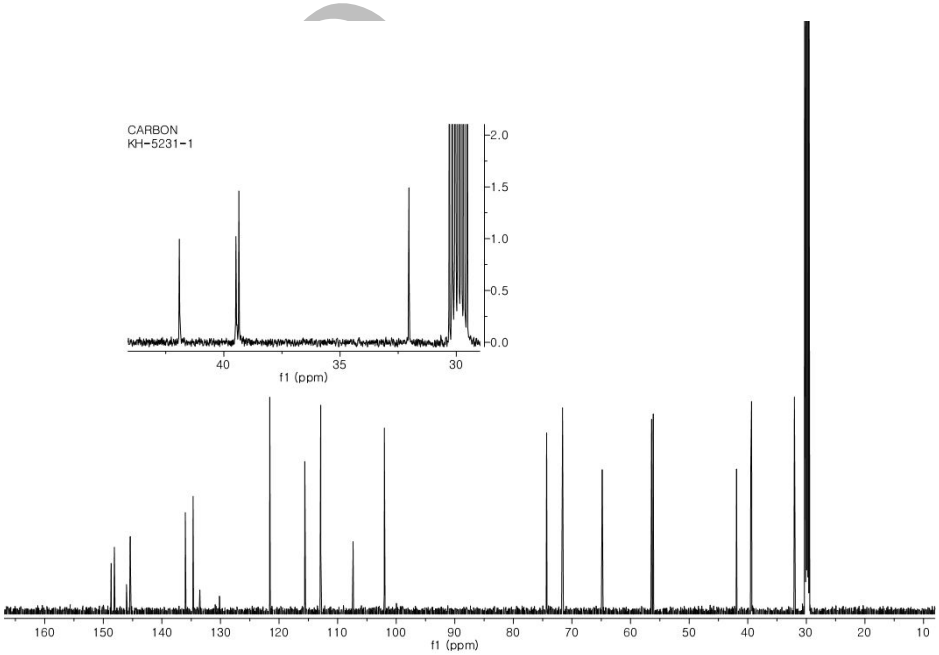

Fig. 103. ^{13}C-NMR spectrum of curcumalongin D (**3**)

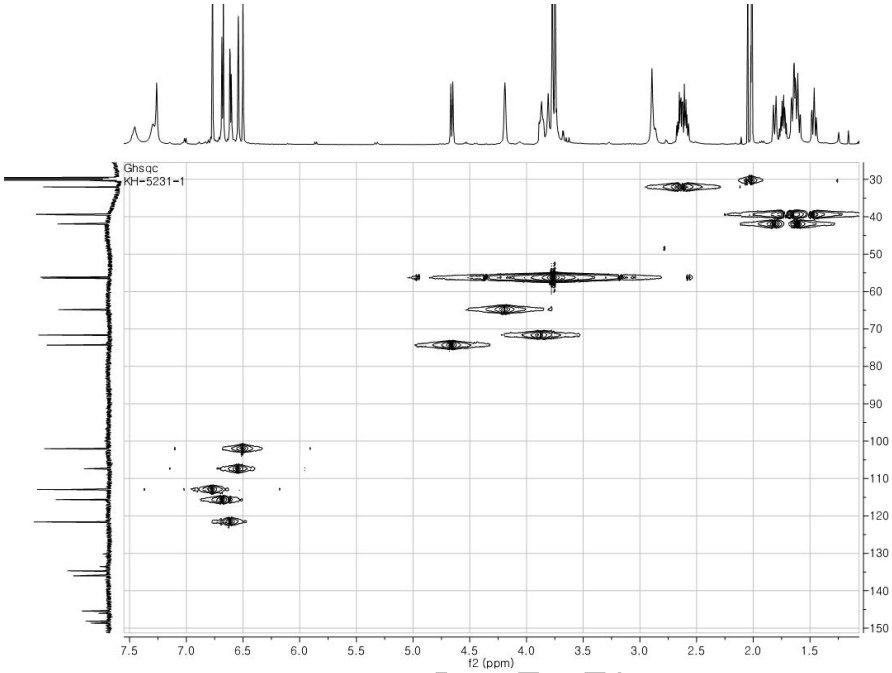

Fig. 104. HSQC spectrum of curcumalongin D (**3**)

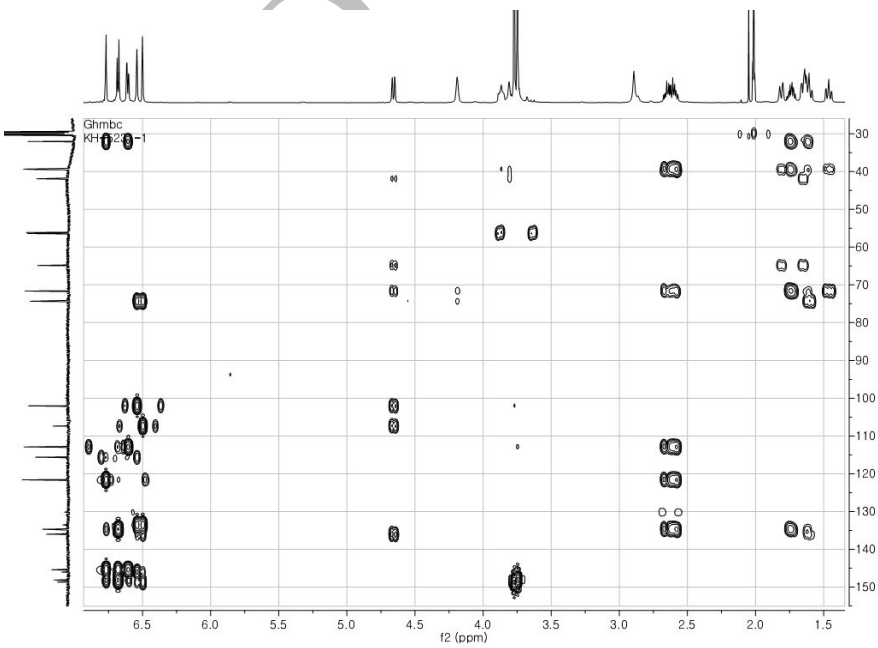

Fig. 105. HMBC spectrum of curcumalongin D (**3**)

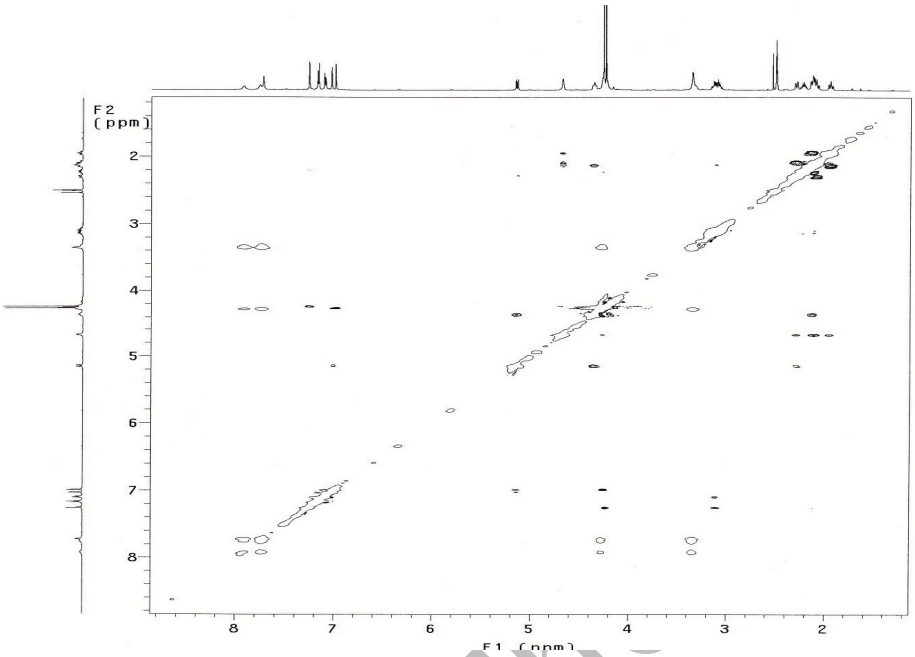

Fig. 106. NOESY spectrum of curcumalongin D (**3**)

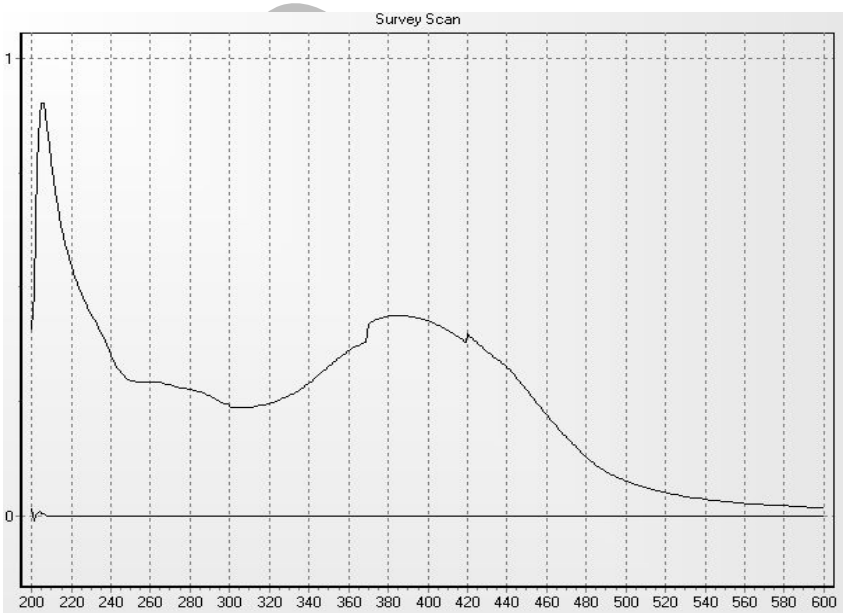

Fig. 107. UV spectrum of curcumalongin D (**3**)

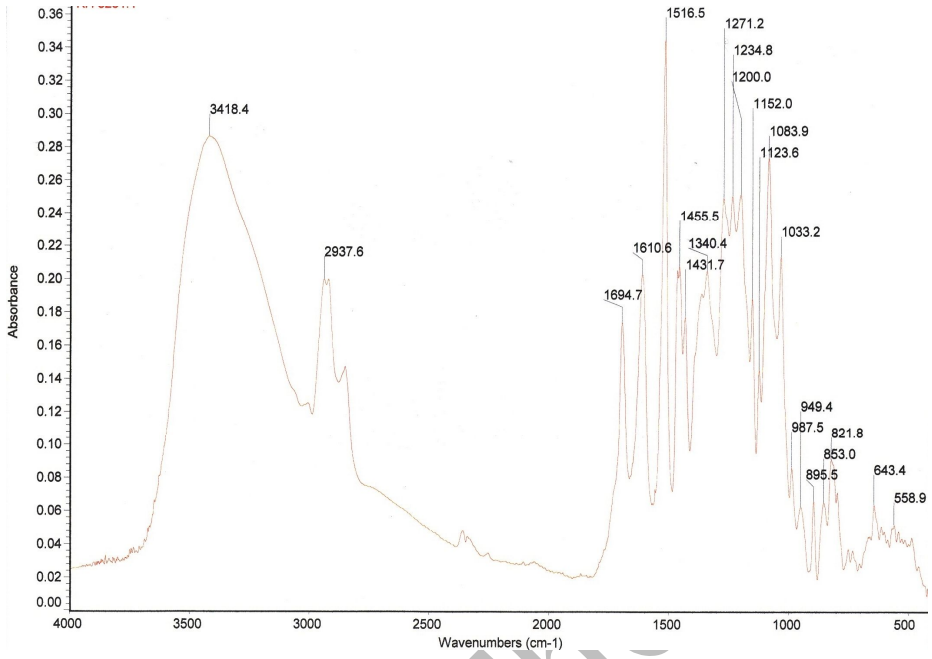

Fig. 108. IR spectrum of curcumalongin D (**3**)

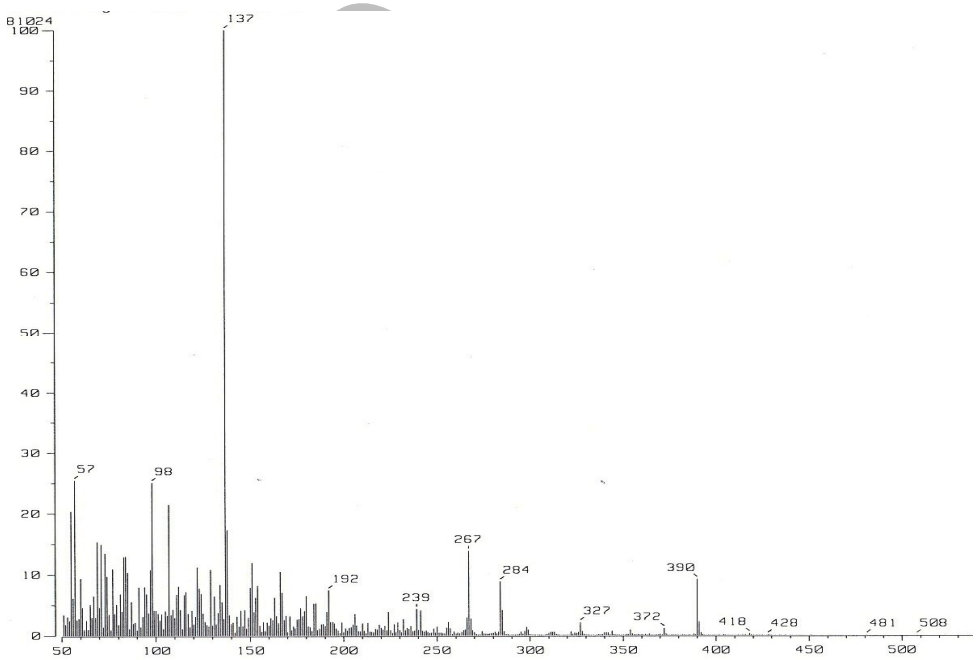

Fig. 109. EIMS spectrum of curcumalongin D (**3**)

Table 12. ^{1}H and ^{13}C-NMR data of curcumalongin D (**3**)[a] (in CD_3COCD_3)

Position	δ_H mult. (*J* in Hz)	δ_C	HMBC (H→C)
1	4.66 d (10.5)	74.6	C-2, C-3, C-2′, C-6′
2	1.81 d (10.5)	41.9	C-4
	1.61 m		C-1, C-3, C-4
3	3.87 m	71.6	C-1, C-2, C-4, C-5
4	1.64 m	39.5	C-5, C-6
	1.46 m		C-3, C-6
5	4.19 m	64.8	C-3
6	1.74 m	39.4	C-4, C-7
	1.60 m		C-4, C-5, C-7
7	2.63 m	32.0	C-6, C-1", C-2", C-6"
	2.56 m		C-6, C-1", C-2", C-6"
1′		133.5	
2′	6.50 s	102.1	C-1′, C-3′, C-4′
3′		148.7	
4′		136.0	
5′		146.0	
6′	6.54 s	107.4	C-1′, C-4′, C-5′
1"		134.7	
2"	6.77 d (2.0)	112.9	C-3", C-4", C-6"
3"		148.1	
4"		145.4	
5"	6.67 d (8.5)	115.6	C-1", C-3", C-4", C-6"
6"	6.62 dd (8.5, 2.0)	121.6	C-1", C-2", C-4", C-5"
3′-OCH_3	3.77 s	56.1	C-3′
3"-OCH_3	3.75 s	56.4	C-3"

[a] Assignments were based on HSQC, HMBC experiments.

2.5. Stimulatory effects of the isolated compounds on SIRT1 activity

The effects on SIRT1 of isolated compounds were tested in vitro according to the above methods, with using resveratrol as a positive control. All compounds except for **10** exhibited an increasingly stimulating SIRT1 activity (see **Fig. 110**). Among tested compounds, the basic skeleton required for the activity seems to be the oxyaryl unit with the unsaturated -C=C-CO- moiety. In contrast, the presence of saturated carbons of the C_7 linker as in compounds **3**, **10**–**12** might be responsible for the decreased activity compared to the others. Remarkablly, compounds **1** and **2** with a furan ring formation significantly enhance SIRT1 activity nearly same as the positive control (**Fig. 110**).

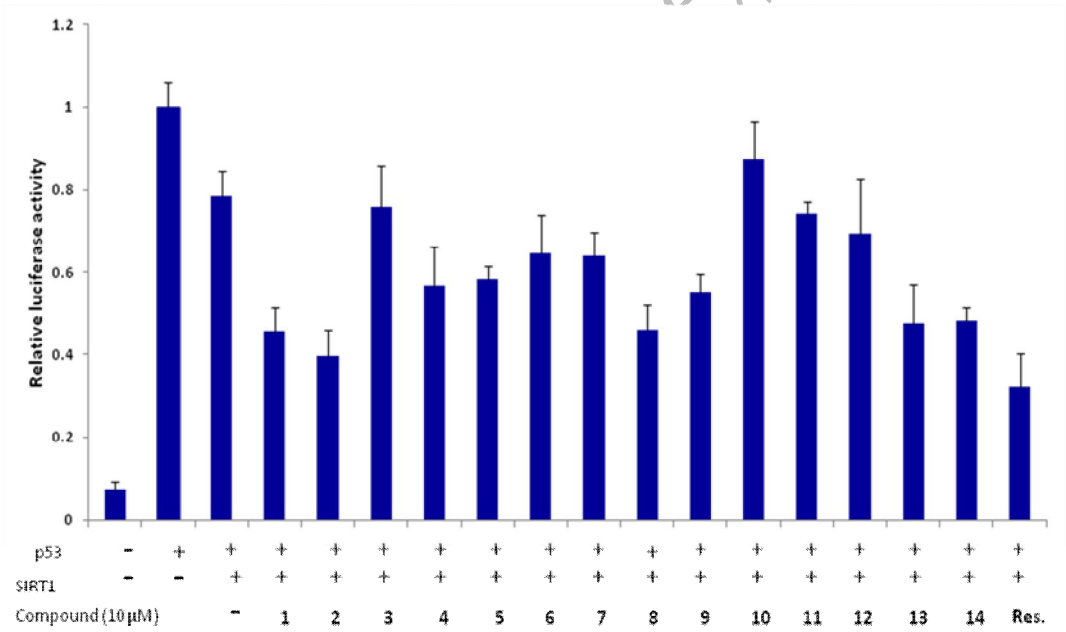

Fig. 110. The effects of isolated compounds on the transcription activity of p53 in HEK293 cells. The cells were transfected with p53-luc, myc-p53, flag-SIRT1 and *β*–gal vectors. After 1 day, cells were treated with the compounds and resveratrol for 12 h.

To further confirm the effect of these derivatives, the strongest compounds (**1**, **2**), the weak compound **3**, and demethoxycurcumin **4** (one of the three majors) were tested at different concentrations. As shown in **Fig. 111**, compounds **1**, **2** and **4** exhibited strongly effects on SIRT1 stimulation in a dose-dependent manner, while compound **3** showed weak effect as discussed in the SAR above.

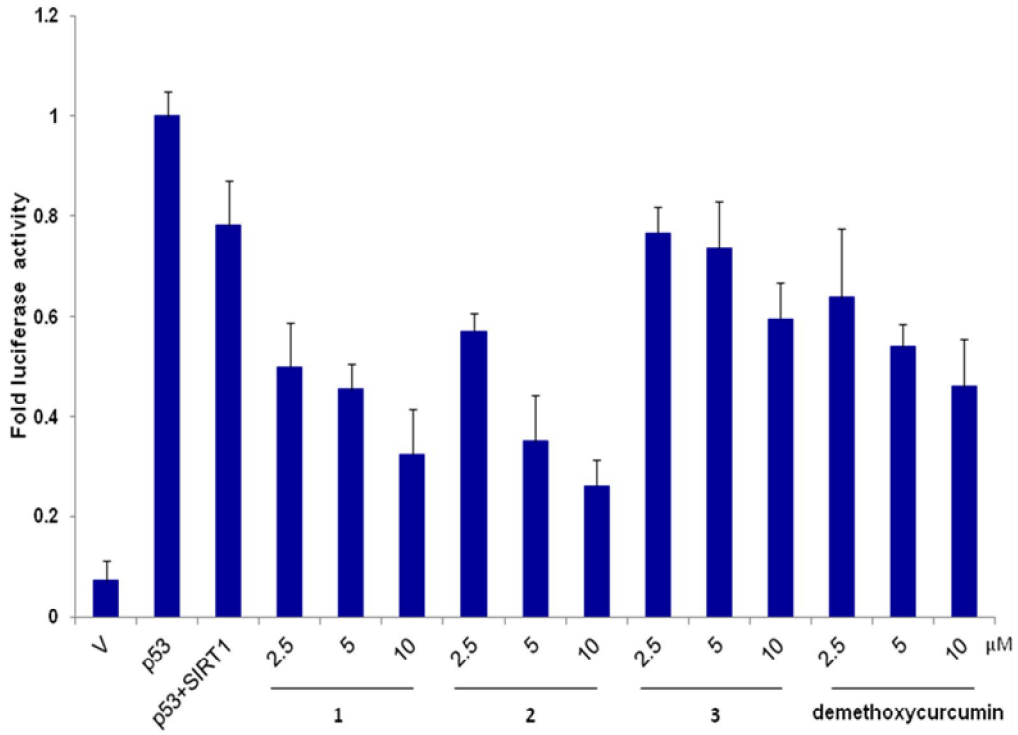

Fig. 111. Compounds **1**–**4** increased SIRT1 activity in a dose-dependent manner.

IV. DISCUSSIONS

Once people have achived the goals of a good quality of life in which basic needs are met, and where this combines with access to good health services and drugs successfully treat most diseases, the next step is to increase life expectancy. It thus becomes necessary to develop drugs that act on different organs and tissues of the body to preserve their functioning. One way of accomplishing this would be through the development of drugs with antiaging properties, which should help to prevent or treat aging-associated diseases. Because of the complex and multifactor nature of aging, it would appear to be almost impossible to find molecules with such a variety of antiaging properties. However, nature has the ability to reveal surprising antiaging tools. For example, it was observed that the French population, through the commonly consumption of red wine, showed reduced mortality from coronary heart disease. Researchers subsequently realized that resveratrol, a naturally occurring polyphenolic compound, was responsible for the beneficial effects on the cardiovascular system. Initial attempts to ascertain its mechanisms showed that it was mainly due to the strong antioxidant property (Orallo *et al*., 2006). However, this property alone cannot explain the pharmacological effects of resveratrol, which, in recent years, has been shown to have anti-inflammatory, antitumor, cardioprotective and antiaging properties. Therefore, there must be additional pathways activated by resveratrol that could explain its antiaging and beneficial coronary effects. Interestingly, the discovery of protein SIRT1, might explain the target for resveratrol and responsible for its physiological actions. SIRT1 has thus emerged as an attractive task for scientists in terms of its effects on longevity, metabolism and other

aging-related disorders (Baur *et al.*, 2006; Feige *et al.*, 2008; Lagouge *et al.*, 2006; Milne *et al.*, 2007; Yamazaki *et al.*, 2009; Pallas *et al.*, 2008; Firestein *et al.*, 2008). In 2008, pharma giant GlaxoSmithKline bought Sitris for $720 million, which is a company formed by Dr. David Sinclair (Havard Medical School) to develop drugs based on compounds stimulating SIRT1 activity. While several small-molecule activators of SIRT1 have been identified by utilizing a commercially available deacetylase activity assay, almost all of them are synthetic compounds (Vu *et al.*, 2009; Bernis *et al.*, 2009; Smith *et al.*, 2009; Yamazaki *et al.*, 2009; Mai *et al.*, 2009). Howitz and colleagues have identified some compounds of natural origin, such as resveratrol, fisetin and butein, but these compounds have a low bioavailability (Howitz *et al.*, 2003). Moreover, the particular method for determination of SIRT1 activity is still controversial due to its dependence on the use of a specific fluorophore substrate (Borra *et al.*, 2005; Pacholec *et al.*, 2010). Other previous researchers have reported synthesized compounds with SIRT1 stimulatory activity, including quinoxalines, SRT derivatives, oxazolo-[4,5-*b*]pyridines, dihydropyridines and imidazol-[1,2-*b*]thiazoles (Vu *et al.*, 2009; Bernis *et al.*, 2009; Smith *et al.*, 2009; Yamazaki *et al.*, 2009; Mai *et al.*, 2009). In this study, we showed a series of natural metabolites, including terpenylated coumarins from *A. altissima* and curcumin derivatives from *C. longa*, that stimulate SIRT1 deacetylase activity, accompanied by SIRT1 binding to enhance SIRT1-mediated deacetylation of p53.

To our knowledge, this is the first retport of terpenylated coumarin with a directly stimulation on SIRT1 enzyme activity. Though the content of these ompounds in *A. altissima* is not high, these terpenylated coumarins show a clear increasning effects on SIRT1 activity. It will be a valuable source for further studies on chemical designing

analoges for pharmacological investigations. Additionally, these compounds have a maintenance of a high [NAD^+]/[NADH] ratio in mitochondrial, that might support to the notion of indirectly stimulation on SIRT1 activity in vivo.

Curcumin, which is the major component from *C. longa*, has a range of biological properties with cardiovascular protection, antitumor, antioxidant, anti-inflammatory, anti-Alzheimer, antiviral and anti-hepatotoxic activities (Chen *et al*., 2010; Miriyala *et al*., 2007; Park & Kim, 2002; Simon *et al*., 1998; Masuda *et al*., 1993). However, its full pharmacological utility is restricted for the limited aqueous solubility, degradation at alkaline pH and poor absorption as well as rapid metabolism (Kurien *et al*., 2007). To date, there are no reports of SIRT1 activity of curcumin derivatives from *C. longa* because of difficulty to isolate these compounds due to their similar retentive properties on chromatography and the low abundance (Li *et al*., 2009). In our extensive research, these derivatives exhibited strong stimulation effects on SIRT1 activity.

V. CONCLUSIONS

It has been postulated that SIRT1 activators might be beneficial for the pharmaceutical interventions that are aimed at delaying or ameliorating the pathologies associated with aging and metabolic and cardiovascular diseases.

However, only a few SIRT1 activators have been reported. Moreover, it is uncertain whether or not these compounds are direct activators of SIRT1 for the mechanism by which they enhance SIRT1 activity remains poorly defined. So, more activators are still needed to improve the understanding of SIRT1 biological functions and to discover its possible therapeutic indication. Since natural products are a promising source for the development of new SIRT1 activators, we have undertaken a screen of thousands of plants on SIRT1 deacetylase activity.

Methanol-soluble extracts of *A. altissima* and *C. longa* were thus found to strongly increase SIRT1 activity at a concentration of 30 µg/mL. The MeOH solutions were then concentrated, suspended in H_2O, and sequentially partitioned with a gradually increasing polarity of organic solvents.

Bioassay-guided fractionation of these extracts has resulted in the isolation of twelve new compounds, including 9 terpenylated coumarins (**1–9**) from the stem barks of *A. altissima* and 3 curcumin derivatives (**1–3**) from the rhizomes of *C. longa* along with a series of other known compounds using chromatography methods (silica gel, C-18, and preparative HPLC). Their structures were elucidated on the basic of spectral (including 1D, 2D-NMR, UV, IR, and MS) and physicochemical analyses. The SIRT1 stimulation effects of tested compounds were also evaluated on different SIRT1 assays.

Fig. 112. Chemical structures of new compounds from the stem barks of *A. altissima*

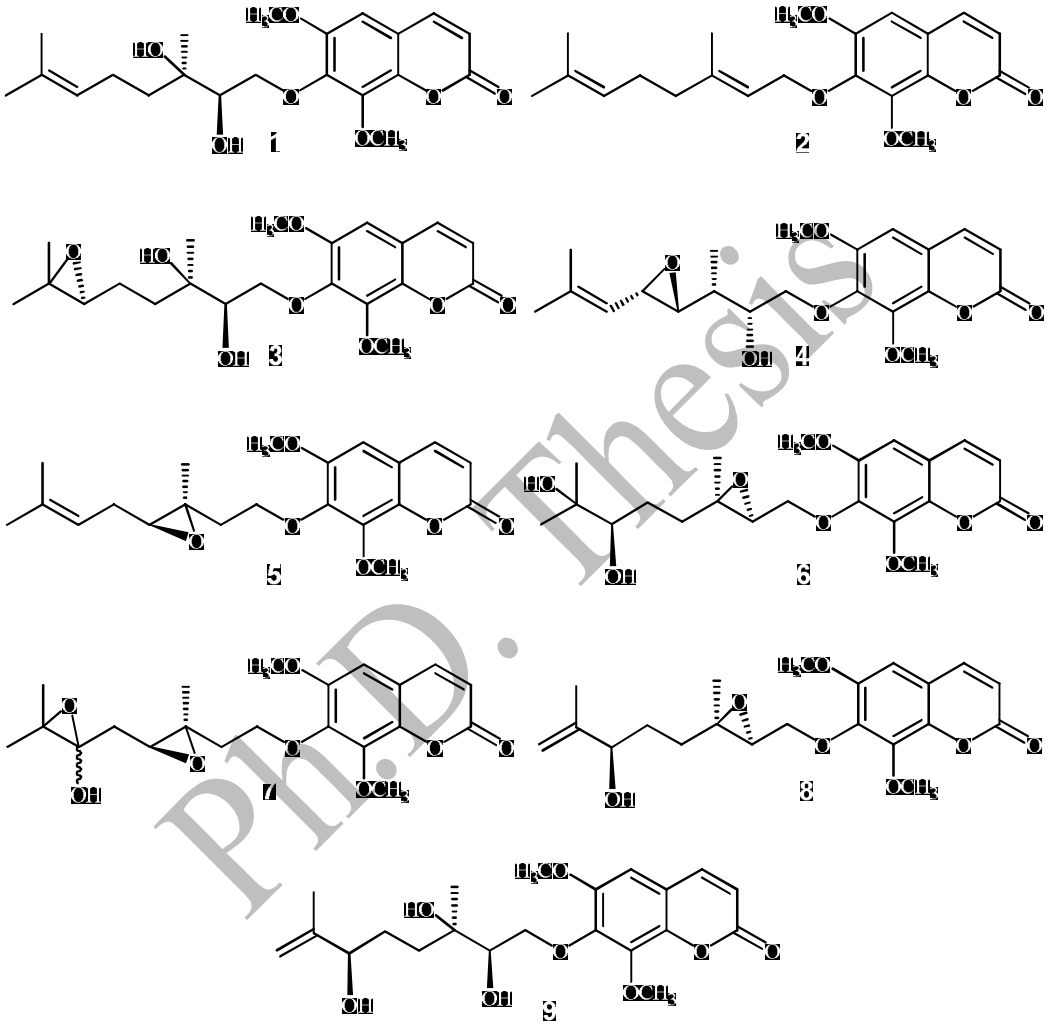

Fig. 113. Chemical structures of new compounds from the rhizomes of *C. longa*

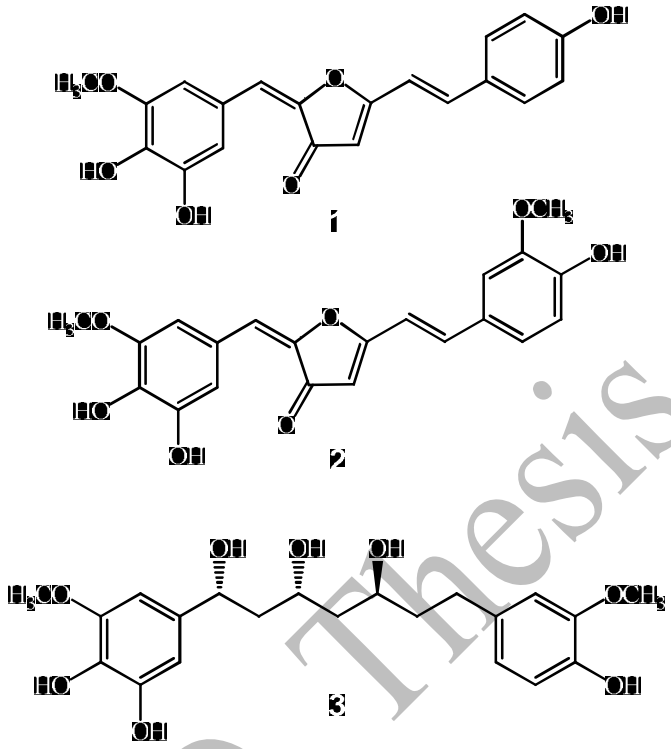

Curcumalongin A (**1**) and curcumalongin B (**2**) are new type of curcuminoid, and this is the first report on the presence of this skeleton in literature.

Although structure-activity relationships of these compounds were not thoroughly investigated, these results suggest that terpenylated coumarins and curcumin derivatives can be considered as promising classes of SIRT1 activators. Therefore, further investigation, optimization on chemical and confirmation of SIRT1 effects of these naturally occurring compounds in aging cells, as well as evaluation of their potential lifespan efficacy in model organisms, such as yeast or *Drossophila*, might enable the discovery of new agents in the treatment of metabolic and age-related diseases.

VI. REFERENCES

Ammon, H.P., Wahl, M.A.: Pharmacology of *Curcuma longa*. *Planta Med.* **1991**, *57*, 1-7.

Anderson, R.M., Bitterman, K.J., Wood, J.G., Medvedik, O., Sinclair, D.A.: Nicotinamide and PNC1 govern lifespan extension by calorie restriction in *Saccharomyces cerevisiae*. *Nature* **2003**, *423*, 181-185.

Araki, T., Sasaki, Y., Milbrandt, J.: Increased nuclear NAD biosynthesis and SIRT1 activation prevent axonal degeneration. *Science.* **2004**, *350*, 1010-1013.

Arany, Z., He, H., Lin, J., Hoyer, K., Handschin, C., Toka, O., Ahmad, F., Matsui, T., Chin, S., Wu, P.H. *et al.*: Transcriptional coactivator PGC-1alpha controls the energy state and contractile function of cardiac muscle. *Cell. Metab.* **2005**, *1*, 259-271.

Banthorpe, D.V., Brown, G.D.: Two unexpected coumarin derivatives from tissue cultures of compositae secies. *Phytochemistry* **1989**, *28*, 3003-3007.

Baur, J.A., Pearson, K.J., Price, N.L., Jamieson, H.A., Lerin, C., Kalra, A., Prabhu, V.V., Allard, J.S., Lopez-Lluch, G., Lewis, K., *et al.*: Resveratrol improves health and survival of mice on a high calorie diet. *Nature* **2006**, *444*, 337-342.

Bedalov, A., Gatbonton, T., Irvine, W.P., Gottschling, D.E., Simon, J.A.: Identification of a small molecule inhibitor of Sir2p. *Pro. Natl. Acad. Sci. U. S. A.* **2001**, *98*, 15113-15118.

Beher, D., Wu, J., Cumine, S., Kim, K.W., Lu, S.C., Atangan, L., Wang, M.: Resveratrol is not a direct activator of SIRT1 enzyme activity. *Chem. Biol. Drug Des.* **2009**, *74*, 619-624.

Bernis, J.E., Vu, C.B., Xie, R., Nunes, J.J., Ng, P.Y., Disch, J.S., Milne, J.C., Carney, D.P.,

Lynch, A.V., Jin, L., Smith J.J., Lavu, S., Iffland, A., Jirousek, M.R., Perni, R.B.: Discovery of oxazolo[4,5b]pyridines and related heterocyclic analogs as novel SIRT1 activators. *Bioorg. Med. Chem. Lett.* **2009**, *19*, 2350-2353.

Bitterman, K.J., Anderson, R.M., Cohen, H.Y., Latorre-Esteves, M., Sinclair, D.A.: Inhibition of silencing and accelerated aging by nicotinamide, a putative negative regulator of yeast sirt2 and human SIRT1. *J. Biol. Chem.* **2002**, *277*, 45099-45107.

Boily, G., He, X.H., Pearce, B., Jardine, K., McBurney, M.W.: SirT1-null mice develop tumors at normal rates but are poorly protected by resveratrol. *Oncogen* **2009**, *28*, 2882-2893.

Bordone, L., Cohen, D., Robinson, A., Motta, M.C., van Veen, E., Czopik, A., Steele, A.D., Crowe, H., Marmor, S., Luo, J., *et al.*: SIRT1 transgenic mice show phenotypes resembling calorie restriction. *Aging Cell* **2007**, *6*, 759-767.

Borra, M.T., Smith, B.C., Denu, J.M.: Mechanism of human SIRT1 activation by resveratrol. *J. Biol. Chem.* **2005**, *280*, 17187-17195.

Brachmann, C.B., Sherman, J.M., Devine, S.E., Cameron, E.E., Pillus, L., Boeke, J.D.: The SIR2 gene family, conserved from bacteria to humans, functions in silencing, cell cycle progression, and chromosome stability. *Genes. Dev.* **1995**, *9*, 2888-2902.

Braunstein, M., Rose, A.B., Holmes, S.G., Allis, C.D., Broach, J.R.: Transcriptional silencing in yeast is associated with reduced nucleosome acetylation. *Genes. Dev.* **1993**, *7*, 592-604.

Chen, D., Steele, A.D., Lindquist, S., Guarente, L.: Increase in activity during calorie restriction requires Sirt1. *Science* **2005**, *310*, 1641.

Chen, D.Y., Shien, J.H., Tiley, L., Chiou, S.S., Wang, S.Y., Chang, T.J., Lee, Y.J., Chan,

K.W., Hsu, W.L.: Curcumin inhibits influenza virus infection and haemagglutination activity. *Food Chemistry* **2010**, *119*, 1346-1351.

Chen, I.Y., Lypowy, J., Pain, J., Sayed, D., Grinberg, S., Alcendor, R.R., Sadoshima, J., Abdellatif, M.: Histone H2A.z is essential for cardiac myocyte hypertrophy but opposed by silent information regulator 2α. *J. Biol. Chem.* **2006**, *281*, 19369-19377.

Cohen, H.Y., Lavu, S., Bitterman, K.J., Hekking, B., Imahiyerobo, T.A., Miller, C., Frye, R., Ploegh, H., Kessler, B.M., Sinclair, D.A.: Acetylation of the C terminus of Ku70 by CBP and PCAF controls Bax-mediated apoptosis. *Mol. Cell* **2004**, *13*, 627-638.

Coleman, M.P., Perry, V.H.: Axon pathology in neurological disease: a neglected therapeutic target. *Trends Neurosci.* **2002**, *25*, 532-537.

Comte, G., Allais, D.P., Chulia, A.J., Vercauteren, J., Delage, C.: Two furanone glucoside derivatives from *Juniperus phoenicea*. *Phytochemistry* **1996**, *41*, 1329-1332.

Dai, J.M., Wang, Z.Y., Sun, D.C., Lin, R.X., Wang, S.Q.: SIRT1 interacts with p73 and suppresses p73-dependent transcriptional activity. *J. Cell Physiol.* **2007**, *210*, 161-166.

Dao, T.T., Nguyen, P.H., Won, H.K., Kim, E.H., Park, J., Won, B.Y., Oh, W.K..: Curcuminoids from Curcuma longa and their inhibitory activities on influenza A neuraminidases. *Food Chem.* **2012**, *134*, 21-28.

Das, D.K., Maulik, N.: Resveratrol in cardioprotection: a therapeutic promise of alternative medicine. *Mol. Interv.* **2006**, *6*, 36-47.

Delmas, D., Jannin, B., Latruffe, N.: Resveratrol: preventing properties against vascular alterations and ageing. *Mol. Nutr. Food Res.* **2005**, *49*, 377-395.

Derbyshire, M.K., Weinstock, K.G., Strathern, J.N.: HST1, a new member of the SIR2

family of genes. *Yeast* **1996**, *12*, 631-640.

Feige, J.N., Lagouge, M., Canto, C., Strehle, A., Houten, S.M., Milne, J.C., Lambert, P.D., Mataki, C., Elliott, P.J., Auwerx, J.: Specific SIRT1 activation mimics low energy levels and protects against diet induced metabolic disorders by enhancing fat oxidation. *Cell Metab.* **2008**, *8*, 347-358.

Feo, V.D., Martino, L.D., Quaranta, E., Pizza, C.: Isolation of phytotoxic compounds from tree-of-heaven (*Ailanthus altissima* Swinggle). *J. Agric. Food Chem.* **2003**, *51*, 1177-1180.

Firestein, R., Blander, G., Michan, S., Oberdoerffer, P., Ogino, S., Campbell, J., Bhimavarapu, A., Luikenhuis, S., deCabo, R., Fuchs, C., Hahn, W.C., Guarente, L.P., Sinclair, D.A.: The SIRT1 deacetylase suppresses intestinal tumorigenesis and colon cancer growth. *PLoS. ONE* **2008**, *3*, e2020.

Gan, L., Mucke, L.: Paths of convergence: sirtuins in aging and neurodegeneration. *Neuron* **2008**, *58*, 10-14.

Gershenzon, J., Mabry, T.J.: Furanoheliangolides from *Helianthus schweinitzii*. *Phytochemistry* **1984**, *23*, 2557-2559.

Ghosh, H.S., Spencer, J.V., Ng, B., McBurney, M.W., Robins, P.D.: Sirt1 interacts with transducin-like enhancer of split-1 to inhibit nuclear factor kappaB-mediated transcription. *Biochem. J.* **2007**, *408*, 105-111.

Guarente, L.: Calorie restriction and SIR2 genes-towards a mechanism. *Mech. Ageing. Dev.* **2005**, *126*, 923-928.

Guarente, L., Picard, F.: Calorie restriction-the SIR2 connection. *Cell* **2005**, *120*, 437-428.

Hashimoto, T.; Tori, M.; Asakawa, Y.: Five new diarylheptanoids from the male flowers

of *Alnus sieboldiana*. *Chem. Pharm. Bull.* **1986**, *34*, 1846-1849.

Hendrie, H.C., Ogunniyi, A., Hall, K.S., Baiyewu, O., Unverzagt, F.W, Gureje, O., Gao, S., Evans, R.M., Ogunseyinde, A.O., Adeyinka, A.O., *et al*.: Incidence of dementia and Alzheimer disease in 2 communities: Yoruba residing in Ibadan, Nigeria, and African Americans residing in Indianapolis, Indiana. *JAMA*. **2001**, *285*, 739-747.

Houtkooper, R.H., Canto, C., Wanders, R.J., Auwerx, J.: The secret life of NAD^+: an old metabolite controlling new metabolic signaling pathways. *Endocr. Rev.* **2009**, *31*, 194-223.

Howitz, K.T., Bitterman, K.J., Cohen, H.Y., Lamming, D.W., Lavu, S., Wood, J.G., Zipkin, R.E., Chung, P., Kisielewski, A., Zhang, L.L., Scherer, B., Sinclair, D.A.: Small molecule activators of sirtuins extend *Saccharomyces cerevisiae* lifespan. *Nature* **2003**, *425*, 191-196.

Hwang S.W., Lee, J.R. Lee, J., Kwon, H.S. Yang, M.S. Park, K.H.: New coumarins from the *Ailanthus altissima*. *Heterocycles* **2005**, *65*, 1963-1966.

Ito, C., Furukawa, H., Ishii, H., Ishikawa, T., Haginiwa, J.: The chemical position of *Murraya paniculata*. The structure of five new coumarins and one new alkaloid and the stereochemistry of murrangatin and related coumarins. *J. Chem. Soc. Perkin Trans. 1* **1990**, *7*, 2047-2055.

Ito, C., Itoigawa, M., Onoda, S., Hosokawa, A., Ruangrungsi, N., Okuda, T., Tokuda, H., Nishino, H., Furukawa, H.: Chemical constituents of Murraya siamensis: three coumarins and their anti-tumor promoting effect. *Phytochemistry* **2005**, *66*, 567-572.

Ivy, J.M., Hicks, J.B., Klar, A.J.: Map position of yeast gene SIR1, SIR3 and SIR4. *Genetics* **1985**, *111*, 735-744.

Jackson, M.D., Denu, J.M.: Structural identification of 2 -and 3 -*O*-acetyl-ADP-ribose as novel metabolites derived from the Sir2 family of beta-NAD^+-dependent histone/protein deacetylases. *J. Biol. Chem.* **2002**, *277*, 18535-18544.

Jayaprakasha, G.K., Rao, L.J.M., Sakariah, K.K.: Improved HPLC method for the determination of curcumin, demethoxycurcumin, and bisdemethoxycurcumin. *J. Agric. Food Chem.* **2002**, *50*, 3668-3672.

Jin, M.H., Yook, J., Lee, E., Lin, C.X., Quan, Z., Son, K.H., Bae, K.H., Kim, H.P., Kang, S.S., Chang, H.W.: Anti-inflammatory activity of *Ailanthus altissima* in ovalbumin-induced lung inflammation. *Biol. Pharm. Bull.* **2006**, *29*, 884-888.

Kaeberlein, M., McDonagh, T., Heltweg, B., Hixon, J., Westman, E.A., Caldwell, S.D., Napper, A., Curtis, R., DiStefano, P.S., Fields, S., Bedalov, A., Kennedy, B.K.: Substrate-specific activation of sirtuins by resveratrol. *J. Biol. Chem.* **2005**, *280*, 17038-17045.

Kaeberlein, M., McVey, M., Guarente, L.: The SIR2/3/4 complex and SIR2 alone promote longevity in *Saccharomyces cerevisiae* by two different mechanisms. *Genes. Dev.* **1999**, *13*, 2570-2580.

Kikuzaki, H.; Kobayashi, M.; Nakatani, N.: Diarylheptanoids from rhizomes of *Zingiber officinale*. *Phytochemistry* **1991**, *30*, 3647-3651.

Kim, E.J., Kho, J.H., Kang, M.R., Um, S.J.: Active regulator of SIRT1 cooperates with SIRT1 and facilitates suppression of p53 activity. *Mol. Cell* **2007**, *28*, 277-290.

Klar, A.J., Fogel, S., Macleod, K.: Mar1-a regulator of the HMa and HMalpha loci in *Saccharomyces cerevisiae*. *Genetics* **1979**, *93*, 37-50.

Kowarik, I.: Clonal growth in *Ailanthus altissima* on a natural site in West Virgina. *J. Veg.*

Sci. **1995**, *6*, 853-856.

Kurien, B.T., Singh, A., Matsumoto, H., Scofield, R.H.: Improving the solubility and pharmacological efficacy of curcumin by heat treatment. *Assay Drug Dev. Technol.* **2007**, *5*, 567-576.

Labinskyy, N., Csiszar, A., Veress, G., Stef, G., Pacher, P., Oroszi, G., Wu, J., Ungvari, Z.: Vascular dysfunction in aging: potential effects of resveratrol, an anti-inflammatory phytoestrogen. *Curr. Med. Chem.* **2006**, *13*, 989-996.

Lagouge, M., Argmann, C., Gerhart-Hines, Z., Meziane, H., Lerin, C., Daussin, F., Messadeq, N., Milne, J., Lambert, P., Elliott, P., Geny, B., Laakso, M., Puigserver, P., Auwerx, J.: Resveratrol improves mitochondrial function and protects against metabolic disease by activating SIRT1 and PGC-1 alpha. *Cell* **2006**, *127*, 1109-1122.

Langley, E., Pearson, M., Faretta, M., Bauer, U.M., Frye, R.A., Minucci, S., Pelicci, P.G., Kouzarides, T.: Human SIR2 deacetylases p53 and antagonizes PML/p53-induced cellular senescence. *EMBO J.* **2002**, *21*, 2383-2396.

Lappas, M., Mitton, A., Lim, R., Barker, G., Riley, C., Permezel, M.: SIRT1 is a novel regulator of key pathways of human labor. *Biol. Reprod.* **2011**, *84*, 167-178.

Leiro, J., Arranz, J.A., Fraiz, N., Sanmartin, M.L., Quezada, E., Orallo, F.: Effect of *cis*-resveratrol on genes involved in nuclear factor kappa B signaling. *Int. Immunopharmacol.* **2005**, *5*, 393-406.

Li, W., Wang, S., Feng, J., Xiao, Y., Xue, X., Zhang, H., Wang, Y., Liang, X.: Structure elucidation and NMR assignments for curcuminoids from the rhizomes of *Curcuma longa*. *Magn. Reson. Chem.* **2009**, *47*, 902-908.

Lin, S.J., Defossez, P.A., Guarente, L.: Requirement of NAD and SIR2 for life-span

extension by calorie restriction in *Saccharomyces cerevisiae*. *Science* **2000**, *289*, 2126-2128.

Liu, Y., Gerber, R., Wu, J., Tsuruda, T., McCarter, J.D.: High-throughput assays for sirtuin enzymes: a microfluidic mobility shift assay and a bioluminescence. *Anal. Biochem.* **2008**, *378*, 53-59.

Luchsinger, J.A., Tang, M.X., Shea, S., Mayeux, R.: Caloric intake and the risk of Alzheimer disease. *Arch. Neurol.* **2002**, *59*, 1258-1263.

Luo, J., Nikolaev, A.Y., Imai, S., Chen, D., Su, F., Shiloh, A., Guarente, L., Gu, W.: Negative control of p53 by Sir2α promotes cell survival under stress. *Cell* **2001**, *107*, 137-148.

Mai, A., Valente, S., Meade, S., Carafa, V., Tardugno, M., Nebbioso, A., Galmozzi, A., Mitro, N., De Fabiani, E., Altucci, L., Kazantsev, A.: Study of 1,4-dihydropyridine structural scaffold: discovery of novel sirtuin activators and inhibitors. *J. Med. Chem.* **2009**, *52*, 5496-5504.

Masuda, T., Jitoe, A., Isobe, J., Nakatani, N., Yonemori, S.: Anti-oxidative and anti-inflammatory curcumin-related phenolics from rhizomes of *Curcuma domestica*. *Phytochemistry* **1993**, *32*, 1557-1560.

Mattagajasingh, I., Kim, C.S., Naqvi, A., Yamamori, T., Hoffman, T.A., Jung, S.B., DeRicco, J., Kasuno, K., Irani, K.: SIRT1 promotes endothelium dependent vascular relaxation by activating endothelial nitric oxide synthase. *Proc. Natl. Acad. Sci. U. S. A.* **2007**, *104*, 14855-14860.

Mattson, M.P.: Gene-diet interactions in brain aging and neurodegenerative disorders. *Ann. Intern. Med.* **2003**, *139*, 441-444.

Michishita, E., Park, J.Y., Burneskis, J.M., Barrett, J.C., Horikawa, I.: Evolutionally conserved and nonconserved cellular localization and functions of human SIRT proteins. *Mol. Biol. Cell* **2005**, *16*, 4623-4635.

Milne, J.C., Lambert, P.D., Schenk, S., Carney, D.P., Smith, J.J., Gagne, D.J., Jin, L., Boss, O., Perni, R.B., Vu, C.B., *et al.*: Small molecule activators of SIRT1 as therapeutics for the treatment of type 2 diabetes. *Nature* **2007**, *450*, 712-716.

Minor, R.K., Baur, J.A., Gomes, A.P., Ward, T.M., Csiszar, A., Mercken, E.M., Abdelmohsen, K., Shin, Y.K., Canto, C., Schebye-Knudsen, M., *et al.*: SRT1720 improves survival and healthspan of obese mice. *Sci. Rep.* **2011**, *1*, 70.

Miriyala, S., Panchatcharam, M., Rengarajulu, P.: Cardioprotective effects of curcumin. *Adv. Exp. Med. Biol.* **2007**, *595*, 359-377.

Nayagam, V.M., Wang, X., Tan, Y.C., Poulsen, A., Goh, K.C., Ng, T., Wang, H., Song, H.Y., Ni, B., Entzeroth, M., Stükel, W.: SIRT1 modulating compounds from high throuput screening as anti-inflammatory and insulin sensitizing agents. *J. Biomol. Screen* **2006**, *11*, 959-967.

Nishiyama, T., Mae, T., Kishida, H., Tsukagawa, M., Mimaki, Y., Kuroda, M., Sashida, Y., Takahashi, K., Kawada, T., Nakagawa, K., Kitahara, M.: Curcuminoids and sesquiterpenoids in turmeric (*Curcuma longa* L.) suppress an increase in blood glucose level in type 2 diabetic KK-A^y mice. *J. Agric. Food Chem.* **2005**, *53*, 959-963.

Okano, M., Fukamiya, N., Lee, K.H.: In *Studies in Natural Products Chemistry*; Atta-ur-Rahman, Ed.; Elsevier Science Publishers: Amsterdam, **1990**; Vol. 7, pp 369-404.

Orallo, F.: Comparative studies of the antioxidant effects of cis-and trans-resveratrol. *Curr. Med. Chem.* **2006**, *13*, 87-98.

Pacholec, M., Bleasdale, J.E., Chrunyk, B., Cunnigham, D., Flynn, D., Garofalo, R.S., Griffith, D., Griffor, M., Loulakis, P., Pabst, B., Stockman, B., Thanabal, V., Varghese, A., Ward, J., Withka, J., Ahn, K.: SRT1720, SRT2183, SRT1406, and resveratrol are not direct activators of SIRT1. *J. Biol. Chem.* **2010**, *285*, 8340-8351.

Pallas, M., Verdaguer, E., Tajes, M., Gutierrez-Cuesta, J., Camins, A.: Modulation of sirtuins: new targets for antiageing. *Recent Patents CNS Drug Discov.* **2008**, *3*, 61-69.

Park, S.Y., Kim, D.S.: Discovery of natural products from *Curcuma longa* that protect cells from beta-amyloid insult: a drug discovery effort against alzheimer's disease. *J. Nat. Prod.* **2002**, *65*, 1227-1231.

Phoopichayanun, C., Phuwapraisirisan, P., Tip-Pyang, S., Jongaramruong, J.: Complete NMR assignment and absolute configuration of feronielloside, a new acetylcholinesterase inhibitor from Feroniella lucida. *Nat. Prod. Res.* **2008**, *22*, 1297-1303.

Porcu, M., Chiarugi, A.: The emerging therapeutic potential of sirtuin interacting drugs: from cell death to lifespan extention. *Trends Pharmacol. Sci.* **2005**, *26*, 94-103.

Pruitt, K., Zinn, R.L., Ohm, J.E., McGarvey, K.M., Kang, S.H., Watkins, D.N., Herman, J.G., Baylin, S.B.: Inhibition of SIRT1 reactivates silenced cancer genes without loss of promoter DNA hypermethylation. *PLoS. Genet.* **2006**, *2*, e40.

Rajendrasozhan, S., Yang, S.R., Kinnula, V.L., Rahman, I.: SIRT1, an antinflammatory and antiaging protein, is decreased in lungs of patients with COPD. *Am. J. Respir. Crit. Care Med.* **2008**, *177*, 861-870.

Ramsey, K.M., Mills, K.F., Satoh, A., Imai, S.: Age-associated loss of Sirt1 mediated enhancement of glucose stimulated insulin secretion in beta cell specific Sirt1

overexpressing (BESTO) mice. *Aging Cell* **2008**, *7*, 78-88.

Rine, J., Herskowitz, I.: Four genes responsible for a position effect on expression from HML and HMR in *Saccharomyces cerevisiae*. *Genetics* **1987**, *116*, 9-22.

Rogina, B., Helfand, S.L.: Sir2 mediates longevity in the fly through a pathway related to calorie restriction. *Proc. Natl. Acad. Sci. U. S. A.* **2004**, *101*, 15998-16003.

Salminen, A., Ojala, J., Huuskonen, J., Kauppinen, A., Suuronen, T., Kaarniranta, K.: Interaction of aging-associated signaling cascades: Inhibition of NF-κB signaling by longevity factors FoxOs and SIRT1. *Cell Mol. Life Sci.* **2008**, *65*, 1049-1058.

Saunders, L.R., Verdin, E.: Sirtuins: critical regulators at the crossroads between cancer and aging. *Oncogen* **2007**, *26*, 5489-5504.

Sauve, A.A., Schramm, V.L.: Sir2 regulation by nicotinamide results from switching between base exchange and deacetylation chemistry. *Biochemistry* **2003**, *42*, 9249-9256.

Sauve, A.A., Wolberger, C., Schramm, V.L., Boeke, J.D.: The biochemistry of sirtuins. *Annu. Rev. Biochem.* **2006**, *75*, 435-465.

Seco, J. M., Quiñoá, E., Riguera, R.: The assignment of absolute configuration by NMR. *Chem. Rev.* **2004**, *104*, 17-117.

Shore, D., Squire, M., Nasmyth, K.A.: Characterization of two genes required for the position-effect control of yeast mating-type genes. *EMBO J.* **1984**, *3*, 2817-2823.

Simon, A., Allais, D.P., Duroux, J.L., Basly, J.P., Durand, S.F., Delage, C.: Inhibitory effect of curcuminoids on MCF-7 cell proliferation and structure-activity relationships. *Cancer Lett.* **1998**, *129*, 111-116

Sinclair, D.A.: Toward a unified theory of caloric restriction and longevity regulation.

Mech. Ageing. Dev. **2005**, *126*, 987-1002.

Smith, J.J., Kenney, R.D., Gagne, D.J., Frushour, B.P., Ladd, W., Galonek, H.L., Israelian, K., Song, J., Razvadauskaite, G., Lynch, A.V., Carney, D.P., Johnson, R.J., Lavu, S., Iffland, A., Elliott, P.J., Lambert, P.D., Elliston, K. O., Jirousek, M.R., Milne, J.C., Boss, O.: Small molecule activators of SIRT1 replicate signaling pathways triggered by calorie restriction in vivo. *BMC Syst. Biol.* **2009**, *3*, 31-44

Stef, G., Csiszar, A., Lerea, K., Ungvari, Z., Veress, G.: Resveratrol inhibits aggregation of platelets from high-risk cardiac patients with aspirin resistance. *J. Cardiovasc. Pharmacl.* **2006**, *48*, 1-5.

Talapatra, S.K., Chaudhuri, M.K., Talapatra, B.: Coumarins of the root bark of Feronia elephantum. *Phytochemistry* **1973**, *12*, 236-237.

Teisseyre, A., Michalak, K.: Inhibition of the activity of human lymphocyte Kv 1.3 potassium channels by resveratrol. *J. Membr. Biol.* **2006**, *214*, 123-129.

Tissenbaum, H.A., Guarente, L.: Increased dosage of a sir2 gene extends lifespan in *Caenorhabditis elegans*. *Nature* **2001**, *410*, 227-230.

Um, J.H., Park, S.J., Kang, H., Yang, S., Foretz, M., McBurney, M.W., Kim, M.K., Viollet, B., Chung, J.H.: AMP-activated protein kinase-deficient mice are resistant to the metabolic effects of resveratrol. *Diabetes* **2010**, *59*, 554-563.

Vaziri H., Dessain, S.K., Ng-Eaton, E., Imai, S.I., Frye, R.A., Pandita, T.K., Guarente, L., Weinberg, R.A.: hSIR2(SIRT1) fuctions as an NAD-dependent p53 deacetylase. *Cell* **2001**, *107*, 149-159.

Venkateswarlu, S., Ramachandra, M.S., Subbaraju, G.V.: Synthesis and biological evaluation of polyhydroxycurcuminoids. *Bioorg. Med. Chem.* **2005**, *13*, 6374-6380.

Vergnes, B., Secreno, D., Madjidian-Sereno, N., Lemesre, J.L., Ouaissi, A.: Cytoplasmis SIR2 homologue overexpression promotes survival of *Leishmania parasites* by preventing programmed cell death. *Gene* **2002**, *296*, 139-150.

Vu, C.B., Bernis, J.E., Disch, J.S., Ng, P.Y., Nunes, J.J., Milne, J.C., Carney, D.P., Lynch, A.V., Smith J.J., Lavu, S., Lambert, P.D., Gagne, D.J., Jirousek, M.R., Schenk, S., Olefsky, J.M., Perni, R.B.: Discovery of imidazol[1,2-b]thiazole derivatives as novel SIRT1 activators. *J. Med. Chem.* **2009**, *52*, 1275-1283.

Walker, A.K., Yang, F., Jiang, K., Ji, J.Y., Watts, J.L., Purushotham, A., Boss, O., Hirsch, M.L., Ribich, S., Smith, J.J., *et al*.: Conserved role of SIRT1 orthologs in fasting dependent inhibition of the lipid/cholesterol regulator SREBP. *Genes Dev.* **2010**, *24*, 1403-1417.

Wang, J., Zhai, Q., Chen, Y., Lin, E., Gu, W., McBurney, M.W., He, Z.: A local mechanism mediates NAD-dependent protection of axon degeneration. *J. Cell Biol.* **2005**, *170*, 349-355.

Xin, Z.Q. Lu, J.J., Ke, C.Q., Hu, C.X., Lin, L.P., Ye, Y.: Constituents from *Clausena excavata*. *Chem. Pharm. Bull.* **2008**, *56*, 827-830.

Yamazaki, Y., Usui, I., Kanatani, Y., Matsuya, Y., Tsuneyama, K., Fujisaka, S., Bukhari, A., Suzuki, H., Senda, S., Imanishi, S., *et al*.: Treatment with SRT1720, a SIRT1 activator, ameliorates fatty liver with reduced expression of lipogenic enzymes in MSG mice. *Am. J. Physiol. Endocrinol. Metab.* **2009**, *297*, 1179-1186.

Yeung, F., Hoberg, J.E., Ramsey, C.S., Keller, M.D., Jones, D.R., Frye, R.A., Mayo, M.W.: Modulation of NF-kappaB-dependent transcription and cell survival by the SIRT1 deacetylase. *EMBO J.* **2004**, *23*, 2369-2380.

Yoshizaki, T., Schenk, S., Imamura, T., Babendure, J.L., Sonoda, N., Bae, E.J., Oh, D.Y., Lu, M., Milne, J.C., Westphal, C., Bandyopadhyay, G., Olefsky, J.M.: SIRT1 inhibits inflammatory pathways in macrophages and modulates insulin sensitivity. *Am. J. Physiol. Endocrinol. Metab.* **2010**, *298*, E419-428.

Zbikowska, H.M., Olas, B., Wachowicz, B., Krajewski, T.: Response of blood platelets to resveratrol. *Platelets* **1999**, *10*, 247-252.

Zhang, Y., Liu, Y., Wang, T., Li, B., Li, H., Wang, Z., Yang, B.: Resveratrol, a natural ingredient of grape skin: antiarrhythmic efficacy and ionic mechanisms. *Biochem. Biophys. Res. Commun.* **2006**, *340*, 1192-1199.

Zhao, K., Harshaw, R., Chai, X., Marmorstein, R.: Structural basis for nicotinamide cleavage and ADP-ribose transfer by NAD^+-dependent Sir2 histone/protein deacetylase. *Proc. Natl. Acad. Sci. U. S. A.* **2004**, *101*, 8563-8568.

VII. ACKNOWLEDGMENTS

Foremost, I would like to express my sincere gratitude to my advisor, Prof. Oh Won Keun, for the continuous support of my Ph.D study and for his facilitating me to grow as a research scientist. His encouragement, enthusiasm and suggestions for high quality research in natural products biochemistry have been inspirational throughout my work and stay in Korea. It is a great privilege for me, and I believe, for all of those who have ever had an opportunity to work under his guidance. His advice on my both research and career will always be invaluable.

I am grateful to my colleagues, Jaeyon, Phi Hung, Van Thu, Thanh Tung, Huwon, Thai Trung, Tien Lam, Nasir, Govinda, Yang, Phuong Dong, Kim Quy, Basanta, and many thanks to my senior Dr. Phuong Thien Thuong for his first help.

I am also greatly thankful to Dr. Nguyen Minh Khoi, Director of Vietnam Institute of Medicinal Materials (VIMM) for the trust and support me in order to study abroad.

Besides, I wish to express my sincere gratitude to Prof. Kang Keon Wook for offering our family the opportunity to study and live together in Korea.

My sincere thanks also go to Dr. Nguyen Bich Thu and Dr. Hoang Thanh Phong, two of my greatest teachers in Vietnam for their help in my study and everything of my life.

Finally, I keep my most deeply sincere gratitude to my parents, my honey and my daughter, whose moral support has meant so much to me in my road of study and research.

Korea, December, 2012

Dao Trong Tuan